7-1995

Non-linear analysis of composite beams with web opening

Ahemd Abdel-Baset Hassanein
The American University in Cairo AUC

NON-LINEAR ANALYSIS
OF COMPOSITE BEAMS
WITH WEB OPENING

BY

Ahmed Abdel-Baset Hussanein

1995

THE AMERICAN UNIVERSITY IN CAIRO
ENGINEERING DEPARTMENT

NON-LINEAR ANALYSIS OF COMPOSITE BEAMS WITH WEB OPENING

Thesis Submitted in Partial Fulfillment of the Requirements
for the Master of Science Degree

BY

Ahmed Abdel-Baset Hassanein

Supervised By

Dr. Ezzat Hassan Fahmy
Head, Construction Engineering Unit,
American University in Cairo

July, 1995

1166

The American University in Cairo
Department of Engineering

M.Sc. Thesis Oral Exam Report

Student's Name: Ahmed Abdel Baset Hassanein

Thesis Title: Non-Linear Analysis of Composite Beams with Web Opening

The student answered the questions adequately, and the Thesis is of the level of Master of Science in Engineering.

Thesis Committee:

Dr. Mohamed Helmy El Haddad
Professor, Cairo University

Dr. Emad Imam,
Associate Professor, AUC

Dr. Ezzat Fahmy,
Associate Professor,AUC

Dr. Fawzia Kouta,
Professor and Chair, AUC

Date: July 10, 1995

ABSTRACT

. The finite difference approach was used to conduct a non-linear analysis of symmetric steel-concrete composite beams with web openings. The presented model accounts for material non-linearity, and for the slip at the interface between the steel beam and the concrete slab, and can analyze composite beams with slabs cast on cellular metal decking. The vertical shear is assumed to be resisted by both the steel beam and the concrete slab, and is divided amongst them by the ratios of their respective shear strength. The model also accounts for shear variation along the opening, and hence composite beams subjected to uniform loading can be analyzed. Von-mises criterion was followed to describe yielding of the steel beam. Strain-hardening of the steel beam was not considered. The model can analyze composite beams subjected to single or two-point loads, as well as uniform loading.

In order to verify the validity of the proposed model, results of the experimental tests available in the literature were compared to the predictions of the current model, and the model proved to be in close agreement with the experimental results.

Having verified the validity of the finite difference model, the model was extended to analyze composite beams with web openings by plotting their interaction diagrams. A parametric study was conducted to determine the impact of varying the opening height, opening length, eccentricity of the opening with respect to the depth of the steel beam, and the number of connectors used in the shear span on the ultimate moment and shear capacities of the composite beam.

The variation of the extreme fiber strain with the applied moment at different locations along the opening was investigated. Also, the effect of varying the opening height, eccentricity of the opening with respect to the depth of the beam and the degree of interaction achieved between the steel beam and the concrete slab on the extreme fiber strain was investigated.

To the memory of my Grand-father, Dr. Abdel-Rahman A. Badran

ACKNOWLEDGMENT

I would like to express my deep appreciation and gratitude to Dr. Ezzat Fahmy, Head of Construction Unit, American University in Cairo, for his constant supervision, encouragement, sincere advice and patience throughout the progress of this work.

I also wish to express my gratitude to Eng. Tarek Ghoneim for his assistance in making the final output of this thesis possible.

I would also like to thank the staff of the Construction Unit, American University in Cairo, for their assistance throughout the progress of this work.

CONTENTS

LIST OF FIGURES

LIST OF TABLES

LIST OF SYMBOLS

A_b	The cross-sectional area of the beam.
A_s	The cross-sectional area of the slab.
A_{wn}	Net web area.
B	The effective width of the slab.
b_f	Breadth of the flange of the steel beam.
$C_{(i)}$	Compressive force in the concrete slab in panel (i).
D, d	Total depth of the steel beam.
d_i	Intercept corresponding to load Q_i of connector "i".
D_s	Depth of the concrete slab including the height of the cellular decking.
d_w	Depth of the web of the steel beam.
E_b	Young's Modulus of the steel of the beam.
E_s	Young's Modulus of the concrete slab.
$F_{1(i)}$	Compressive force in the steel beam in panel (i).
$F_{2(i)}$	Tensile force in the steel beam in panel (i).
$F_{b(i)}$	Force in the steel beam in panel (i).
$F_{s(i)}$	Force in the concrete slab in panel (i).
f_c'	The strength of the concrete.
h	Opening height.
I_b	Moment of inertia of the steel beam.
I_s	Moment of inertia of the concrete slab.
K_i	Slope of the load-slip curve of connector "i".
M	Moment at mid-length of the opening at failure.
$M_{b(i)}$	Moment resisted by the steel beam in panel (i).
M_{DL}	Moment due to dead load.
$M_{s(i)}$	Moment resisted by the concrete slab in panel (i).
M_{ult}	The ultimate moment capacity of the composite beam.
N_{ci}	Number of connectors needed for complete interaction.
N_{used}	Number of connectors used in the shear span.
Q_i	Force on connector "i".
r_i	Slip of connector "i".
$S_{(i)}$	Spacing of connectors in panel (i).
$T_{(i)}$	Net tensile force in the steel beam in panel (i).
t_f	Thickness of the flange of the steel beam.
t_s	Solid thickness of the concrete slab.
V	Shear at mid-length of the opening at failure.
V_b	Vertical shear force resisted by the steel beam.
V_s	Vertical shear force resisted by the concrete slab.
V_{ult}	The ultimate shear capacity of the composite beam.
Z	The distance between the centroids of the steel beam and the concrete slab.
ε_b	Strain at the top of the steel beam.
ε_{bb}	Strain at the bottom of the steel beam.
ε_s	Strain at the top of the concrete slab.
ε_{ss}	Strain at the bottom of the concrete slab.

ε_{wb}	Strain at the bottom of the steel web.
ε_{wt}	Strain at the top of the steel web.
$\varepsilon_{wy'}$	Strain at which yielding will occur.
ϕ_b	Curvature of the steel beam.
ϕ_{DL}	Curvature of the steel beam due to dead load alone.
ϕ_s	Curvature of the concrete slab.
σ	The equivalent stress due to the combined effect of normal and shear forces.
σ_n	The normal stress in the steel beam.
$\sigma_{wy'}$	The equivalent stress at which yielding will occur.
σ_{wy}	The nominal yield stress of the steel.
σ_y	Yield stress of the steel.
τ	The shear stress.

CHAPTER 1
INTRODUCTION

1.1. GENERAL:

Composite structures are often used in construction nowadays. The most common type of composite structures consists of a concrete slab supported on a steel beam, and connected together in a way which causes shear transfer from one element to the other. Ribbed metal decking is now used as formwork for the concrete slab and forms, together with the hardened concrete, the structural floor. The use of composite steel-concrete construction provides great economy as lighter steel sections can be used for a given span and load. The composite construction results in a shallower beam depth and consequently smaller floor-to-floor heights, with all the savings that implies.

Often, utility ducts are required to pass from one side to the other of the composite beam. Passing these utility ducts under the beam results in larger floor-to-floor height and loss of the advantage gained by using the composite construction. The demand for economical and efficient structures led the engineers to develop a way to reduce the storey-to-storey height in high-rise buildings by eliminating the space below the beams and girders which was usually provided for the utility passage. The use of web openings in the composite beam offers an engineering solution for this problem. However, the presence of such openings affects the moment and shear capacities of the composite beam, and influences its behavior.

Before the engineer can make use of the tangible benefits of using composite beams with web openings, the behavior and strength of such beams should be thoroughly investigated and fully comprehended.

1.2. Objectives of This Thesis:

All previous models were only concerned with determining the ultimate moment and shear capacities of composite beams with web openings. The behavior of the composite beams with web openings at working loads was never investigated. Most previous models assumed that no slip would occur between the steel beam and the concrete slab, which is not a realistic assumption. Moreover, the assumption that the shear is constant along the opening could lead to faulty results.

This study aims to investigate the behavior of composite beams with web openings at all loading stages, and determine the ultimate load-carrying capacity of composite beams with web opening. As slip at the interface between the steel beam and the concrete slab can be accounted for, the predictions of the current model will be more accurate than those of previous models.

As the model can accommodate uniform loading conditions, the shear at both ends of the opening could be unequal, which is also more realistic, as beams are primarily subjected to uniform loading conditions. The model is discussed in detail in chapter 3.

CHAPTER 2
LITERATURE REVIEW

2.1. General:

The behavior of composite steel-concrete beams has been the subject of investigation by many researchers, and is well documented in the literature. Many researchers have investigated the effect of web openings in steel beams. Although composite beams with web openings provide a very economic construction system, specially in high-rise buildings, their behavior has not been thoroughly investigated. Limited research effort has been conducted to determine the behavior of composite beams with web openings. A few researchers have attempted to analytically study the behavior of composite beams with web openings, and presented models to predict the ultimate strength and mode of failure of the composite beam. The behavior of composite beams with web openings at all stages of loading has not been previously investigated.

A literature review of the published research in areas related to the study of the behavior of composite beams with web openings is presented in this chapter. The literature review is divided into the following three sections 1) the behavior of composite beams 2) the behavior of steel beams with web openings, and 3) the behavior of composite beams with web openings.

2.2. Composite Beams:

The connection provided by the shear connectors between the steel beam and the concrete slab was the focus of many researchers as part of their investigations to study the behavior of composite beams. The fact that the connection becomes a comparatively flexible one when cellular metal decking is used in composite beams made such investigation of particular interest.

Robinson[20] carried out an experimental program to determine the effect of rib geometry on the strength of the connection. The results of the experimental

investigation showed that rib geometry affects both the magnitude of slip and the mode of failure. When the height-to-width ratio of the ribs was greater than one cracking of the ribs occurred in the elastic range. On decreasing the height-to-width ratio of the ribs to one, cracking of the ribs shortly followed the onset of local yielding of the beam. On further decreasing the ratio, a load in excess of the first yield load was achieved.

He concluded that in order to achieve the theoretical ultimate moment capacity, the ribs should be wide enough to provide a sufficient cover for the studs. Increasing the width of the ribs provides a sufficient cover of concrete in the lateral direction to prevent punching out of the rib, as well as a better seating of the ribs and preventing them from rotating.

The variation of connector slip along the length of the beam was investigated by Robinson[21]. He concluded that the slip of the connector, and thus the force to which it is subjected, is minimal at the locations of the applied loads in case of concentrated loads, figure 2.1. He also concluded that the efficiency of the connection is also decreased as the shear span decreases. Also, the degree of interaction at the mid-span of the composite beam is higher for two-point loading conditions than that for uniform loading.

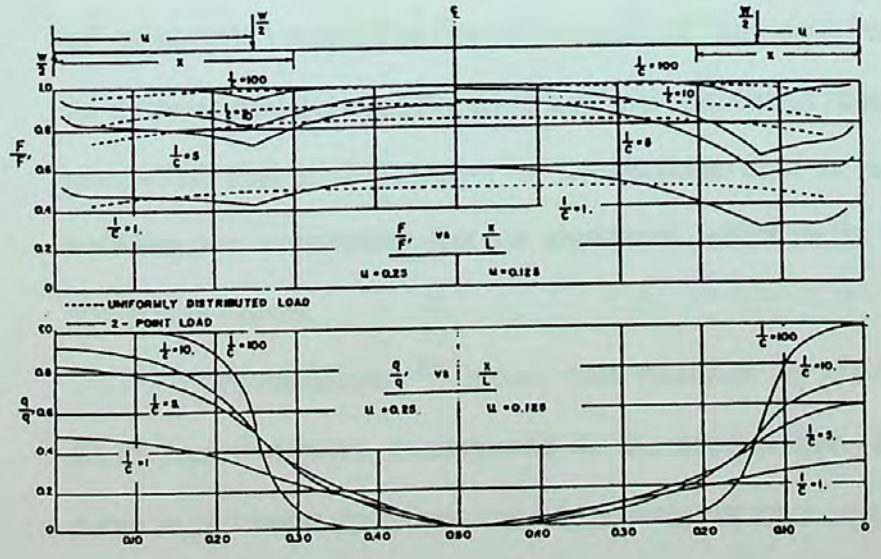

F,F' : Interaction forces for complete and incomplete interaction, respectively
q,q' : Horizontal shear per unit length of composite beam for complete and incomplete interaction, respectively

Figure 2.1- Variation of Connector Slip Along Beam Span[21].

A computer model was presented by Thiruvengadam[23] to analyze composite beams. Using the finite difference approach, he presented a numerical method that calculated the strains, curvatures and the deflection at all points along the span of the beam, at all loading stages. The model accounts for the slip at the interface between the steel beam and the concrete slab, and all types of connections between the slab and the beam. Composite beams with concrete slabs on cellular metal decking could also be analyzed by that model. The model also accounted for strain-hardening. However, it did not take the effect of the vertical shear forces, on the steel beam and the concrete slab, into consideration in the analysis. Only the normal stresses and the resulting strains were considered.

Robinson and Wallace[22] conducted experimental tests on various composite beams with various number and arrangements of connectors to study the effect of using cellular metal decking on the strength of the connection between the steel beam and the concrete slab. The results of their study showed that the strength of the connection between the slab and the steel beam depends on the height and width of the ribs, as well as the length and diameter of the stud. Their experiments also showed that the strength of the connection increased with increasing the length of the stud embedded in the solid part of the slab. They also showed that the use of fewer connectors than that required for full interaction reduces the ultimate flexural capacity of composite beams. The flexural capacity of composite beams was reduced to 82% of its ultimate flexural capacity when a partial connection ratio of 0.5 was used. They also concluded that if the number of connections used is satisfactory, then the spacing between the connectors has no significant effect on the ultimate flexural capacity of composite beams.

Thiruvengadam's[23] model was modified by Ma[14] to overcome some of the difficulties that were encountered in the computation. He used a smooth load-slip curve to represent the shear connectors, which is more accurate than the representation presented by Thiruvengadam[23]. When compared with experimental tests[22], this

model proved to be rather accurate in predicting the deflection and strains along the span of composite beams.

2.3. Steel Beams With Web Openings:

Steel beams with web openings present one of the units of the composite beam. Understanding it's behavior is therefore a very important step in comprehending the behavior of the composite beam as a whole. Steel beams with web openings, however, present a less-complicated problem than composite beams with web openings. This is because the interaction between the steel beam and the concrete slab in the case of composite slabs should be taken into consideration. The behavior of the concrete slab is another factor controlling the behavior, and thus must also be studied. Studying the behavior of steel beams when an opening is introduced in their web was therefore a necessary step to understanding the behavior of composite beams with web openings.

Based on the dimensions of the opening, and the geometry of the steel beam, Redwood[15] presented an analytical method to plot the interaction diagrams for steel beams with concentric reinforced or unreinforced rectangular openings. He also suggested a method to analyze steel beams with circular and extended-circular web openings by approximating them to rectangular holes (fig. 2.2). He suggested a vertical cut-off in the interaction diagrams for steel beams with circular openings due to the reduced shear capacity.

Aglan and Redwood[1] presented an analytical model to study the behavior of non-composite steel beams with two concentric, reinforced rectangular web openings. In their model, they included the effect of strain-hardening, as well as lateral buckling of the web post. The rigid-plastic strain-hardening theory presented by Horne and Medland was applied. The results of their analysis was in close agreement with experimental results. Their method could also be used to calculate the critical moment for the post between two non-rectangular openings.

Fahmy[11] conducted a study to determine the ultimate strength of steel beams with web openings. Bassed on the ultimate strenght design, he plotted the interaction

diagrams of steel beams with web openings. The openings could be either concentric or eccentric with respect to the depth of the beam.

Design recommendations for steel beams with or without reinforced rectangular or circular web openings were presented by Redwood and Shrivastava[18]. They conducted a study which was based on the assumption that the steel used in the beam would be ductile, and thus have $F_y \leq 0.8F_u$. The study was conducted for steel beams with opening heights between 30% and 70% of the total beam depth, and the opening length was not to be greater than triple the opening height. Concentrated loads were not to be applied within the length of the opening. They also studied the stability of the compression zone above the opening, and suggested that it should be treated as an axially-loaded column with its effective length equal to the length of the opening. The effect of multiple holes was also studied. A minimum distance between the openings was recommended to avoid interaction between the holes.

2.4. Composite Beams with Web Opening:

Todd and Cooper[24] presented an analytical model to determine the ultimate strength of composite beams with unreinforced rectangular openings. They assumed complete interaction between the slab and the beam, and neglected strain hardening of the steel. They also assumed constant vertical shear along the length of the opening. In their model, the ability of the slab to support tension and shear was neglected. Also, failure was assumed to be due to the formation of plastic hinges at the two ends of the opening. Buckling and instability failures were not considered in their model. Yielding in the web was assumed to follow von Mises' yield criterion. They plotted the interaction diagrams of various composite beams with web openings, and also conducted a parametric study to determine the effect of changing some variables on the overall behavior of the beam. Their analysis indicated that the moment capacity of composite beams was much higher than that of steel beams, despite the fact that they neglected the shear resistance of the concrete slab.

According to their analysis, the thickness of the slab did not significantly affect the moment capacity of composite beams. Their analysis also showed that the ultimate shear and moment capacities of composite beams decreased with increasing the opening height. The effect of varying the opening eccentricity with respect to the beam depth was more complex; the ultimate shear capacity of composite beams decreased with increasing the eccentricity of the opening, while the ultimate moment capacity increased as the opening approached the concrete slab. When compared with experimental results, their model was found to be over-conservative.

Clawson and Darwin[4] carried out experimental tests on 6 composite beams with web openings. The openings were located at different locations along the span of the beam to enable studying the effect of varying the "M/V" ratio at the mid-length of the opening on the overall performance of the beam, as well as the mode of failure at the opening. From their experimental analysis, they concluded that the mode of failure at the opening is greatly affected by the "M/V" ratio. They found that beams that had openings at locations of high "M/V" ratio failed by general yielding in the steel below the neutral axis, and crushing in the concrete above the neutral axis. On the other hand, beams with medium or low "M/V" ratios failed by the formation of plastic hinges in the bottom tee, accompanied by a diagonal tension failure in the concrete. From the results of their experimental study they concluded that the concrete contributes significantly to the moment and shear capacities of composite beams.

Based on their experimental results, they plotted an interaction diagram for a composite beam. They tested three identical composite beams except for the location of the opening, which was varied along the beam span.

Figure 2.1 shows an interaction diagram developed by Clawson and Darwin[4]. The figure shows that beam B_5, which was a larger beam, failed at a load combination higher than that necessary to cause failure of the smaller beams. Also, the figure shows that the ultimate shear capacities of beams B_1 and B_6 are higher than those for beams B_2, B_3 and B_4. The authors attributed this to the contribution of the concrete slab in resisting the shear forces. The authors also deduced that strain-hardening plays an

important role in resisting the applied moment, specially at the point of high "M/V" ratio.

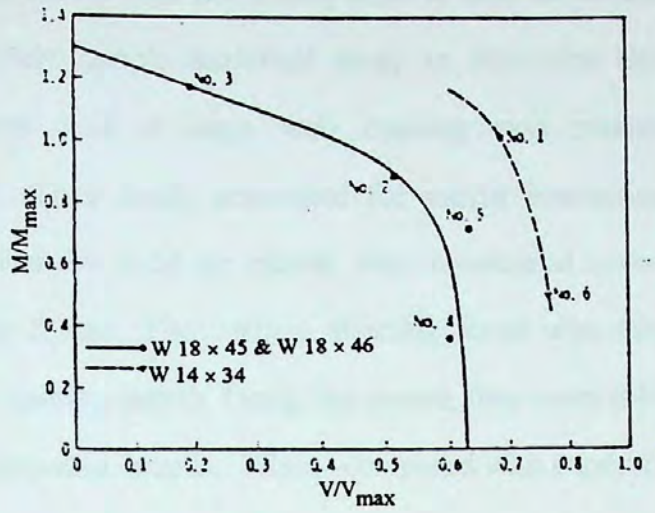

Figure 2.2- Interaction Diagrams Presented by Clawson et al[4].

Another analytical model to determine the ultimate strength of composite beams with concentric or eccentric unreinforced rectangular openings was presented by Clawson and Darwin[5]. Unlike the model suggested by Todd et al, the ability of the slab to resist the shear stresses was taken into account. Strain hardening of the steel beam was not taken into consideration, and the shear was assumed to be constant along the opening length. Also, the slip between the concrete and the steel was not included in the model.

When compared with experimental results[4], this model was found to present a conservative estimation of the strength of composite beams with web openings. The prediction of the strength of the composite beam was more realistic than that of the model presented by Todd et al. This could be attributed to their considering the strength of the concrete slab in resisting the shear forces.

Based on experimental tests carried out on five composite beams with large unreinforced rectangular web openings, Redwood and Wong[19] suggested a model to predict the ultimate strength of composite beams with web openings. Partial interaction between the steel beam and the concrete slab was taken into consideration. The ability

of the concrete slab to resist shearing forces was taken into account, and they analytically plotted an interaction diagram of composite beams with web openings. The predictions of the model were acceptably close to their test results.

A relatively simple analytical study to determine the ultimate strength of composite beams with a large web opening was presented by Redwood and Poumbouras[17]. Their study accounted for partial interaction. The concrete slab, which could either be solid or ribbed, was considered to contribute in resisting the vertical shearing forces. The vertical shearing force was considered to be constant throughout the opening length. Using this model, they were able to plot the interaction diagrams of composite beams. When compared with experimental results the model showed good agreement, and its predictions were slightly more conservative than the predictions of Redwood and Wong[19], which was a more complicated model.

The deflection of composite beams with web openings was studied by Donahey[8]. He calculated the deflection of composite beams with web openings using the stiffness method of matrix analysis. Two models were presented and compared with experimental test results; one in which the deflection due to bending only was considered, while in the other the effect of both shear and moment on the deflection was considered. The test results showed that the model in which the effect of shear on the deflection of the composite beam was considered yielded more accurate results than the model in which shear was neglected. The importance of including the effect of shear on the deflection of the beam became more pronounced as the opening height increased. The opening height, as well as the opening location along the span of the beam, proved to affect the overall deflection of the beam, but the effect of the opening height was much more significant.

The ultimate strength of composite beams with unreinforced rectangular web opening was investigated by Darwin and Donahey[6] using the load and resistance factor design (LRFD). The method adapted to both solid and ribbed slabs. The study includes reasonable solutions for the pure moment and pure shear strengths at the opening, as well as a solution for the capacity of the composite beam at the opening

under combined shear and moment. The predictions of the model were compared to those of some experimental beams, and proved the method to be comparatively accurate.

Fahmy[10] presented a study on composite beams with unreinforced rectangular openings, based on the ultimate strength analysis. The contribution of the slab in resisting the shear forces was taken in consideration, and the interaction between the slab and the beam was assumed to be full. Buckling and instability failures were not considered in this analysis, and the strain hardening of the steel beam was not taken into consideration. The shear along the opening was also assumed to be constant. Comparison was made between the analytical results of the model, and some experimental tests, and the model was found to be in close agreement in most cases, with a tendency to be on the conservative side. This can be attributed to the fact that the beneficial effects of strain hardening were not considered.

Another study using the LRFD approach to determine the strength of composite beams with reinforced or unreinforced rectangular web openings was later conducted by Darwin and Lucas[7]. They conducted a study to determine the resistance factors for design. The predictions of the model were compared with experimental results from 50 steel beams and 35 composite beams and the comparisons were used to determine the resistance factors for design.

An experimental study was conducted by Lawson, Chung and Price[13]. In order to justify current design methods[12], they experimentally loaded three composite beams with five web openings till failure. They concluded that the current design methods were over-conservative in cases when the opening was in the low-moment, high-shear region. They also concluded that stiffeners welded to one side of the web did not enhance the performance of the beam. Based on their experimental study, they developed an analytical method to design composite beams with rectangular web openings, which they claim to provide more economic sections for composite beams with web openings.

The behavior of the concrete slab in resisting the vertical shear stresses at the region of the opening was investigated by Cho and Redwood [2]. They presented a model which could be applied to both solid and ribbed slabs to determine the ultimate strength of the slab in the region of the opening using a truss analogy. They assumed that the shear was carried by both the steel beam and the concrete slab only in the vicinity of the opening, and beyond the studs just before and just after the opening the steel beam was considered to be resisting all the vertical shear stresses. In their study the truss capacity was limited by failure of the concrete around the studs, and related the strength of the slab in resisting vertical shear stresses to the location and spacing of the studs. Three models were presented, in which the location of the studs with regard to the opening were varied to suit most practical locations of the studs. From their study they concluded that placing the studs close to the low-moment end of the opening provides the most efficient shear-carrying mechanism in composite beams at web holes. The spacing between shear connectors also proved to be a major factor controlling the shear strength of the concrete. On comparing the results of their analysis with experimental beams, these models proved to yield conservative results.

Cho and Redwood[3] carried out experimental tests on six full-scale composite beams with nine web openings to determine the validity of the above-mentioned truss analogy. The tested beams had different stud arrangements of both single and double studs. Openings with both high and low M/V ratios were tested. From this experimental study, they concluded that shear connectors placed over the hole and close to the opening's edges were the major factors controlling the capacity of the slab to resist vertical shear stresses in the opening. The tensile strength of the connectors placed near the high moment end of the opening also contributed greatly to the slab shear-carrying capacity. Compared to the predictions of Darwin and Donahey[6], the predictions of the truss analogy model were more conservative in solid slabs as well as ribbed slabs, but the predictions were only slightly more conservative in the case of beams with ribbed slabs, and the scatter was significantly less in the case of ribbed slabs.

CHAPTER 3
ANALYTICAL MODEL

3.1. General Introduction:

Theoretical approaches to predict the behavior of composite beams have been developed by various researchers. The most recent development in this field is the finite difference approach developed by Thiruvengadam[23] and modified by Ma[14] to overcome the numerical difficulties encountered in the analysis presented by Thiruvengadam[23].

This chapter contains the description of the analytical model developed to analyze composite beams with web openings. The method presented by Ma[14] was extended to account for both the opening in the web of the steel beam and the vertical shear stresses applied on the composite beam. Von-Mises yield criterion was used to describe yielding of the steel beam under the combined effect of flexural and shear stresses.

3.2. General Definitions:

A single span composite steel-concrete beam with a web opening is presented in figure 3.1(a). The beam has "n" panel and "n+1" shear connectors. The panel between connectors "i" and "i+1" is referred to as the "(i)"th panel. The number of the panel will be written between parenthesis, while the connector number will be written without parenthesis. In the analysis, tensile normal forces and moments producing tension in the bottom fibers are considered positive.

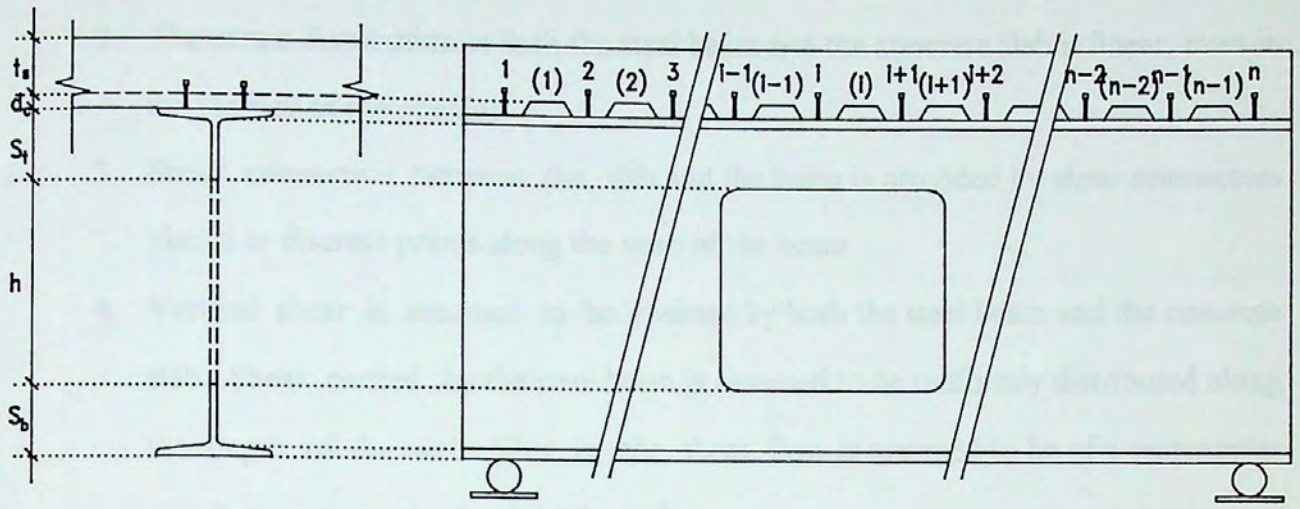

a) Connector and Panel Numbering

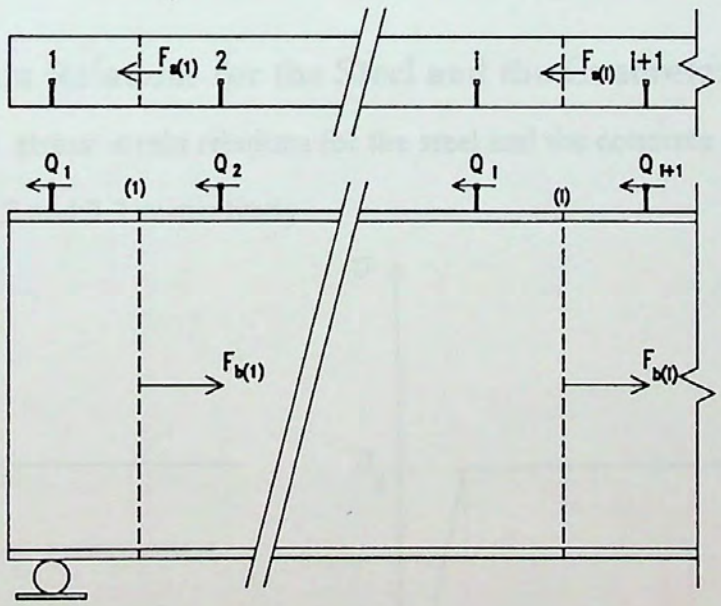

b) Forces in the Slab and the Beam

Figure 3.1- General Definitions

3.3. Basic Assumptions:

The basic assumptions used throughout the analysis are:

1. The slab and the beam deflect equally at all points along the span.
2. The strain distribution in both the steel beam and the concrete slab is linear, even in the vicinity of the opening.
3. Shear connection between the slab and the beam is provided by shear connectors placed at discrete points along the span of the beam.
4. Vertical shear is assumed to be resisted by both the steel beam and the concrete slab. Shear carried by the steel beam is assumed to be uniformly distributed along the depth of the web. That is, the shear flow is assumed to be of a rectangular distribution along the depth of the web.
5. Stress concentrations at the beginning of the opening are neglected, as the corners of the opening are considered to be smoothed so as not to induce stress concentrations.
6. Failure due to local buckling and web instability is not considered in the analysis.

3.4. Stress-Strain Relations for the Steel and the Concrete:

The actual stress strain relations for the steel and the concrete are idealized as shown in figures 3.2 and 3.3 respectively.

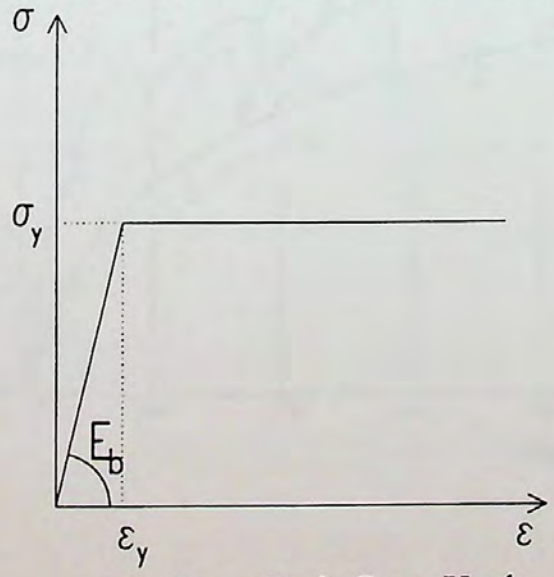

3.2- Stress-Strain Curve Used for Steel

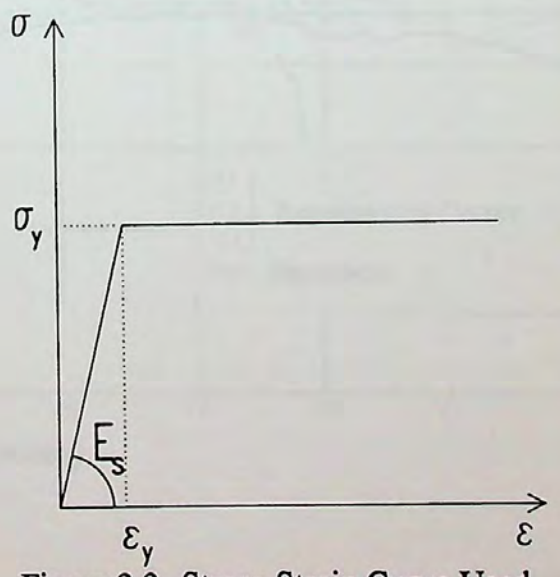

Figure 3.3- Stress-Strain Curve Used for Concrete

3.5. Load-Slip Curve of the Connector:

A smooth curve defined analytically is used to represent the load-slip curve of the connectors. For composite beams with cellular deck, the load-slip relation for the connector is represented by a hyperbola the equation of which is

$$Q = \frac{C}{r - A} + B \qquad [3.1]$$

Where A, B and C are three constants determined by three points through which the curve passes. One of these points is the origin (0,0), and the other two are (r_2,Q_2) and (r_3,Q_3). The constants are given by

$$A = \frac{C}{B}$$

$$B = \frac{r_2 Q_2 Q_3 - r_3 Q_2 Q_3}{r_2 Q_3 - r_3 Q_2}$$

$$C = \frac{B r_2 Q_2 - B^2 r_2}{Q_2}$$

Ma[14] proved that the hyperbola gives a close approximation to the load-slip curve as can be seen in figure 3.4.

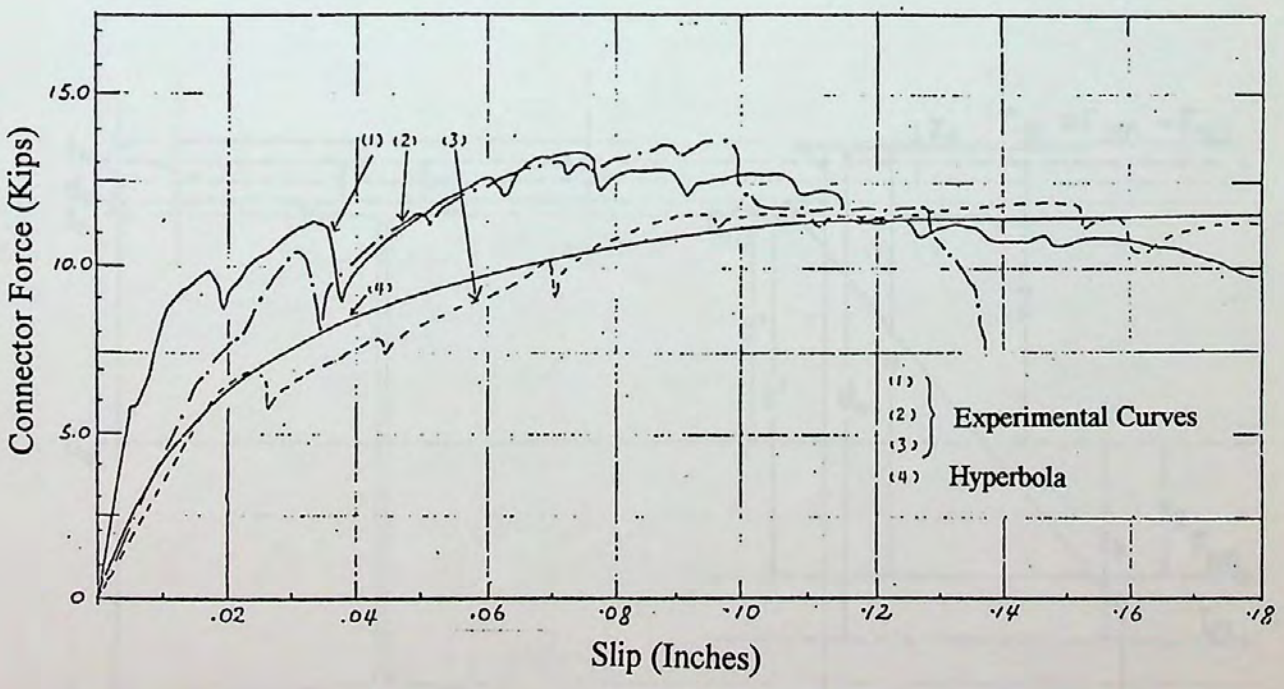

Figure 3.4- Experimental Load-Slip Curves and the Hyperbola Representation[14]

3.6. Equilibrium Conditions:

At any panel in the composite beam, the net compressive force in the slab must be equal to the net tensile force in the steel beam for the equilibrium to be satisfied. From figure 3.1(b);

$$F_s = -F_b \qquad [3.2]$$

Where F_s and F_b are the net forces in the slab and the beam respectively. From figure 3.1(b), it can also be seen that

$$F_{b(i)} - F_{b(i-1)} = Q_i \qquad [3.3]$$

Where: $F_{b(i)}$ is the force in the beam in panel (i),

$F_{b(i-1)}$ is the force in the beam in panel (i−1),

Q_i is the load on the connector i.

Also, for equilibrium, the total external moment must be equal to the resisting moment of the section. Figure 3.5 shows the forces in panel (i) in a composite beam.

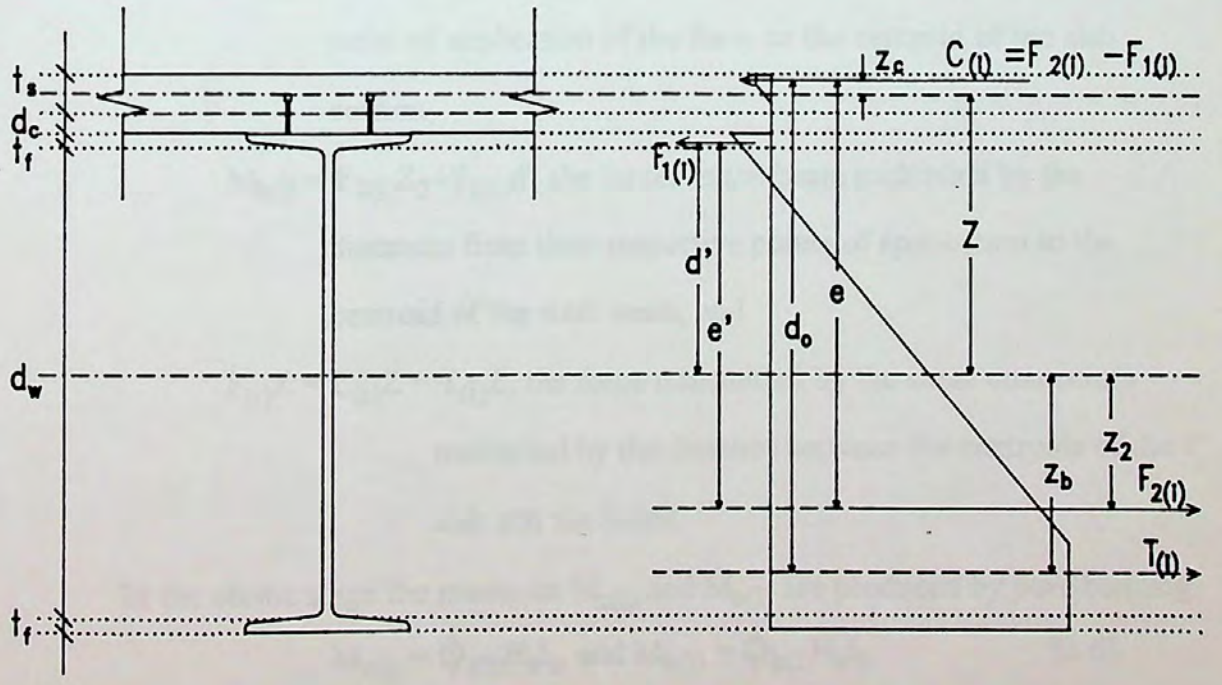

Figure 3.5- Stress Distribution in Panel (i)

From figure 3.5

$$T_{(i)} = F_{2(i)} - F_{1(i)} \qquad [3.4]$$

$$C_{(i)} + F_{1(i)} = F_{2(i)} \quad \Rightarrow C_{(i)} = T_{(i)} = F_{(i)}$$

where: $C_{(i)}$ is the compressive force in the slab,

$F_{1(i)}$ is the compressive force in the beam,

$F_{2(i)}$ is the tensile force in the beam,

$T_{(i)}$ is the net tensile force in the beam.

The moment in the composite beam can be determined by the following method:

From figure 3.5:

$$M_{(i)} = C_{(i)} \times e + F_{1(i)} \times e'$$

$$M_{(i)} = C_{(i)} \times (Z_c + Z + Z_2) + F_{1(i)} \times (d' + Z_2)$$

$$= C_{(i)}Z_c + C_{(i)}Z + C_{(i)}Z_2 + F_{1(i)}d' + F_{1(i)}Z_2$$

$$= C_{(i)}Z_c + (C_{(i)} + F_{1(i)})Z_2 + C_{(i)}Z + F_{1(i)}d'$$

$$= C_{(i)}Z_c + F_{2(i)}Z_2 + F_{1(i)}d' + C_{(i)}Z$$

$$\therefore \quad M_{(i)} = M_{s(i)} + M_{b(i)} + F_{(i)}Z \qquad [3.5]$$

Where $M_{s(i)} = C_{(i)}Z_c$, the force in the slab multiplied by the distance from the point of application of the force to the centroid of the slab section,

$M_{b(i)} = F_{2(i)}Z_2 + F_{1(i)}d'$, the forces in the beam multiplied by the distances from their respective points of application to the centroid of the steel beam, and

$F_{(i)}Z = C_{(i)}Z = T_{(i)}Z$, the force transmitted by the shear connectors multiplied by the distance between the centroids of the slab and the beam.

In the elastic stage the moments $M_{s(i)}$ and $M_{b(i)}$ are produced by pure bending.

$$M_{s(i)} = \phi_{s(i)}E_sI_s, \text{ and } M_{b(i)} = \phi_{b(i)}E_bI_b \qquad [3.6]$$

where: $\phi_{s(i)}$ and $\phi_{b(i)}$ are the curvatures of the slab and beam at panel (i) respectively.

I_s and I_b are the moments of inertia of the slab and beam respectively.

E_s and E_b are the Young's Modulii of the slab and the beam respectively.

3.7. Compatibility Condition:

Slip at the interface between the slab and the beam is resisted by the shear connectors. These connectors deform under the loads to which they are subjected, and slip occurs. It is assumed that no vertical separation takes place between the slab and the beam.

From figure 3.6;

$$S_{(i)}+\int_{s(i)}\varepsilon_s ds + r_{i+1} = S_{(i)}+\int_{s(i)}\varepsilon_b ds + r_i$$

$$\therefore \quad r_{i+1} = r_i + \int_{s(i)}(\varepsilon_b - \varepsilon_s) ds \qquad [3.7]$$

where: $S_{(i)}$ is the distance between connectors in panel (i)

r_i is the slip of connector i

r_{i+1} is the slip of connector i+1

ε_s and ε_b are the strains in the bottom of the slab and top of the beam respectively.

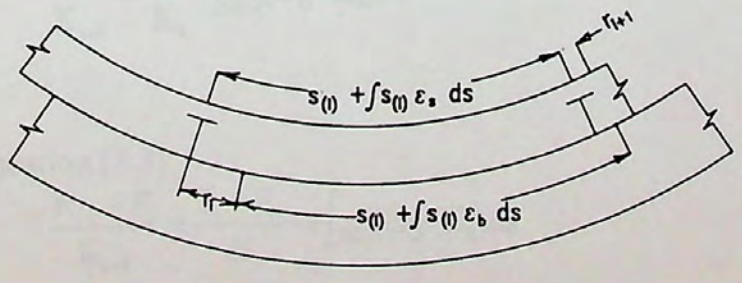

Figure 3.6- Bending of a Panel with Slip

3.8. Finite Difference Equations:

Although the load-slip relation for the shear connectors is non-linear, it will be illustrated on an elastic case to simplify the behavior The inelastic case will be explained later. Assuming the load-slip curve of the connector to be linearly-elastic as shown in figure 3.7, the load-slip relation of the connector would be

$$Q=Kr \qquad [3.8]$$

Where: Q is the load on the connector

K is the slope of the curve

r is the slip of the connector

$$\therefore \quad r=\frac{Q}{K}$$

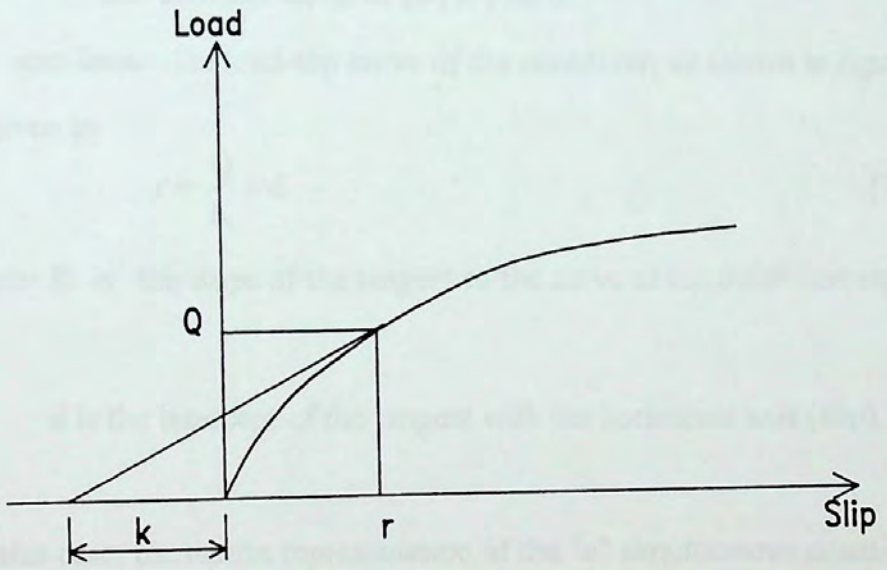

Figure 3.7- Load-Slip Curve for a Connector

Substituting in equation [3.7]

$$\frac{Q_{i+1}}{K_{i+1}}=\frac{Q_i}{K_i}+\int_{S(i)}(\varepsilon_b-\varepsilon_s)ds$$

and from equation [3.3]

$$\frac{F_{i+1}-F_i}{K_{i+1}}=\frac{F_i-F_{i-1}}{K_i}+\int_{S(i)}(\varepsilon_b-\varepsilon_s)ds$$

$$\frac{F_{i-1}}{K_i}-\left(\frac{1}{K_{i+1}}+\frac{1}{K_1}\right)F_i+\frac{F_{i+1}}{K_{i+1}}=\int_{S(i)}(\varepsilon_b-\varepsilon_s)ds \qquad [3.9]$$

Putting "n" equations for "i" (between 1 and "n"), we get "n" simultaneous equations. These equations can be presented in a matrix form

$$[B][F]=[A] \qquad [3.10]$$

where: [F] is a vector whose i^{th} term is "F_i".

[A] is a vector whose i^{th} term is $(A_{(i)}=\int_{S(i)}(\varepsilon_b-\varepsilon_s)ds)$.

[B] is a banded diagonal matrix

$$B_{ii}=-\left(\frac{1}{K_{i+1}}+\frac{1}{K_1}\right),$$

$$B_{i(i-1)}=B_{(i-1)i}=\frac{1}{K_i},$$

$$B_{i(i+1)}=B_{(i+1)i}=\frac{1}{K_{i+1}},$$

and all other terms of [B] are zero.

For non-linear the load-slip curve of the connector, as shown in figure 3.7, the relation is given by

$$r=\frac{Q}{K}+d \qquad [3.11]$$

where: K is the slope of the tangent to the curve at the point corresponding to "Q".

d is the intercept of the tangent with the horizontal axis (slip).

In this case, the matrix representation of the "n" simultaneous equations would be

$$[B][F]=[A]+[D] \qquad [3.12]$$

Where $D_{(i)} = d_i-d_{i+1}$, where d_i and d_{i+1} are the intercepts corresponding to loads Q_i and Q_{i+1} at connectors "i" and "i+1" respectively, and [B], [F], and [A] are as defined in equation [3.10].

3.9. Modifications in Terms of the Basic Equation:

3.9.1. Elastic Case:

When the both the slab and the beam are elastic, the strains in the slab and the beam can be given by:

$$\varepsilon_b = \frac{1}{E_b}\left(\frac{F}{A_b} - \frac{M_b C_b}{I_b}\right) \qquad [3.13]$$

$$\varepsilon_s = \frac{1}{E_s}\left(-\frac{F}{A_s} + \frac{M_s C_s}{I_s}\right) \qquad [3.14]$$

where: ε_b is the strain at the top of the steel beam.

ε_s is the strain at the bottom of the slab.

E_b is the Modulus of Elasticity of the beam.

A_b is the cross-sectional area of the beam.

I_b is the moment of inertia of the steel beam.

C_b is the distance from the centroid of the beam to the top of the beam.

C_s is the distance from the centroid of the slab to the bottom of the slab.

E_s , A_s and I_s are the same as quantities as above but for the slab.

Substituting in for the value of $A_{(i)}$

$$A_{(i)} = \int_{s(i)} (\varepsilon_b - \varepsilon_s) ds$$

$$= \int_{s(i)} \left[\frac{1}{E_b}\left(\frac{F}{A_b} - \frac{M_b C_b}{I_b}\right) \div \frac{1}{E_s}\left(-\frac{F}{A_s} + \frac{M_s C_s}{I_s}\right)\right] ds$$

$$= \int_{s(i)} \left[\left(\frac{1}{E_b A_b} + \frac{1}{E_s A_s}\right) F - \left(\frac{M_b C_b}{E_b I_b} + \frac{M_s C_s}{E_s I_s}\right)\right] ds$$

Since the assumption is made that the slab and the beam deflect equally at all points, therefore, for small values of deflection equal curvature can be assumed.

$$\phi_s = \phi_b$$

$$\therefore \quad \frac{M_b}{E_b I_b} = \frac{M_s}{E_s I_s} = \frac{M_b + M_s}{I_b E_b + I_s E_s}$$

From equation [3.5]

$$M = M_s + M_b + ZF$$

$$\therefore \quad \frac{M_b + M_s}{I_b E_b + I_s E_s} = \frac{M - ZF}{E_b I_b + E_s I_s}$$

$$\therefore \quad A_{(i)}=\int_{S(i)}\left[\left(\frac{1}{E_bA_b}+\frac{1}{E_sA_s}\right)F-\frac{M-ZF}{E_bI_b+E_sI_s}(C_s+C_b)\right]ds$$

But $C_s+C_b=Z$

$$\therefore \quad A_{(i)}=\int_{S(i)}\left[\left(\frac{1}{E_bA_b}+\frac{1}{E_sA_s}\right)F-\frac{M-ZF}{E_bI_b+E_sI_s}(Z)\right]ds$$

$$\therefore \quad A_{(i)}=\int_{S(i)}\left[F\left(\frac{1}{E_bA_b}+\frac{1}{E_sA_s}+\frac{Z^2}{E_bI_b+E_sI_s}\right)-\frac{MZ}{E_bI_b+E_sI_s}\right]ds$$

E_s, E_b, A_s, A_b, I_s, I_b and Z are all section properties of the composite beam.

Let $\alpha=\frac{1}{E_bA_b}+\frac{1}{E_sA_s}+\frac{Z^2}{E_bI_b+E_sI_s}$,

and $\beta=\frac{Z}{E_bI_b+E_sI_s}$,

$$\therefore \quad A_{(i)}=\int_{S(i)}\left[\alpha\ F-\beta M\right]ds \qquad [3.15]$$

And since "F" is constant within a panel

$$A_{(i)}=F_{(i)}\alpha_{(i)}S_{(i)}-\int_{S(i)}\beta M ds$$

Substituting in equation [3.9]

$$\frac{F_{i-1}}{K_i}-\left(\frac{1}{K_{i+1}}+\frac{1}{K_i}+\alpha_{(i)}S_{(i)}\right)F_i+\frac{F_{i+1}}{K_{i+1}}=-\int_{S(i)}\beta M ds \qquad [3.16]$$

which can also be written in a matrix form, with

$$B_{ii}=\frac{1}{K_{i+1}}+\frac{1}{K_i}+\alpha_{(i)}S_{(i)}$$

and $$A_{(i)}=-\int_{S(i)}\beta M ds. \qquad [3.17]$$

If panel (i) is divided into $N_{(i)}$ sub-panels, equation [3.17] can be replaced by a summation

$$A_{(i)}=-\sum_{j=1}^{N_{(i)}}B_{(ij)}M_{(ij)}S_{(ij)} \qquad [3.18]$$

where: $S_{(ij)}$ is the length of sub-panel "j" in panel "i".

$M_{(ij)}$ is the moment at the mid-point of sub-panel "j".

3.9.2. Inelastic Case:

As given in equation [3.11]

$$r = \frac{Q}{K} + d \qquad [3.11]$$

substituting in equation [3.6]

$$\frac{Q_{i+1}}{K_{i+1}} = \frac{Q_i}{K_i} + \int_{s(i)} (\varepsilon_b - \varepsilon_s) ds + (d_i - d_{i-1}) \qquad [3.19]$$

and going through the same procedure described earlier, equation [3.19] can be written in a matrix form

$$[B][F]=[A]+[D]$$

with [B], [F] and [A] as defined is equation [3.12], and "[D]" is a vector whose i^{th} term is $(d_i - d_{i-1})$.

Panel (i) could also be sub-divided into N(i) sub-panels, and then the integration could be replaced by a summation

$$A_{(i)} = \sum_{j=1}^{N_{(i)}} (\varepsilon_b - \varepsilon_s)_{(ij)} \Delta S_{ij} \qquad [3.20]$$

where $(\varepsilon_b - \varepsilon_s)_{(ij)}$ is the relative slip between the slab and the beam interface between the slab and the beam, at the mid-point of the sub-panel "j" within panel "i".

3.10. Calculation of Inertia and Area of the Steel Beam:

In order that the program locate the opening, the program was modified. The data file contains information about the location and size of the opening. When the program calculates the cross-sectional area of the beam, and its moment of inertia, a check is made to determine whether the distance from the support to the location at which the area and inertia are being calculated lies within the opening length. If the check proves the element to be located within the opening, the area of the web consumed by the opening is not considered in calculating the area and inertia of the beam. Using this approach, the area and moment of inertia of the steel beam that will be calculated will be the net steel area at the location of the opening.

3.11. Strain Distribution:

If the strain at the bottom of the steel beam, ε_{bb}, is known, as well as the curvature of the steel beam, ϕ_b, then strain at any point at a distance "Y" from the bottom of the steel beam can be known from

$$\varepsilon=\varepsilon_{bb}-\phi_b Y.$$

This equation is also valid for determining the strain at any point in the slab, if the strain at the bottom of the slab and the curvature, ε_{ss} and ϕ_s, are known.

Also, it is worth noting that ϕ_b and ϕ_s are not two independent variables, but are related by

$$\phi_b=\phi_s+\phi_{DL} \qquad [3.21]$$

and ϕ_{DL} is equal to zero if the beam is shored, and is equal to $\frac{M_{DL}}{E_b I_b}$ if the beam is unshored, where M_{DL} is the moment due to dead loads.

3.12. Computation of the Force and its Point of Application in the Slab from a Known Strain Distribution:

If "ε_{ss}" and "ϕ_s" are known, then the strain distribution throughout the depth of the slab can be determined. Knowing the strain distribution, and with the use of the stress-strain diagram of the concrete (fig.(3.3)), the stress distribution throughout the depth of the slab can also be determined.

The concrete is assumed to be cracked in the zone of tensile stresses. Thus, the depth of the uncracked section can be calculated by

$$H=\frac{\varepsilon_{ss}}{\phi_s}$$

If the value of "H" exceeds the thickness of the slab, then the whole cross-section of the slab is subjected to compressive stresses, and no cracking due to tension occurs in the slab.

$$\sigma_{ss}=E_s\varepsilon_{ss}$$

or $$\sigma_{ss}=\sigma_{sy} \quad \text{if } E_s\varepsilon_{ss}\geq\sigma_{sy}$$

and $\sigma_s'=E_s\varepsilon_s'$

or $\sigma_s'=\sigma_{sy}$ if $E_s\varepsilon_s'\geq\sigma_{sy}$

where "ε_s'" is the strain at the bottom fiber, and "σ_s'" is its corresponding stress.

Figure 3.8 shows an example for the strain and stress distributions in the slab.

$$\Delta\sigma=\sigma_{ss}-\sigma_s'$$

and "h" is taken to be the smallest of $\frac{\varepsilon_y-\varepsilon_s'}{\phi_s}$ or "H".

Now the stress distribution in the slab is known, and the forces in the slab can be calculated.

$$F_1=\sigma_{ss}HB$$

$$F_2=\tfrac{1}{2}(\sigma_{ss}-\sigma_s')hB$$

$$F=F_1-F_2 \qquad [3.22]$$

The point of application of the resultant "F" can be determined by calculating moments about the bottom of the slab.

$$\frac{F_1H}{2}-\frac{F_2H}{3}=F\overline{Y}$$

$$\overline{Y}=\frac{\frac{F_1H}{2}-\frac{F_2h}{3}}{F} \qquad [3.23]$$

and $M_s=F\left(\frac{H}{2}-\overline{Y}\right)$

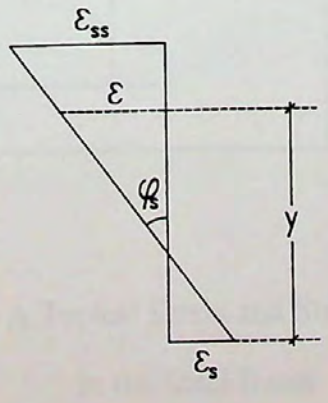

Figure 3.8- Strain Distribution in the Slab

3.13. Computation of the Force and its Point of Application in the Beam for a Known Strain Distribution:

The steel beam does not have a constant breadth throughout its depth, therefore the method used to determine the force in the slab cannot be applied to determining the force in the beam. The method of sub-division is used. Figure 3.9 shows the parameters used in the following equations.

$$F_i=\varepsilon_i A_i E_b$$

or $$F_i=\sigma_y A_i \qquad \text{if } \varepsilon_i \geq \varepsilon_y$$

$$F=\sum_{i=1}^{i=N} F_i \qquad [3.24]$$

Point of application of the force "F" is at a distance $\overline{Y}$,

where $$\overline{Y}=\frac{\sum F_i Y_i}{\sum F_i} \qquad [3.25]$$

and $$M_b = F\left(\overline{Y}-\frac{D}{2}\right)$$

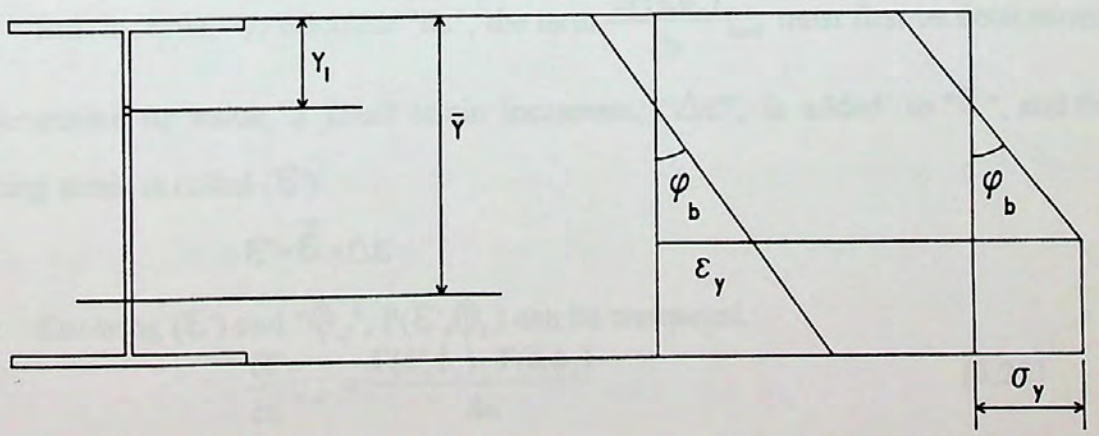

Figure 3.9- A Typical Strain and Stress Distribution in the Steel Beam

3.14. Computation of the Extreme Fiber Strain in the Slab for a Known Curvature and Force:

There is only one force for a given strain distribution as described earlier. The strain distribution is determined by "ϕ" and "ε", so it is only normal to say that $F=F(\phi,\varepsilon)$. "F" and "ϕ" are known, and so there is only one value of the extreme fiber strain to satisfy the above equation.

A trial-and-error approach will be used. "ϕ" will be fixed to its given value "ϕ_o", and values will be assumed for "ε" and the corresponding "F" computed, until the calculated value for "F" is satisfactorily close to its given value. A value should be assumed for "ε" and the corresponding value for "F" calculated, and these values will be referred to as "$\bar{\varepsilon}$" and "$\bar{F}$" in the first cycle.

Taylor's expansion formula will be used and only the linear term will be kept.

$$F(\varepsilon,\phi_o)=\bar{F}(\bar{\varepsilon},\phi_o)+\frac{\partial F(\varepsilon,\phi_o)}{\partial\varepsilon}\Big|_{\varepsilon=\bar{\varepsilon}}d\varepsilon \qquad [3.26]$$

$$\therefore \quad d\varepsilon=\frac{F(\varepsilon,\phi_o)-\bar{F}(\bar{\varepsilon},\phi_o)}{\partial F(\varepsilon,\phi_o)/\partial\varepsilon} \qquad [3.27]$$

For this equation to yield satisfactory results, $\bar{F}(\bar{\varepsilon},\phi_o)$ should be in the close neighborhood of $F(\varepsilon,\phi_o)$. When added to "$\bar{\varepsilon}$", "$d\varepsilon$" yields "ε". This way when "$d\varepsilon$" is determined, "ε" will consequently be known.

$$\varepsilon=\bar{\varepsilon}+d\varepsilon \qquad [3.28]$$

But in order to calculate "$d\varepsilon$", the term $\frac{\partial F(\varepsilon,\phi_o)}{\partial\varepsilon}\Big|_{\varepsilon=\bar{\varepsilon}}$ must first be determined. To determine its value, a small strain increment, "$\Delta\varepsilon$", is added to "$\bar{\varepsilon}$", and the resulting strain is called (ε').

$$\varepsilon'=\bar{\varepsilon}+\Delta\varepsilon$$

Knowing (ε') and "ϕ_o", $F(\varepsilon',\phi_o)$ can be computed.

$$\frac{\partial F}{\partial\varepsilon}\Big|_{\varepsilon=\bar{\varepsilon}}=\frac{F(\varepsilon',\phi_o)-F(\bar{\varepsilon},\phi_o)}{\Delta\varepsilon} \qquad [3.29]$$

Substituting in equation [3.27] into equation [3.28] yields;

$$\varepsilon=\bar{\varepsilon}+\frac{F(\varepsilon,\phi_o)-\bar{F}(\bar{\varepsilon},\phi_o)}{\partial F(\varepsilon,\phi_o)/\partial\varepsilon}$$

Having calculated $\frac{\partial F(\varepsilon,\phi_o)}{\partial \varepsilon}$ from equation [3.29], we can calculate ε from the following equation

$$\varepsilon = \bar{\varepsilon} + \frac{F(\varepsilon,\phi_o) - \bar{F}(\bar{\varepsilon},\phi_o)}{F(\varepsilon',\phi_o) - \bar{F}(\bar{\varepsilon},\phi_o)} \Delta\varepsilon \qquad [3.30]$$

Now "ε" is known, then "F" corresponding to "ε" and "ϕ_o" is calculated. If the calculated "F" is in the close neighborhood of the given "F", then "ε" is the required strain, and the computation is complete. If not, then the cycle is repeated, and the "F" computed from the last cycle, and the corresponding "ε", are used as "$\bar{F}$" and "$\bar{\varepsilon}$" for the following cycle. These steps are repeated until the required accuracy in "F" is achieved.

3.15. Computation of Strain Distribution for the Composite Beam for a Known Force and External Moment:

In order to determine the strain distribution, ε_s, ϕ_s, ε_b and ϕ_b must be known. ϕ_s and ϕ_b are related as shown in equation [3.21]. If ε_b and ϕ_b are known F_b can be determined as described in section 3.13. After knowing F_b, F_s can be determined from equation [3.2]. Knowing F_s and ϕ_s, we can calculate ε_s as described in section 3.14. This way, the independent variables are only ε_b and ϕ_b, and after determining their values all other variables can be derived. So we may write $F = F(\varepsilon_b, \phi_b)$, and $M = M(\varepsilon_b, \phi_b)$.

At the beginning two values for ε_b and ϕ_b are chosen and referred to as $\bar{\varepsilon}_b$ and $\bar{\phi}_b$, and the force and moment corresponding to this combination of strain and curvature are calculated following the procedure outlined in section 3.13, and are nominated $\bar{F}$ and $\bar{M}$.

Taylor's expansion formula for the two-dimensional case is used, and again only the linear terms are retained.

$$F(\varepsilon_b,\phi_b)=\bar{F}(\bar{\varepsilon}_b,\bar{\phi}_b)+\frac{\partial F}{\partial \varepsilon}\Big|_{\substack{\varepsilon_b=\bar{\varepsilon}_b\\ \phi_b=\bar{\phi}_b}} d\varepsilon_b+\frac{\partial F}{\partial \phi}\Big|_{\substack{\varepsilon_b=\bar{\varepsilon}_b\\ \phi_b=\bar{\phi}_b}} d\phi_b \qquad [3.31]$$

$$M(\varepsilon_b,\phi_b)=\bar{M}(\bar{\varepsilon}_b,\bar{\phi}_b)+\frac{\partial M}{\partial \varepsilon}\Big|_{\substack{\varepsilon_b=\bar{\varepsilon}_b\\ \phi_b=\bar{\phi}_b}} d\varepsilon_b+\frac{\partial M}{\partial \phi}\Big|_{\substack{\varepsilon_b=\bar{\varepsilon}_b\\ \phi_b=\bar{\phi}_b}} d\phi_b \qquad [3.32]$$

A small strain increment, $\Delta\varepsilon_b$, is then added to $\bar{\varepsilon}_b$ to obtain ($\varepsilon_b'=\bar{\varepsilon}_b+\Delta\varepsilon_b$) and the curvature is kept $\bar{\phi}_b$. The force $\bar{F}_b$ corresponding to ε_b' and $\bar{\phi}_b$ is calculated as described in section 3.13. From equation [3.21] the curvature in the slab is determined. From equation [3.2] the force in the slab is also determined. Since the force and the curvature of the slab are known, the extreme strain at the bottom of the concrete slab could be determined as described in section 3.14. Knowing the force in the slab, and its location, and the force in the beam and it's location, the moment of the composite beam can be determined.

Then a small increment $\Delta\phi_b$ is added to $\bar{\phi}_b$ to obtain $\phi_b' = \Delta\phi_b + \bar{\phi}_b$ keeping $\varepsilon_b=\bar{\varepsilon}_b$, and the force in the beam corresponding to ϕ_b' and $\bar{\varepsilon}_b$, $F(\bar{\varepsilon}_b,\phi_b')$, is computed, as well as the moment, $M(\bar{\varepsilon}_b,\phi_b')$, following the same steps described above. Then the following equations are used to determine the force and moment gradients:

$$\frac{\partial F}{\partial \varepsilon_b}\Big|_{\substack{\varepsilon_b=\bar{\varepsilon}_b\\ \phi_b=\bar{\phi}_b}} = \frac{F(\varepsilon_b',\bar{\phi}_b)-F(\bar{\varepsilon}_b,\bar{\phi}_b)}{\Delta\varepsilon_b}$$

$$\frac{\partial M}{\partial \varepsilon_b}\Big|_{\substack{\varepsilon_b=\bar{\varepsilon}_b\\ \phi_b=\bar{\phi}_b}} = \frac{M(\varepsilon_b',\bar{\phi}_b)-M(\bar{\varepsilon}_b,\bar{\phi}_b)}{\Delta\varepsilon_b}$$

$$\frac{\partial F}{\partial \phi_b}\Big|_{\substack{\varepsilon_b=\bar{\varepsilon}_b\\ \phi_b=\bar{\phi}_b}} = \frac{F(\bar{\varepsilon}_b,\phi_b')-F(\bar{\varepsilon}_b,\bar{\phi}_b)}{\Delta\phi_b}$$

$$\frac{\partial M}{\partial \phi_b}\Big|_{\substack{\varepsilon_b=\bar{\varepsilon}_b\\ \phi_b=\bar{\phi}_b}} = \frac{M(\bar{\varepsilon}_b,\phi_b')-M(\bar{\varepsilon}_b,\bar{\phi}_b)}{\Delta\phi_b}$$

Equations [3.33] and [3.34] can now be solved for $d\varepsilon_b$ and $d\phi_b$ as follows:

$$d\varepsilon_b = \frac{\frac{\partial F}{\partial \phi_b}(F(\varepsilon_b,\phi_b)-\bar{F}(\bar{\varepsilon}_b,\bar{\phi}_b))-\frac{\partial F}{\partial \phi_b}(M(\varepsilon_b,\phi_b)-\bar{M}(\bar{\varepsilon}_b,\bar{\phi}_b))}{(\frac{\partial F}{\partial \varepsilon_b})(\frac{\partial M}{\partial \phi_b})-(\frac{\partial F}{\partial \phi_b})(\frac{\partial M}{\partial \varepsilon_b})} \qquad [3.33]$$

$$d\phi_b = \frac{F-\bar{F}-\frac{\partial F}{\partial \varepsilon_b}\times d\varepsilon_b}{\frac{\partial F}{\partial \phi_b}} \qquad [3.34]$$

Now, and can be computed from the following equations

$$\varepsilon_b = \bar{\varepsilon}_b + d\varepsilon_b,$$

and $$\phi_b = \bar{\phi}_b + d\phi_b.$$

Now $F(\varepsilon_b,\phi_b)$ and $M(\varepsilon_b,\phi_b)$ corresponding to ε_b and ϕ_b can be calculated and compared to the given F and M. If they are in the close vicinity of the given values, then the computation is complete. If not, then the whole computation is repeated, taking the computed values for F and M as the assumed values for the next cycle. This procedure is repeated until the required accuracy is attained.

3.16. Computation of the Panel Force $F_{(i)}$ and the Connector Slip r_{i+1} from the Known Panel Force $F_{(i-1)}$ and Connector Slip r_i:

In order to avoid these difficulties, a method that does not require solving the simultaneous equations was developed by Ma[14]. The steps of this method are:

1. Since the slip of connector "i" is known, the load corresponding to this slip can be determined from the load-slip curve of the connector

   $$Q_i=Q_i(r_i).$$

2. The force in panel (i) can be computed from equation [3.3]

   $$F_{b(i)} - F_{b(i-1)} = Q_i \qquad [3.3]$$

3. If the panel is elastic, the slip in panel (i+1) can be determined from

   $$r_{i+1}=r_i+\alpha_i S_i F_i-\int_{s(i)}\beta M ds$$

and the integral can be replaced by a summation as follows

$$A_{(i)} = \sum_{j=1}^{N_{(i)}} B_{(ij)} M_{(ij)} S_{(ij)} \qquad [3.17]$$

If the panel is inelastic equation [3.7] could be used

$$r_{i+1} = r_i + \int_{S(i)} (\varepsilon_b - \varepsilon_s) ds \qquad [3.7]$$

the integral could be approximated by a summation as shown in equation [3.20]

$$A_{(i)} = \sum_{j=1}^{N_{(i)}} (\varepsilon_b - \varepsilon_s)_{(ij)} \Delta S_{ij} \qquad [3.20]$$

and by following the method described in section 3.15, the strains ε_b and ε_s can be determined, as the force and the moment in the panel and sub-panels are known.

3.17. Distribution of Vertical Shear:

The vertical shear stresses are assumed to be resisted by both the steel beam and the concrete slab. The model divides the vertical shear stresses between the beam and the slab according to "the shear factor", which is the shear resisted by the steel beam divided by the total shear to which the composite beam is subjected

The model calculates the value of the shear factor on the basis of ultimate shear capacities of the steel beam and the concrete slab. Clawson and Darwin[5] concluded that the ultimate shear capacity of the concrete slab, V_s, in N, is given by

$$V_s = 0.9 t_s^2 \sqrt{f_c'}, \qquad [3.35]$$

where: t_s is the thickness of the solid slab in mm,

f_c' is the strength of the concrete in MPa,

while the shear resisted by the steel beam, V_{beam}, according to von-Mises yield criterion, is given by

$$V_b = \frac{A_{wn} F_y}{\sqrt{3}}. \qquad [3.36]$$

Where: A_{wn} is the net area of the web

F_y is the yield stress of the steel

It is worth noting that when calculating the web area, the areas in common between the flanges and the web were neglected. According to the shear flow

diagrams, these areas make very little participation in resisting the shearing forces, and can therefore be neglected. This assumption leads to more conservative results, as the area considered is less than the actual area resisting shear, and thus the strength of the composite beam in resisting shear will be under-estimated by a relatively small degree. For the full beam

$$A_{wn} = (d - (2t_f))t_w \qquad [3.37]$$

Where t_f is the thickness of the flange, and d is the total depth of the steel beam. For parts of the beam where there is an opening, the net web area can be given by

$$A_{wn} = (d - h - (2t_f))t_w \qquad [3.38]$$

where: "h" is the opening height.

The amount of vertical shear resisted by the steel web is based on the net web area of the steel beam. Therefore, the shear factor at the location of the opening is not equal to the shear factor in parts where the beam is full.

The vertical shear resisted by the steel beam, V_b, is therefore equal to

$$V_b = V \times SHFAC \qquad [3.39]$$

where: V is the total vertical shear applied at the panel due to live load.

SHFAC is the shear factor at the panel.

The vertical shear resisted by the concrete slab, V_s, is equal to

$$V_s = V \times (1 - SHFAC) \qquad [3.40]$$

Where "V" and "SHFAC" are as defined in [3.39].

3.18. Check for Yielding:

The presented model follows the von Mises yield criterion. The panel should be declared plastic when the equivalent stress at any panel reaches a value greater than that of the yield of steel. Von Mises yield criterion states that

$$\sigma^2 = \sigma_n^2 + 3 \times \tau^2 \qquad [3.41]$$

Where σ is the equivalent stress due to the combined effect of normal and shear stresses,

σ_n is the normal stress, and

τ is the shear stress.

The normal stress at any element "n" in panel (i) was calculated by multiplying the strain at that element by the Young's Modulus of steel. As the shear stress was assumed to be divided equally among all elements of the steel web, the shear stress at any element was obtained by dividing the total shear force by the area of the steel web.

$$\tau = \frac{V_b}{A_{wn}} \qquad [3.42]$$

Where : τ is the shear stress.

V_b is the vertical shear resisted by the beam.

A_{wn} is the net area of the web.

Failure due to shear would occur if

$$\tau_{max} = \frac{F_y}{\sqrt{3}} \qquad [3.43]$$

Where σ_y is the yield strain of the steel.

The steps made to determine if yielding has occurred can be summarized in the following steps:

1. The strains at the top and bottom of the steel beam in each panel were calculated, as well as the shear. The strains at the top and bottom of the web were also calculated.
2. The strain of the top and bottom of the beam were then compared to the yield strains of the steel flange. If the strain was found to have exceeded the yield strain of the flange the panel was declared inelastic and treated accordingly.
3. The strain at which the yielding will occur in the steel web can be calculated as follows:

$$\sigma_{wy'} = \sqrt{\sigma^2_{wy} - 3\tau^2} \qquad [3.44]$$

and $\varepsilon_{wy'} = \sigma_{wy'}/E_s$

Where: $\sigma_{wy'}$ is the equivalent stress at which yielding will occur.

σ_{wy} is the nominal yield stress of the steel of the web.

τ is the shear stress in the panel as calculated in equation [3.42].

E_s is the Young's Modulus of the steel.

4. The calculated strain at the top and bottom of the steel web are then compared to the yield value obtained from equation [3.44]. If the value of the strain is found to exceed this value in any panel, this panel was declared inelastic and treated accordingly in the analysis.

3.19. Analysis:

3.19.1. Elastic Case:

The same steps used by Ma[14] in his program to analyze the beam in the elastic state were also used, with some alterations in the steel area calculation and the check for yielding, as described above. Also, his model did not consider vertical shear stresses, while the presented analysis accounted for it. These steps can be summarized in the following steps:

1. The moment and shear force are calculated at the mid-point of each panel or sub-panel.

   The shear stress at each panel is calculated from equation [3.42]:

$$\tau = \frac{V_b}{A_{wn}} \qquad [3.42]$$

   Where: τ is the shear stress in the panel.

   V_b is the vertical shear resisted by the steel beam.

   A_{wn} is the net area of the steel web, as calculated from either equation [3.37] or [3.38].

2. Reasonable values of "k" is assumed for each connector. The initial slope of the load-slip curves of the connectors can be assumed.
3. From the assumed values for "k", the corresponding values for "d" are determined form the load-slip curve of the connector.
4. All the terms in [B] can be determined from the relation $B_{ii}=\frac{1}{K_{i+1}}+\frac{1}{K_i}+\alpha_{(i)}S_{(i)}$.

5. All the terms in [D] can be determined from the relation $D_{(i)} = d_i - d_{i+1}$.
6. Since [B], [D] and [A] are known, the elements of [F] can be determined from equation [3.12].
7. Knowing the terms in [F], the load on each connector, Q, can be calculated from equation [3.3].
8. The slope of the load-slip curve corresponding to the load connector "Q" can now be determined, and compared to the assumed value of "k". If the calculated values of "k" are found to be different that the assumed values, the steps from 3-8 are repeated, taking the calculated values of "k" as the assumed values for the next cycle. These steps are repeated until the allowable error limit is achieved.
9. From one dimensional beam theory, the curvature at any panel in the beam can be calculated by

$$\phi = \frac{M - Z \times F}{\Sigma E \times I}$$

where: ϕ is the curvature of the composite beam at the panel.

M is the applied moment at the panel.

Z is the distance between the points of application of the forces in the slab and the beam.

F is the force due to interaction.

Σ EI is equal to $E_s I_s + E_b I_b$. E_s and I_s are the Young's Modulus and moment of inertia of the concrete slab respectively, and E_b and I_b are the same quantities for the steel beam.

For the shored beam, "M" is the total moment due to both dead and live loads, and in this case $\phi_b = \phi_s = \phi$.

In case of an unshored beam, "M" is the induced moment due to live loads alone. In this case $\phi_b = \phi_s + \phi$, and $\phi_s = \phi$.

For both the above cases, calculation of strains can be made as follows:

$$\varepsilon_b = \frac{F}{E_b \times A_b} - \phi_b \times C_b \qquad [3.13]$$

$$\varepsilon_{bb} = \varepsilon_b + \phi_b \times d_b$$

$$\varepsilon_s = -\frac{F}{E_s \times A_s} + \phi_s \times C_s \qquad [3.14]$$

$$\varepsilon_{ss} = \varepsilon_s - \phi_s \times D_s$$

$$\varepsilon_{wt} = \varepsilon_b + \phi_b \times t_f \qquad [3.45]$$

$$\varepsilon_{wb} = \varepsilon_b + \phi_b \times (d_b - t_f) \qquad [3.46]$$

Where: ε_s is the strain at the top of the concrete slab.

ε_{ss} is the strain at the bottom of the concrete slab.

C_s is the distance between the centroidal axes of the slab and the interface between the slab and the beam.

D_s is the depth of the concrete slab (including the depth of the cellular decking, if present).

ε_b is the strain at the top of the steel beam.

ε_{bb} is the strain at the bottom of the steel beam.

ε_{wt} and ε_{wb} are the strains at the top and bottom of the steel web respectively.

C_b is the distance between the centroidal axes of the steel beam and the interface between the beam and the slab.

10. Strains at the top and bottom of the web at mid-points of all panels and sub-panels are compared with the yield strain as calculated from equation [3.44], and the strains at the top and bottom of the steel beam are compared with the yield strain of the steel. If the strain at either the top or bottom of the web, or the top or bottom of the steel beam at any panel or sub-panel exceeds its respective yield strain, that panel is declared inelastic, and is analyzed accordingly.

3.19.2. Inelastic Case:

If the check for plasticity proved a panel to have reached its yield strain, this panel is declared plastic, and is analyzed by the method described below. The plastic analysis is not as simple as the elastic analysis, as super-position is not valid in the inelastic state.

According to Thiruvengadam's[23] program, if a panel is found to have yielded, then all the panels between that panel and the panel in the middle of the span must also be treated plastically. This is because the external moment increases as the distance from the support increases, and accordingly the normal stresses increase. In both Thiruvengadam's[23] and Ma's[14] programs, there was no decrease in the steel beam cross-sectional area along the length. Only if a bottom plate was used was there an increase in the area. This way the only factor causing any increase in normal stresses was the applied moment. Also, Thiruvengadam's[23] program did not consider stresses due to shear in the computation of stresses, and so any yielding due to shear in the panels near the support could not be detected. This approach might be accepted when there are no openings in the web of the steel beam, that would cause the panels in the vicinity of the opening to yield, while the panels between the opening and the mid-span of the beam are still well below the yield strain. Therefore, the sequence the program followed needed to be modified to be able to solve elastic panels located between two yielded panels.

After a panel is declared plastic and analyzed accordingly, a check is made to determine if the panel next to it has also yielded. If it is also found to have yielded it is also analyzed as a yielded panel. On the other hand, if the strains in the next panel are found to be lower than those that cause yielding, then this panel is analyzed as elastic.

The procedure can be summarized as follows:

1. The moment and shear at the mid-points of all panels and sub-panels are calculated.
2. Strains are calculated at the midpoints of all panels and sub-panels as described in 3.3.2.2. If any panels are found to have yielded, that panel is declared inelastic. Assume the number of the yielded panel is (m), where $1 \leq m \leq N$ (where "N" is the number of panels in half-span).
3. A new value for the end slip is assumed. Slip of all connectors i, of all panels (i) is calculated ($1 \leq i \leq m-1$) as described in the elastic case for the elastic panels, until the slip of connector m-1 is calculated.

4. Knowing the force in the panel (m-1), and the force on the connector m-1, the force in the panel (m), and the slip of connector m, can be calculated by using the method described in section 3.16, with the index "i" set to equal "m", solving (m) as a yielded panel.
5. If panel (m+1) is also found to be inelastic, it should be analyzed by the method described in section 3.16 for the inelastic case. If panel (m+1) is found to be elastic, then the method described in section 3.16 for the elastic case is used to calculate the force in the panel (m+1), and the connector m+1.
6. The procedure is repeated until the slip of the connector at the mid-span of the beam is calculated. If any other panel (p), where $m \leq p \leq N$, has also yielded, it is treated as an inelastic panel.
7. If the slip of the connector at the mid-span of the beam is acceptably close to zero, then the assumed end slip in step 1 is the correct end slip. If, however, the slip of the connector at the mid-span is not close enough to zero, a new value for end slip is assumed and the computation is repeated. This is repeated until the value of slip of the connector at the mid-span is acceptably close to zero.
8. The strains in all elastic panels and sub-panels is computed as described in step 9 of the elastic case.
9. The new values of strains for all elastic panels and subpanels is found to have exceeded its respective yield strain, this panel is declared inelastic, and the computation is repeated.
10. A check is then made to determine if the value of shear in any panel or sub-panel has exceeded the failure value according to the von Mises criterion, as given in equation [3.43]. If the value of shear stress is found to have reached that value, computation is terminated.

If there is no connector at the mid-span of the beam, then an imaginary connector is assumed to be located at the mid-span of the beam. Such a connector is called pseudo connector. Pseudo connectors are imaginary connectors that do not carry any loads, but are used to aid in the computation.

3.20. Methods Used to Find a Revised Value for End Slip:

The method of multiplication factors is the method generally used in the model. The Regula Falsi method is also used when the sign of the slip of the connector at the mid-span of the beam changes.

3.20.1. Method of Multiplication Factors:

The method of multiplication factors was adopted by Thiruvengadam[23] to find a revised value for the assumed end-slip. If the slip of the connector was found to be negative after a main cycle, this implies that the trial end slip was too small. If it was found to be positive, then the assumed end slip was too large. In order to assume a more accurate trial value for the end slip in the new main cycle, the assumed end slip of the previous cycle is multiplied by a multiplication factor. This multiplication factor is larger than 1.0 if the calculated slip of the connector at the middle of the span was negative, and less than 1.0 if otherwise. The difference between the value of the multiplication factor and 1.0 increases as the absolute value of the slip of the mid-span connector increases. An example for the elastic case is given below.

If	$r_m \leq .05$	then	$r^{(2)} = r^{(1)} \times 1.04$
If	$-0.5 < r_m \leq -0.001$	then	$r^{(2)} = r^{(1)} \times 1.02$
If	$-0.001 < r_m \leq 0$	then	$r^{(2)} = r^{(1)} \times 1.004$
If	$r_m \geq 0.05$	then	$r^{(2)} = r^{(1)} \times (2\text{-}1.04)$
If	$0.001 \leq r_m < 0.05$	then	$r^{(2)} = r^{(1)} \times (2\text{-}1.02)$
If	$0 \leq r_m < 0.001$	then	$r^{(2)} = r^{(1)} \times (2\text{-}1.004)$

where r_m is the slip of the mid-span connector, and $r^{(1)}$ is the assumed end slip for the cycle just computed, and $r^{(2)}$ is the assumed value for end slip for the next cycle.

Care should be taken when choosing the values of the multiplication factors. The multiplication factors should not differ greatly from unity, specially in the inelastic case. When the multiplication factors are chosen so that they only differ very slightly from unity, the solution is prolonged. On the other hand, if the values of the

multiplication factors is taken to be significantly different from unity, some computational difficulties might be encountered in the analysis. When the value of "r_m" changes sign, this means that the correct value for end slip is between the last two trial values. In the case, the Regula Falsi method gives quicker convergence than the bisection method in finding a better revised value for end-slip.

3.20.2. Regula Falsi Method:

This method is used when the computed values of the mid-span slip corresponding to two values of assumed end slip are of opposite signs. Let X_L be the value of end slip producing a negative mid-span slip, and X_R the value of end slip producing a positive mid-span slip , and let $f(X_L)$ and $f(X_R)$ be the values of mid-span slip corresponding to the assumed end slips X_L and X_R respectively.

The predicted value for end slip, X, for the next cycle can be obtained by

$$X = \frac{X_R f(X_L) - X_L f(X_R)}{f(X_L) - f(X_R)}$$

If this prediction still does not provide a mid-span slip satisfactorily close to zero, the procedure is repeated with "X" replacing either X_L or X_R, depending on whether the obtained mid-span slip was positive or negative; if the mid-span slip obtained from the new cycle is negative, X_L is replaced by "X", and X_R is unchanged, and if the mid-span slip obtained from the new cycle is positive X_R is replaced by "X", and X_L is unchanged.

3.21. The Computer Program:

A computer program coded in FORTRAN 77 was developed to perform the computation on the computer. The computer program consists of the main program and eight subroutines. The program follows an iterative process to analyze the composite beam. A flow chart showing the sequence of the program is presented in Appendix A, and a listing of the computer program is presented in Appendix B.

Input to the program is provided in the data file, which contains the geometric properties, as well as the material properties of the beam to be analyzed. The data file also contains the load increment, multiplication factors, and the acceptable accuracy. A sample data file is presented in Appendix C.

Output of the program is directed to an output file. The program analyzes the composite beam at each load increment, calculating the force and external moment in each panel, the vertical shear, the extreme fiber strains, the curvature of both the steel beam and the concrete slab, and the force on each connector. A typical output file consumes approximately 1 mega byte of hard-disk space. A typical execution of the program consumes almost 2 minutes on a 486, 33 MHz personal computer.

CHAPTER 4
RESULTS AND DISCUSSION

4.1. General:

The developed analytical model was used to analyze 35 series of composite beams of different dimensions, and with varying web opening sizes and locations. The strains at all loading stages were computed, and the failure loads of the beams were recorded, as well as the modes of failure. The moment and shear at the mid-length of the opening were also recorded in order to plot the interaction diagram of each individual beam.

To verify the validity of the proposed analytical model and the developed computer program, it was used to analyze five composite beams having the same dimensions and material properties as five experimentally-tested beams; two composite beams that were tested by Clawson et al[4], and three that were tested by Lawson et al[13].

A parametric study was carried out to investigate the impact of changing the key parameters on the performance of the composite beam. The parameters under investigation were the opening height, opening length, eccentricity of the opening with regard to the beam depth, and the number of connectors used in the shear span.

The variation of the extreme fiber strains with the applied moment was also studied at different locations in the opening, namely:

1. Just before the opening, at the low "M/V" end.
2. At the beginning of the opening, at the low "M/V" end.
3. At the middle of the opening.
4. Just before the end of the opening, at the high "M/V" end.
5. Just after the end of the opening, at the high "M/V" end.

The impact of varying some of the variables on the variation of the extreme fiber strain, at the specified sections, with the moment was also investigated. The

variables studied were the opening height, opening eccentricity, and the number of connectors in the shear span.

4.2. Verification of the Current Model:

In order to verify the validity of the presented model, comparison between the predictions of the model and the results of experimental tests on composite beams was performed. Five experimentally-tested beams were analyzed using the current model, and the results of the analysis were compared with the experimental results. The dimensions and material properties of the selected beams are given in tables 4.1 and 4.2. Beams B_1 and B_2 were identical to beams 5 and 6, respectively, presented in the literature by Clawson et al[4], and beams B_3, B_4 and B_5 were identical to test specimens 2N, 3N and 3S, respectively, presented in the literature by Lawson et al[13]. Beams B_1 and B_2 were manufactured according to Imperial units. However, the dimensions and properties of these beams were converted to the SI units for the purpose of presentation in the current investigation.

Table 4.1. Dimensions of experimental beams.

Beam Number	Designation	Opening			Concrete slab		
		Height (cm)	Length (cm)	Location* (cm)	Thickness (cm)	Rib Height (cm)	Width** (cm)
B_1	W 460×68	27.5	33.3	182.9	10.2	0	122
B_2	W 360×51	20.3	40.6	91.5	10.2	0	122
B_3	533×210×82 UB	35	35	267.5	6	6	200
B_4	533×210×82 UB	25	45	82.5	6	6	200
B_5	533×210×82 UB	20	60	90	6	6	200

* Distance from support to mid-length of opening

** Based on $16t_s+b_o$

Table 4.2. Material Properties of Experimental Beams

Beam	Concrete Strength	Steel Beam			
		Flange		Web	
	(MPa)	Yield (MPa)	ultimate (MPa)	Yield (MPa)	Ultimate (MPa)
B_1	32.3	289.1	462.6	272.3	439.5
B_2	27.7	273	459.6	301.9	462.7
B_3	30.9	317	486	349	501
B_4	34.4	309	481	341	495
B_5	34.4	309	481	341	495

In the experimental programs, beams B_1 and B_2 were subjected to an unsymmetric two-point loading system, while beams B_3 through B_5 were subjected to an eight-point loading system to simulate uniform loading. In the current analysis, beams B_1 and B_2 were subjected to a symmetric two-point loading system as the current model is only capable of solving symmetric beams with symmetric loading. On the other hand, beams B_3, B_4 and B_5 were subjected to uniform loading conditions in the analysis, since the model can analyze a beam subjected to uniform loading. The uniform loading condition caused the shear across the opening to be slightly varying, unlike the experimental test, in which the opening was subjected to constant shear. This caused the M/V ratio at the openings in the analysis to differ from those of the experimental tests.

The ratio of the vertical shear resisted by the slab to that resisted by the steel beam was studied by Lawson et al[13]. From their study, they concluded that this ratio varied from 10% at the elastic loading stage, to 20% at the ultimate loading stage. At elastic loading stages, the web of the steel beam resists most of the vertical shear stresses. As the normal stresses due to flexure increase, and yielding of the steel web occurs, the participation of the steel web in resisting the vertical shear stress decreases, and the slab resists up to 20% of the vertical shear stresses.

Clawson et al[5] had also developed a formula to determine the vertical shear resisted by the slab. They divided the shear between the steel beam and the concrete slab according to their relative shear resistance. By applying their formula to determine the amount of vertical shear resisted by the slab, it was found that the steel beam resisted 65-85% of the vertical shear due to live load in the five experimental beams at the location of the opening.

In the test results of the experimental program carried out by Lawson et al[13], the moment and shear at the low-moment end, rather than at the middle of the opening, were reported. The Vierendeel moment, defined[13] as the shear at the end of the opening multiplied by the opening length, was also reported. The results of the analysis carried out with the current model of the beams tested by Clawson et al[4] and Lawson et al [13] are summarized in tables 4.3 and 4.4 respectively.

4.2.1. Beam B_1:

Beam B_1 was identical to beam #5 presented in the literature by Clawson et al[4], which was a W 460×68 (W 18×46) steel beam supporting a 10.16 cm (4") -thick solid slab. The effective breadth of the slab was 1.22 m (48"). The span of the beam was 6.4 m (21'). The connectors used had 1.9 cm (¾") diameter and 7.5 cm (3.0") height. The number of connectors used was sufficient for complete interaction between the concrete slab and the steel beam. The opening, which was concentric with regard to the beam depth and of 27.5 cm (10 13/16") height and 54.9 cm (21 5/8 ") length, was located so that its mid-length was 182.9 cm (6') from the support. Strain-hardening of the steel beam was neglected in the model used in the verification. The beam in the model was subjected to the same type of loading as that of the experimental beam, which was a two-point load. However, due to limitation of the model, the loading had to be symmetric, so the two loads were applied equidistantly from the supports. The spacing of the connectors was the same as that of the experimental beam.

Table 4.3. Comparison Between Experimental Results and Model Predictions for Clawson's Beams[4].

Beam	Experimental		Model Predictions		$M_{exp}/M_{anal.}$	Failure Mode	
	M_u (LL) (kNm)	V_u (LL) (kN)	M_u (LL) (kNm)	V_u (LL) (kN)		Anal.	Exp.
B_1	381.9	209.2	339.3	185.6	1.13	Shear	Shear
B_2	160.5	175.3	136.7	150.9	1.17	Shear	Shear

Table 4.4. Comparison Between Experimental Results and Model Predictions for Lawson's Beams[13].

Beam	Experimental Results			Model Predictions			Hypothetical Vierendeel Moment (kNm)**	$M_{exp.}/M_{anal.}$	$V_{exp.}/V_{anal.}$	Model Factor**
	M_u* (kNm)	V_u* (kN)	Vierendeel Moment (kNm)	M_u* (kNm)	V_u* (kN)	Vierendeel Moment (kNm)				
B_3	652	174	61	623.3	166.2	53.7	58.2	1.05	1.05	1.05
B_4	242	400	180	229.4	358	151.7	161	1.06	1.12	1.12
B_5	242	400	240	230.1	358.3	200	215	1.05	1.12	1.12

* Values at the low-moment end of the opening.

** Analytical Vierendeel moment computed hypothetically for constant shear across the opening length (V×Opening length).

In the experimental test, the beam failed when the moment and shear due to live-load at the mid-length of the opening reached 381.9 kNm (3'380.0 in-Kip) and 209.15 kN (47.0 Kip), respectively. The model under-estimated the capacity of the beam, and predicted that the beam would fail at a total mid-opening moment and shear of 352.3 kNm (3'117.8 in-Kip) and 190.0 kN (42.7 Kip), respectively. The moment and shear due to live load alone at the mid-length of the opening were 339.3 kNm (3'002.4 in-Kip) and 185.6 kN (41.7 Kip), respectively. In this case, the model predicted the capacity of the beam with a model factor of 1.13.

The shear factor calculated by the model at the location of the opening and for the full beam were 81.2% and 92.3%, respectively. These values are in agreement with Lawson et al[13], as they had concluded that the slab, at the location of the opening, resists 20% of the total vertical shear at the ultimate loading stage.

The model predicted the beam to fail due to shear in the concrete above the opening. In the experimental program, the beam failed in shear.

4.2.2. Beam B_2:

Beam B_2 was identical to beam #6 presented in the literature by Clawson et al[4], which was a W 360×51 (W 14×34) steel beam supporting a 10.16 cm (4") -thick solid slab, and had a concentric opening of dimensions 20.3 cm×40.6 cm (8"×16"). The breadth and thickness of the slab were 1.22 m (48") and 10.16 cm (4") respectively. The span of beam B_2 was 4.57 m (15'). The spacing of the connectors was identical to that of the experimental beam. The center of the opening was at a distance of 91.4 cm (3') from the support. The number and strength of the connectors was sufficient for complete interaction to occur. The beneficial effects of strain-hardening were not considered in the analysis.

In the experimental test, the beam failed at a live-load moment and shear at the mid-point of the opening of 160.5 kNm (1'420.0 in-Kip) and 175.33 kN (39.4 Kip) respectively. The model predicted the beam to fail when the moment and shear at the middle of the opening were 141.8 kNm (1'255.5 in-Kip) and 155.3 kN (34.9 Kip)

respectively. The predicted moment and shear due to the live load were 136.7 kNm (1'209.5 in-Kip) and 150.9 kN (33.3 Kip), respectively. The model predicted the strength of the beam with a model factor of 1.17.

The model calculated the beam to resist 84.6% of the vertical shear due to live load in the solid parts of the beam, and 68.1% of the vertical shear at the region of the opening. A high percentage of the vertical shear was resisted by the concrete slab because a large area of the web was consumed in the opening.

The model predicted beam B_2 to fail in shear. This is in agreement with the results of the experimental program.

4.2.3. Beam B_3:

Beam B_3 was identical to test specimen 2N experimentally tested by Lawson et al[13], which was a 533×210×82 UB, with a concentric square opening in its web. The side of the square was equal to 350 mm. The mid-length of the opening was located 2.675 m from the support. The slab was ribbed, with a solid thickness of 6 cm, and ribs 6 cm high. The breadth of the concrete slab in the experimental test was 2.0 m. The effective width of the slab, based on $16t_s+b_o$, was 116.4 cm. Shear connectors used, which were headed studs of 10 cm height and 1.9 cm diameter, were placed every 30 cm. The used number of studs allowed for complete interaction to develop in the shear span.

In the experimental test the beam failed at a moment and shear of 652 kNm and 174 kN, respectively, at the low-moment end of the opening. The Vierendeel moment, the product of the shear at the low moment end of the opening multiplied by the opening length, was 61 kNm. The current model predicted the moment and shear capacities of the composite beam at the low-moment end to be 623.3 kNm and 166.2 kN respectively. Considering the Vierendeel moment to be the difference between the moments at the two ends of the opening, it was predicted to be 53.7 kNm. The steel beam was predicted to resist 84.1% of the shear due to live load in the vicinity of the opening, and 94.5% of the vertical shear due to live load in parts where

the beam is full. The model had under-estimated the moment and shear capacities of beam B_3 by 4.4% and 6.7%, respectively. The variation in the predicted M/M_{ult} and V/V_{ult} ratios is due to considering uniform distributed load in the analysis, unlike the experimental test, in which the shear across the opening was constant. The Vierendeel moment was under-estimated by 12%. The model factor for the Vierendeel moment, defined by Lawson et al[13] as the experimental Vierendeel moment divided by the predicted Vierendeel moment, for B_3 is 1.14.

Since the Vierendeel moment in the experimental results was defined as the shear at the low moment end multiplied by the opening length, the same definition was used to estimate the Vierendeel moment in the present analysis. Following this approach, the Vierendeel moment would be equal to the shear at the low-moment end of the opening multiplied by the opening length. The Vierendeel moment predicted by the model would be 58.2 kN. This value is 4.6% lower than the Vierendeel moment reported in the experimental program. The model factor in this case would be 1.05.

4.2.4. Beam B_4:

Beam B_4 was identical to test specimen 3N experimentally tested by Lawson et al[13], which was a 533×210×82 UB. Beam B_4 had the same dimensions and span of beam B_4, but the opening height and length were 250 mm and 450 mm, respectively. The mid-length of the opening was 825 mm from the support.

In the experimental test, the beam failed when the moment and shear at the low-moment end of the opening were 242 kNm and 400 kN, respectively. The Vierendeel moment was reported to be 180 kNm. The analytical model predicted that the beam would fail due to shear when the moment and shear at the low-moment end of the opening reach 229.4 kNm and 358 kN, respectively. Calculating the Vierendeel moment to be equal to the difference in moments between the two ends of the opening, it was predicted to be 151.7 kNm by the analytical model. The steel beam was predicted to resist 89.4% of the vertical shear due to live load in the vicinity of the opening, and 94.4% in parts where the beam was full. For beam B_4, the analytical

model had under-estimated the moment and shear capacities by 5.2% and 10.5%, respectively. The Vierendeel moment was under-estimated by 15.7%, and the Vierendeel moment factor was 1.19.

Following the same approach for defining the Vierendeel moment as explained in B_3, the Vierendeel moment would be equal to the shear at the low-moment end of the opening multiplied by the opening length. The Vierendeel moment predicted by the model would be 161 kN. This value is 10.5% lower than the Vierendeel moment reported in the experimental program. The model factor in this case would be 1.12.

4.2.5. Beam B_5:

Beam B_5 was identical to test specimen 3S in the experimental program conducted by Lawson et al[13], which was a 533×210×82 UB, but the height and length of the opening were 20 cm and 60 cm, respectively. The mid-point of the opening was located 90 cm from the support. The area of the opening was almost equal to the area of the opening in beam B_4.

In the experimental program, the beam failed when the moment and shear at the low moment end of the opening were 242 kNm and 400 kN respectively. The Vierendeel moment at the opening was 240 kNm. The analytical model predicted the beam to fail when the moment and shear at the low-moment end of the opening reach 230.1 kNm and 358.3 kN respectively. The Vierendeel moment, which is the difference between the moments at the two ends of the opening, was predicted by the analytical model to be 200 kNm. The model predicted the steel beam to resist 91.0% of the vertical shear due to live load in the vicinity of the opening, and 94.4% in regions where the beam was full. Thus, the analytical model under-estimated the moment and shear capacities of beam B6 by 4.9% and 10.4% respectively. The Vierendeel moment was also under-estimated by 16.7%. The Vierendeel model factor was 1.2.

Assuming that the opening is subjected to constant shear, the Vierendeel moment would be equal to the shear at the low moment end of the opening multiplied by the opening length, the Vierendeel moment predicted by the model would be

215 kN. This value is 10.4% lower than the Vierendeel moment reported in the experimental program. The Vierendeel model factor in this case would be 1.12.

4.3. Comparison Between the Current Model and Previous Analytical Models:

Clawson et al[5] and Fahmy[10] had both attempted to predict the ultimate strength of the beams tested by Clawson et al[4]. As discussed in section 2.4, their models were based on the ultimate strength analysis.

In both models presented by Clawson et al[5] and Fahmy[10], the areas in common between the flanges and the web were considered to be participating in resisting the shear forces, whereas this area was not considered to resist shear in the model presented in this thesis. This explains the difference in the shear capacity between the two models and the present analysis. For example, the top and bottom stub lengths for beam B_1 were 3.06"(7.77 cm) and 3.13"(7.95 cm) respectively , and the thickness of the top and bottom flanges were 0.623"(1.58 cm) and 0.615"(1.56 cm) respectively[4]. Thickness of the web is 0.38"(0.97 cm)[4]. This way, the area considered to be resisting shear would be increased by almost 20%.

Table 4.5 shows the comparison between the experimental results, the predictions of the current model and those of Clawson et al's[5] and Fahmy's[10] models. As can be seen from the table, the current model presented more accurate predictions than those of Clawson et al's model[5] for beam B_1, while the predictions of Clawson et al's model[5] were closer for beam B_2. Fahmy's predictions[10] were always higher than those of the current model. Both Clawson et al[5] and Fahmy[10] assumed complete interaction between the steel beam and the concrete slab, which explains their higher predictions for the capacity of the composite beam.

The modes of failure predicted by the model were more accurate than the predictions of the models of both Clawson et al[5] and Fahmy[10]. Clawson et al[5] had predicted mechanism failure for both B_1 and B_2, while Fahmy[10] predicted a four-

hinge-failure mechanism for beam B_1, and shear failure for beam B_2. The model predicted that both beams would fail due to shear.

The comparison made between the predictions of Clawson et al's model[5], Fahmy's model[10] and the model presented in this thesis, and the ratios between the predicted values and the experimental results are presented in table 4.6.

The predictions of the model were also compared with the predictions of the SCI design guide. Table 4.7 shows a comparison between the predictions of the current model, and those of the SCI design guide for the Vierendeel moments of beams B_3 through B_5.

The current model predictions were consistently lower than the experimental results, lower-bound solution, with the model factor varying from 1.05 to 1.17.

Table 4.5. Results of The Current Model, Clawson et al's[5], Fahmy's [10], and The Experimental Results [4].

Beam	Model			Clawson et al[5].			Fahmy[10]			Experimental [4] & [13]		
	M (kNm)	V (kN)	Predicted Failure	M (kNm)	V (kN)	Predicted Failure	M (kNm)	V (kN)	Predicted Failure	M (kNm)	V (kN)	Mode of Failure
B_1	352.3	190.02	Shear	339.5	182.9	Mechanism	402.6	216.72	Shear	399.0	214.05	Shear
B_2	141.9	155.31	Shear	154.5	167.32	Mechanism	153.6	166.88	4-Hinge	166.1	179.78	Shear

Values due to the effect of both dead and live loads.

Table 4.6. Comparison Between Predictions of The Current Model, Experimental Data, Fahmy[10]'s Model, and Those of Clawson et al[5].

Beam	$\frac{M_{Exp.}}{M_{Pred.}}$	$\frac{M_{Exp.}}{M_{Clawson}}$	$\frac{M_{Exp.}}{M_{Fahmy}}$
B_1	1.13	1.18	0.99
B_2	1.17	1.07	1.08

Values for the effect of both dead and live loads.

Table 4.7. Comparison Between Predictions of the Model and those of SCI Design Guide[13]

Beam	Experimental (kNm)	Model Predictions* (kNm)	SCI Predictions (kNm)	Model Factor for Model (kNm)	Model Factor for SCI (kNm)
B_3	61	58.2	59	1.05	1.04
B_4	180	161	122	1.12	1.48
B_5	240	215	174	1.12	1.4

* Calculated by assuming constant shear along the opening.

4.4. Interaction Diagram Plotted Using the Current Model:

The ultimate capacity of a composite beam with web opening depends on the location of the opening with regard to the beam span. For a composite beam with an opening of specific dimensions and location with regard to the beam depth, the location of the opening along the span controls both the ultimate capacity and the mode of failure of the beam at the opening.

The interaction diagram is a graphical representation showing the effect of varying the location of an opening of specific dimensions and eccentricity along the span of the beam on the ultimate capacity of the composite beam. The interaction diagram represents a safety envelope for the stress resultants at the opening. The

location of the opening is best expressed in terms of "M/V" at the center of the opening, which is the moment at the middle of the opening, divided by the shear at the same location. Knowing the location of a specific opening, hence the M/V at the opening, the ultimate capacity of the composite beam, as well as its mode of failure, can be determined graphically with the aid of the interaction diagram.

In order to plot the interaction diagram, the ultimate capacity of the composite beam for all locations of the opening along the beam span should be determined. Therefore, analysis of the composite beam for various locations covering the whole span of the beam should be made in order to plot the interaction diagram using the proposed model. A typical interaction diagram is presented in figure 4.1.

The interaction diagram shown in figure 4.1 is plotted for a W 310×38 steel beam of 6.4 m span, supporting a ribbed slab of 10 cm solid thickness. The concrete was cast on steel metal decking, and the height of the ribs was 2.5 cm. The beam was uniformly-loaded to failure. The web of the steel beam had a concentric opening of 45 cm length and 18.2 cm height. Stud were used as shear connectors, and were equally-spaced along the length of the beam, and placed at 15 cm intervals. The number of connectors used was sufficient for complete interaction between the steel beam and the concrete slab. The yield stress for the steel was 300.9 MPa, and the compressive strength of the concrete was 20.5 MPa. The Young's Modulus of the used steel was 200'000.0 MPa.

The axes of the interaction diagram are normalized by dividing the moment and shear at failure by the ultimate moment and shear capacities of the full beam, M_{ult} and V_{ult}. M_{ult} and V_{ult}, could be calculated for the composite beam, as shown in Appendix D, or the steel beam alone. The stress block method was used to calculate the ultimate moment capacity of the composite beam. The ultimate shear capacity was calculated for both the steel beam and the concrete slab, or the steel beam only. Von-Mises yield criterion was used to determine the ultimate shear capacity of the steel.

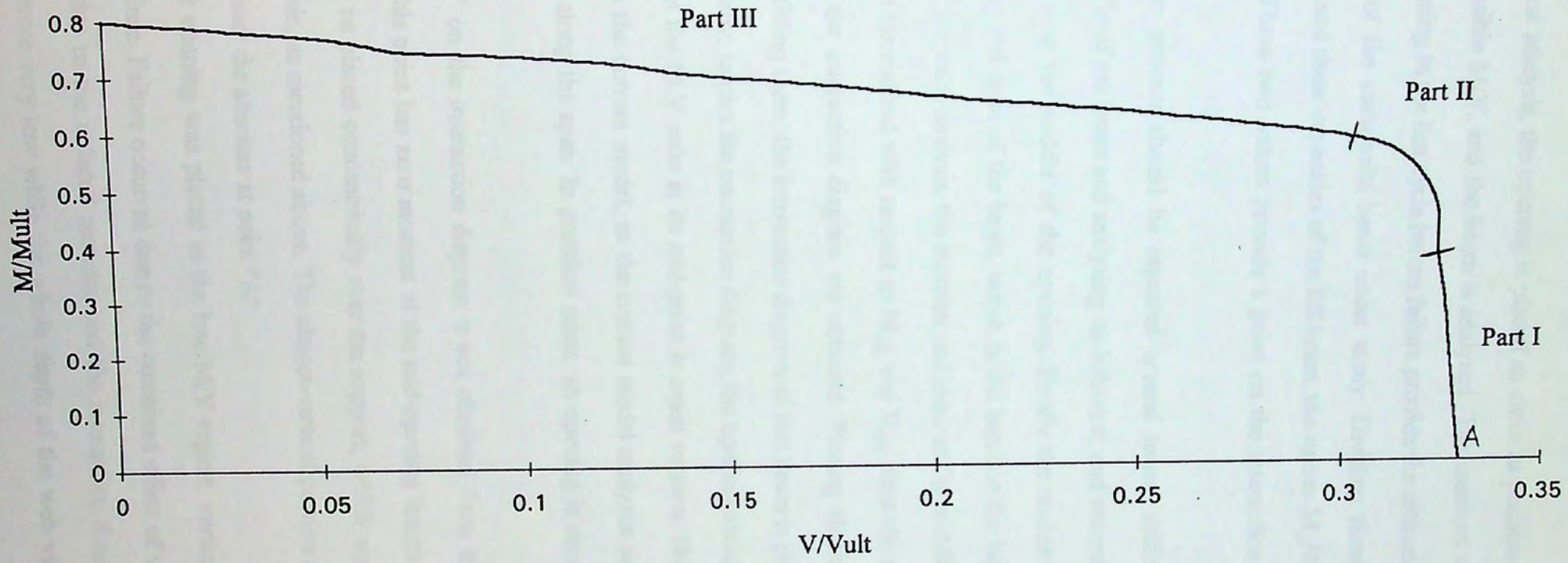

Figure 4.1- Interaction Diagram of Beam B8

For the first analysis, the opening is placed as close as possible to the support, in the lowest possible M/V, and the beam is analyzed. The moment and shear at the middle of the opening in the last cycle before failure provide the ultimate moment and shear capacities of the composite beam under study. Dividing these values by the ultimate moment and shear capacities of the full beam, the values M_1/M_{ult} and V_1/V_{ult} are determined. These two values provide a point on the interaction diagram of the beam.

The above process should be repeated several times, shifting the opening towards the middle of the beam and analyzing its behavior, and recording the ultimate moment and shear at the middle of the opening. Finally the middle of the opening coincides with the mid-span of the beam, which is the location for highest M/V ratio (∞ for V = zero). For each analysis, the moment and shear at the middle of the opening (M_i and V_i) were normalized with respect to M_{ult} and V_{ult}, thus the remaining points required to plot the interaction diagram are obtained. Placing all the points on the graph and curve-fitting them, the interaction diagram of that beam is plotted.

Theoretically, to plot the interaction diagram, the opening should be placed at a location such that the M/V ratio at its mid-point is equal to zero. However, this was not possible with the current model, as the current model analyzes single-span beams with an opening along the span. In practical cases, an opening is rarely required over the support.

Point "A" on the interaction diagram is not obtained from the output of the program. Since this point has zero moment at the mid-opening length, this means that the opening is to be placed concentrically over the support, which was not possible in the present analysis, as mentioned above. The almost-vertical portion of the curve was extended to intersect the abscissa at point "A".

When the opening was placed in the low M/V region, vertical shear was the main cause of failure. Failure occurred due to the combined effect of vertical shear and normal stresses due to the induced moment and the interaction force. However, the normal stresses were very low while the whole depth of the web yielded due to the

vertical shear. Since yielding of the model follows the von-Mises yield criterion and a beam with a M/V ratio equal to zero could not be analyzed by the model, the case of an opening subjected to pure vertical shear conditions was not analyzed by the current model. Thus, the steel beam could never achieve its full shear strength at the location of the opening, as the vertical shear would always be accompanied by some normal forces due to the induced moment. According to the model, the composite beam fails due to shear at the location of the opening only when both the steel beam and the concrete slab achieve their ultimate shear strengths.

When failure is governed by shear, and the steel web yields mainly due to shear, while the normal stress in the flange is well below its yield stress, the failure is termed as shear-governed failure. The full depth of the web in the region of the opening yields in shear, while the normal stresses could still be well below the yield stress. The flange of the steel beam, which is not considered to be resisting any vertical shear stresses in the current analysis, could be subjected to tensile stresses well below its yield stress in the same panel in which the web has yielded due to shear.

For openings placed in a constant shear zone (single and two-point loads) of the span, and for comparatively short openings, the difference between the equivalent stresses in the web at both ends of the opening is not very high. In such cases, the four hinge failure mechanism, shown in figure 4.2, is the prevailing failure mode for low M/V locations for the opening. The current analysis accounts for the own weight of

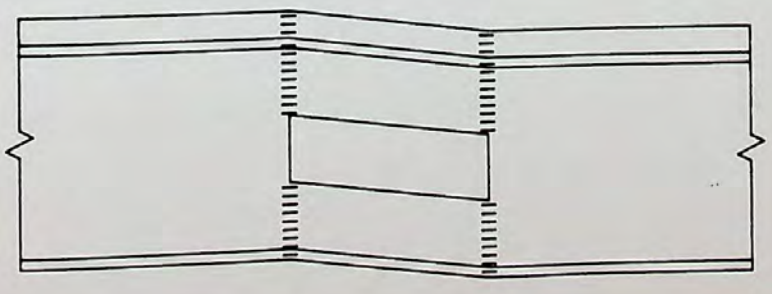

Figure 4.2- Four-Hinge Failure Mechanism

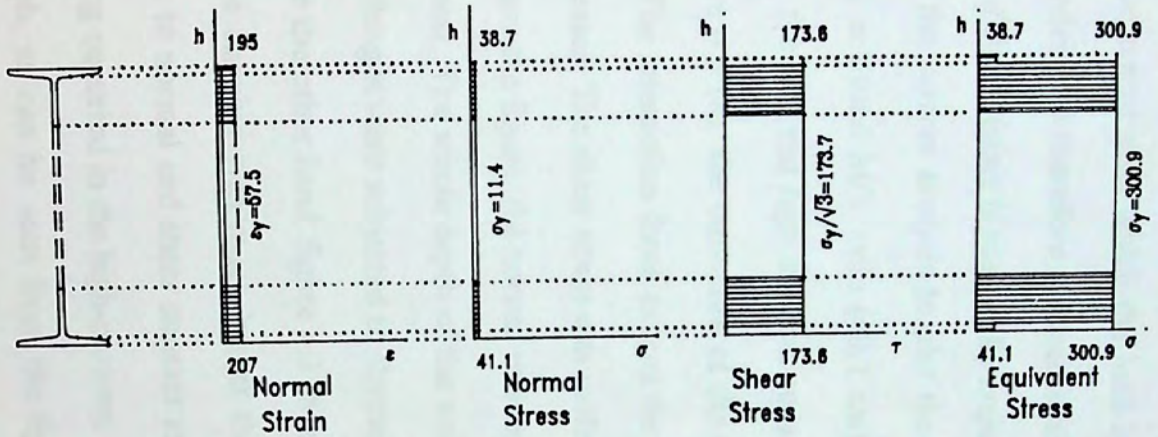

(a)–At Low–Moment End

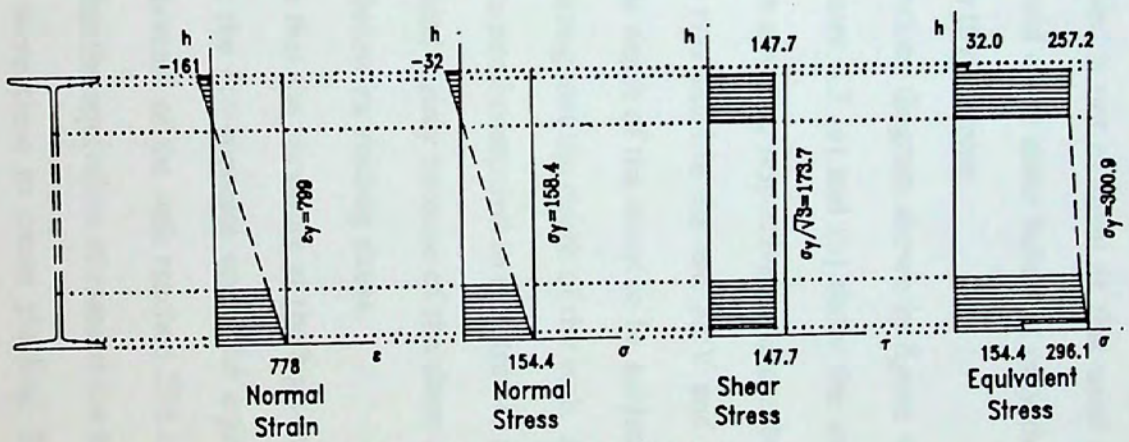

(b)– At High–Moment End

Figure 4.3- Strain and Stress Distributions at M/V=0.4 m
(Stresses in MPa)

the composite beam, and thus there always is a difference between the shear values at both ends of the opening, which causes the low M/V end to fail in shear before the high M/V end has reached its ultimate capacity. Due to the fact that very small loading increments could be used in the current analysis, once failure occurs at the low-moment end of the opening, the program terminates. In experimental tests, however, the load increment with which the load is applied is not as small as that used in the current model, and therefore the load which could cause shear failure at only the low M/V end of the opening is practically impossible to determine.

In the current analysis to plot the interaction diagram shown in figure 4.1, at the lowest analyzed M/V ratio (40.7 cm). Figures 4.3 (a) and (b) show the state of stresses at the low and high moment ends of the opening, respectively. As can be seen from figure 4.3 (a), the curvature of the beam was small in the low M/V end of the opening. The interaction force caused the whole depth of the beam to be subjected to tensile stresses. The shear stress was uniform throughout the depth of the web. As can be seen from the figure, the normal stresses were small compared to the stresses due to vertical shear. The whole depth of the web yielded mainly because of the shear stress, while the flanges were subjected to stresses far below its yielding stress.

On the other hand, figure 4.3 (b) shows that the curvature at the high-moment end of the opening was much higher than at the low-moment end. The equivalent stress due to normal and shear stresses at the bottom of the web reached 296.1 MPa. No yielding occurred in the high-moment end, but the equivalent stresses at the bottom of the web, as can be seen from the figure, were close to cause yielding. Normal stresses were much higher than at the low-moment end due to the higher moment. However, normal stresses were still below yielding in the flange.

The vertical shear stress and normal stress at failure at the low moment end were 173.6 MPa and 41.0 MPa, respectively, at the bottom of the web. At the high-moment end, the vertical shear stress and normal stress were 147.7 MPa and 149.0 MPa, respectively, at the bottom of the steel web. Applying the von-Mises criterion, the whole depth of the web at the low-moment end was found to have

yielded, while the equivalent stress at the bottom of the web at the high-moment end was 296.1 MPa. Therefore, the beam failed at the low-moment end of the opening, and the stresses due to vertical shear were the main cause for failure. It can be seen from these values that the high-moment end of the opening was very close to yielding. Therefore, if a larger load increment had been used, failure would have occurred at both ends of the opening, resulting in a four-hinge mechanism.

The extreme fiber strains due to the normal stresses at the low-moment end of the opening were 195.25 micro strain and 207.13 micro strain at the top and bottom of the steel beam, respectively. At the high-moment end, the extreme fiber strains due to the normal stresses were −161.2 micro strain and 778.5 micro strain at the top and bottom of the steel beam, respectively. As can be seen, these values are well below the yield strain values (1'517.0 micro strain). However, when the von-Mises yield criterion was applied, the whole depth of the steel web was found to have yielded.

The ultimate shear capacity of this beam was only around 33% of the theoretical shear capacity of the full beam. This reduction in shear capacity was caused by a 62.5% reduction in the web area and the existence of the normal stress in the web. The region where the almost-vertical shear is the main cause for failure constitutes the almost-vertical portion of the interaction curve. The mode of failure in this region of the curve is equivalent to the mode of failure that Todd et al[24] referred to as shear or four-hinge failure mechanism.

As the opening approached the point of maximum moment, the moment increased and the shear force decreased at both ends of the opening, as well as at the middle of the opening. Failure was no longer due to shear at the low M/V end of the opening. The increase in moment at the high and low moment ends of the opening, and the decrease in shear force caused the beam to fail at a shear stress less than its maximum shear capacity, and a moment also well below the ultimate moment capacity of the full beam. When the M/V ratio at the opening was 1.21 m, the maximum shear force calculated at the low M/V end of the opening was 11.48 kN, and the shear stress was 167.8 MPa. The strain at the bottom of the web at the low M/V end due to normal

stresses resulting from both the external moment and the interaction force was 1'153.0 micro strain, which is less than the yield strain of steel, which was 1'517.0 micro strain. When the von-Mises yield criterion was applied the strain in the bottom of the web exceeded the yield strain at the low-moment end of the opening. On the other hand, the strain at the bottom of the steel beam at the high M/V end of the beam also exceeded the yield strain. Stress at the web and flanges above and below the opening did not constitute plastic hinges at these two locations.

The strain at the bottom of the steel beam due to normal stresses at the point of maximum moment (mid-span of the beam) was 6'279.0 micro strain. As the beam was uniformly-loaded the shear at the middle of the beam was equal to zero. The strain distribution at this location indicates the formation of plastic hinges at the mid-span of the beam. For this location of the opening, the beam failed due to the excessive yielding of the steel beam at the mid-span, and failure did not occur at the location of the opening.

It is worth noting here that the interaction diagram presented in figure 4.1 is plotted for beam B_8, which was one of the beams used to carry out the parametric study. As can be seen in figure 4.8, at this location the interaction curves of the full beam and that of B_8 coincided, which indicates that the capacity of the full beam was equal to that of B_8 when a concentric opening of this size was introduced at this location.

As the opening was brought closer to the middle of the beam, the increase in external moment affected the strain at the high moment end of the opening, and caused the formation of plastic hinges at both ends of the opening. A plastic hinge can be detected as the strains at the bottom of the steel beam become very high when compared to the strains in the panels before and after it. When the opening was shifted closer to the point of maximum moment, at the location when the M/V at the middle of the opening was 1.5 m, the strain at the bottom of the steel beam in the high M/V end due to normal stresses reached 17'455.0 micro strain. The shear stress at the high-moment end of the opening was 120.1 MPa. Compared with the yield strain of the

steel beam, which was 1'517.0 micro strain, it can be seen that the strains at the bottom of the beam had greatly exceeded the yield strain.

The strain and stress distributions at the low and high moment ends of the opening are presented in figure 4.4 (a) and (b). As can be seen from figure 4.4 (a), the whole depth of the bottom tee at the low-moment end had yielded, and the stresses in the top tee had also caused the equivalent stress to approach the yield stress. From figure 4.4 (b) it can be seen that the bottom tee had also yielded, and that the strains were very high compared to the yield strain.

On the other hand, the shear stress in the web at the low-moment end was 150.0 MPa, while the strain due to normal stresses at the bottom of the web was 1'189.0 micro strain. The combined effect of these stresses, according to the von-Mises yield criterion, caused yielding in the panel. This equivalent stress results in the formation of a plastic hinge at the bottom of the web in the low-moment end of the opening. When another loading increment was added, the strains became excessively large, and the model could not analyze the beam. Practically, the whole depth of the beam at both the high and low moment ends of the opening yielded, forming four plastic hinges. This mode of failure is also termed "four-hinge failure mechanism".

As the opening approached the middle of the span of the beam, the mode of failure changed. Figures 4.5 (a) and (b) show the states of strains and stresses at the low and high moment ends when the M/V ratio at the middle of the opening was 4.68 m. From figure 4.5 (a), it can be seen that the bottom tee had fully-yielded, while the stresses in the top tee were well below the yield stress. The stresses due to vertical shear were low, and yielding of the bottom tee was mainly because of the normal stresses. On the other hand, figure 4.5 (b) shows that the whole depth of the bottom tee at the high-moment end, as well as a large portion of the top tee, had yielded because of the normal force. The effect of shear was negligible, as can be seen when comparing the diagrams showing the normal and equivalent stresses. In this case,

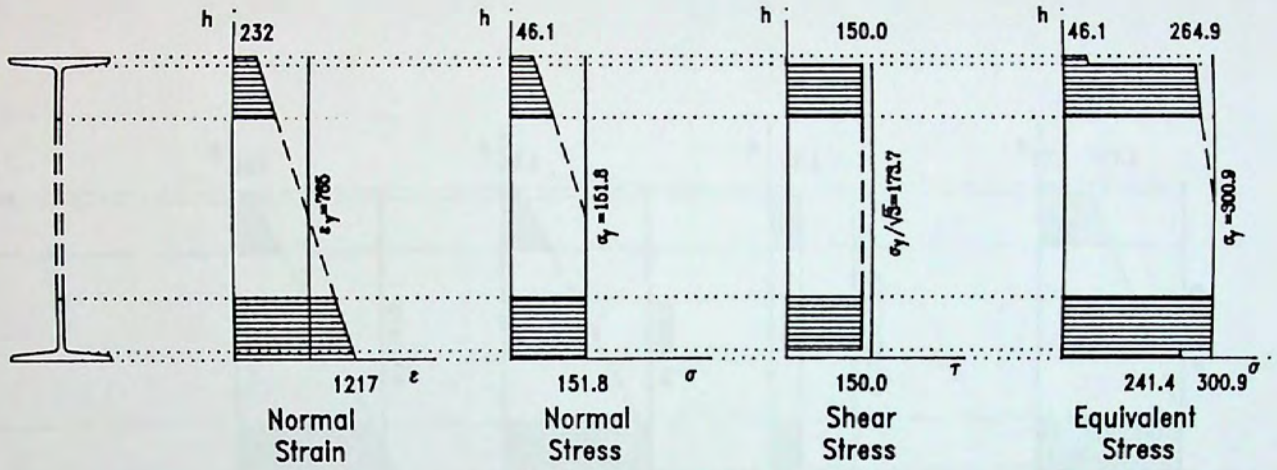

(a)- At Low-Moment End

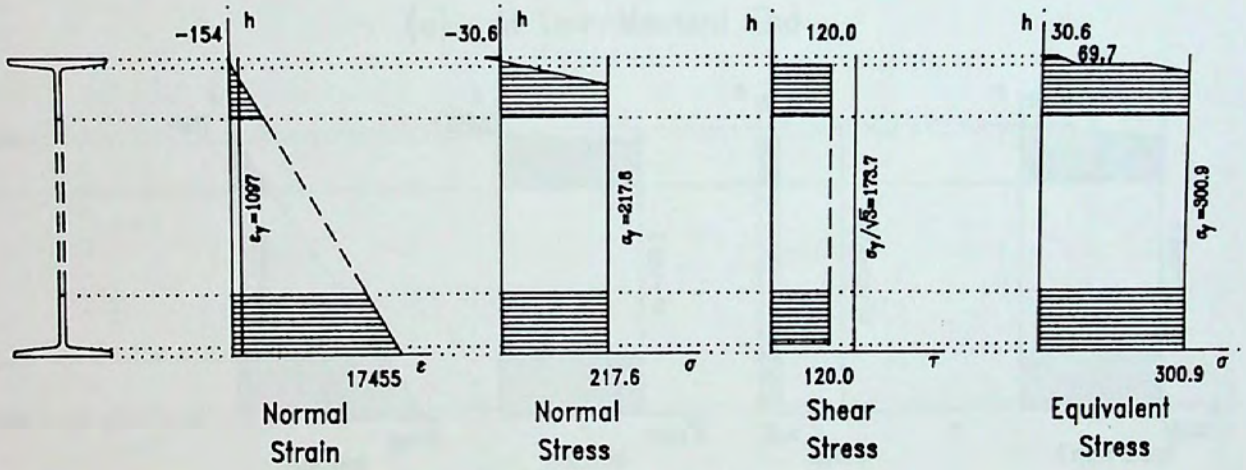

(b)- At High-Moment End

Figure 4.4- Strain and Stress Distributions at M/V=1.5 m
(Stresses in MPa)

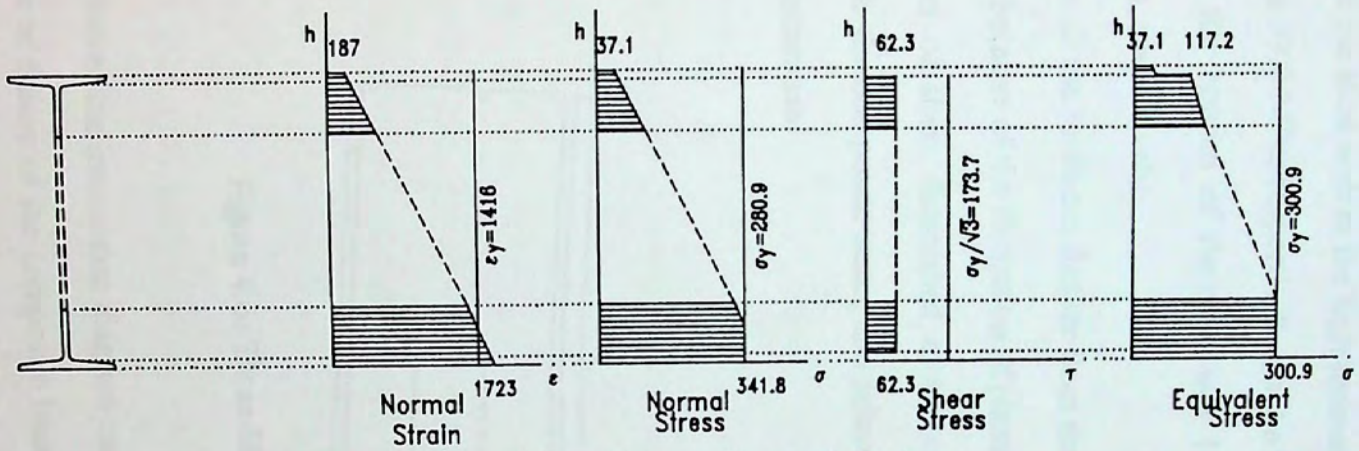

(a)- At Low-Moment End

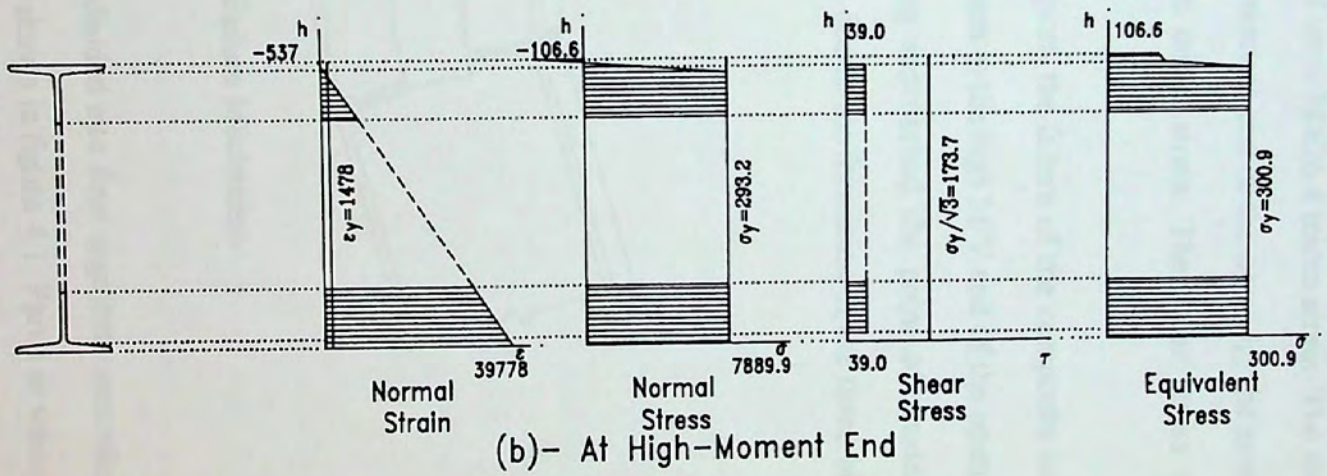

(b)- At High-Moment End

Figure 4.5- Strain and Stress Distributions at M/V= 4.7 m
(Stresses in MPa)

failure was due to a three-hinge mechanism, due to the formation of plastic hinges at both ends of the bottom tee, and at the high-moment end of the top tee. This mode of failure is presented in figure 4.6.

The strain at the bottom of the steel beam at the high-moment end of the opening reached 39'783.4 micro strain. The strain due to the normal forces at the bottom of the steel web at the high-moment end were 38'626.4 micro strain. The shear stress was 39.0 MPa, respectively. At the low-moment end of the opening, the normal strain at the bottom of the web was 1'679.6 micro strain. The shear stress was 62.3 MPa, respectively.

In all the locations further from the support, the failure of the composite beam was also because of the formation of plastic hinges at the high M/V end of the opening. The effect of shear diminished as the opening approached the point of maximum moment in the composite beam, and failure was due to the formation of the three-hinge failure mechanism.

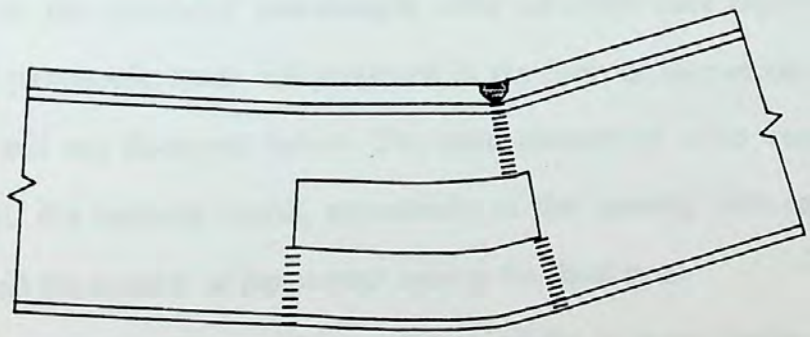

Figure 4.6- Three-Hinge Failure Mechanism

Hence, the interaction diagram can be divided into four segments according to the mode of failure of the composite beam, as shown in figure 4.1. Part I is where the opening is subjected to low moment and high shear. Vertical shear at the low-moment end is mainly responsible for failure of the beam in this part, as the normal stresses are negligible. In part II, failure is in the mid-span of the beam, and not in the vicinity of the opening. In part III, the M/V ratio is high, and failure is due to the formation of

four plastic hinges at both ends of the opening. At the high-moment end plastic hinges are formed due to the high normal forces, while the shear contributes effectively in forming the plastic hinges at the low-moment end of the opening. In Part IV, the M/V ratio is higher than in part III. The effect of shear is less pronounced on the behavior of the composite beam at the opening. This causes the beam to fail due to the formation of three plastic hinges; two at both ends of the bottom tee, and the third in the top tee at the high-moment end. These hinges are mainly caused by the high normal stresses in the beam, as the effect of vertical shear is not pronounced.

4.5. Parametric Study:

Having verified the validity of the finite difference model, it was used to conduct a parametric study to investigate the effect of varying the main parameters on the behavior and capacity of composite beams at the opening, and consequently constructing their interaction diagrams.

In order to study the impact of each parameter on the behavior of the composite beam, this parameter was changed while the others were kept constant. The results of this parametric study are presented in the form of interaction diagrams of these beams, and are discussed below. The main parameters under study were the opening height, the opening length, eccentricity of the opening with respect to the beam depth, and the number of connectors used in the shear span.

The dimensions and material properties of all the analyzed beams were similar in all regards, except for the dimensions and location of the openings. All steel beams used were W 310×28, supporting a ribbed slab of 10 cm solid thickness, and the height of the ribs was 2.5 cm. The yield stress of the used steel was 300.9 MPa. The effective width of the slab was 172.7 cm.

In order to be able to compare between the behavior of a composite beam with a web opening, and that of a full beam, the interaction diagram of a full beam was plotted. The moment and shear at all panels at failure were recorded. Dividing these values by the ultimate moment and shear capacities of the beam, points on the

interaction diagram of the full beam were obtained. Connecting these points, the interaction diagram of the full beam was plotted.

4.5.1. Effect of Varying Opening Height:

The proposed model was used to plot the interaction diagrams of eight composite beams, which were similar in all aspects except the opening heights. These beams were composed of a steel beam W 310×28. All the openings in this study were concentric with respect to the beam depth. The slabs of beams B_6 through B_{13} were 10.0 cm thick, and ribbed perpendicular to the longitudinal direction of the steel beam. The height of the ribs was 2.5 cm. All these beams were over-connected in order to avoid failure of the connectors. The spacing of the connectors was constant along the length of the beam. The beams were subjected to uniform loading. Strain-hardening of the steel beam was not considered. The characteristics of the eight beams and their opening sizes are presented in table 4.8.

Table 4.8. Characteristics of Beams to Study the Effect of Varying Opening Height.

Beam	Designation	Web Height (cm)	Opening Height (cm)	Opening Length (cm)	% Reduction in Web Area
B_6	W 310×28	29.1	13.1	45.7	45
B_7	W 310×28	29.1	15.7	45.7	53.8
B_8	W 310×28	29.1	18.2	45.7	62.5
B_9	W 310×28	29.1	20.7	45.7	71.2
B_{10}	W 310×28	29.1	22.8	45.7	78.2
B_{11}	W 310×28	29.1	23.3	45.7	79.9
B_{12}	W 310×28	29.1	23.8	45.7	81.7
B_{13}	W 310×28	29.1	25.8	45.7	88.7

By varying the opening height it is found that the capacities of the beams varies, as shown in figure 4.7.

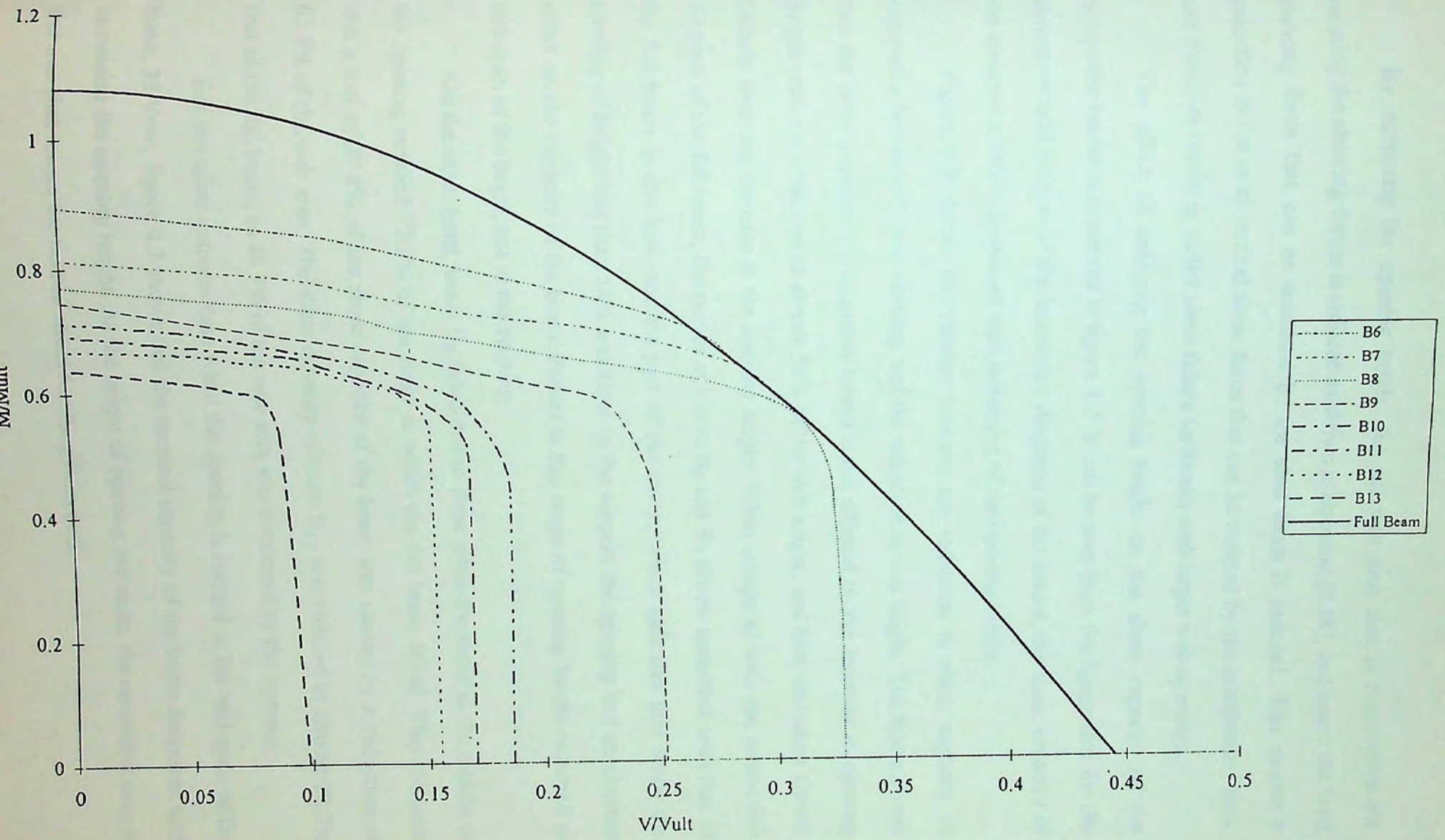

Figure 4.7- Effect of Varying Opening Height

By increasing the opening height, the net web area that is responsible for resisting the shearing forces is reduced as shown in equation [3.38], and hence the total shearing force that can be sustained by the steel beam is reduced. This causes a reduction in the total vertical shear force that can be resisted by the composite beam, and therefore results in earlier shear failure for beams with larger web openings.

The effect of changing the opening height on the shear capacity of the composite beams is presented in figure 4.7. It can be seen from the figure that for the almost-vertical portion of the interaction diagrams of the beams, the shear capacity of the composite beams decreased with increasing of the opening height.

Figure 4.8 shows the relation between the reduction in shear capacity of composite beams with web opening, and the reduction in web height. The figure shows that the shear capacity of composite beams is not affected by the increase in opening height until a a reduction of almost 54% of the web height, and then decreases almost linearly with any increase in the opening height. When compared with the interaction diagram of the full beam, the curves of beams B_6 and B_7 almost coincided with that of the full beam in the low moment part of the curve, which indicates that when the opening of height less than 54% was close to the support the opening had no obvious effect on the capacity of the beam. Failure in this range of opening height occurred at mid-span of the beam, not at the opening.

On the other hand, beam B_8 failed due to shear when the shear at the middle of the opening reached 72.2% of the shear at which the full beam failed. This indicates that a loss of 27.8% of the shear capacity of the beam was caused by a reduction of 62.5% of the web area. The shear capacity of beam B_{13} was reduced to almost 22.2% that of the full beam, as 88.7% of the web area was consumed by the opening.

For the other extreme case when the opening is located at the mid-span of the beam, $M/V=\infty$, figure 4.7 shows that the moment capacity of the beam decreases with increasing the opening height. As the height of opening increases, the remaining area of the web that resists the normal stress resulting from both:

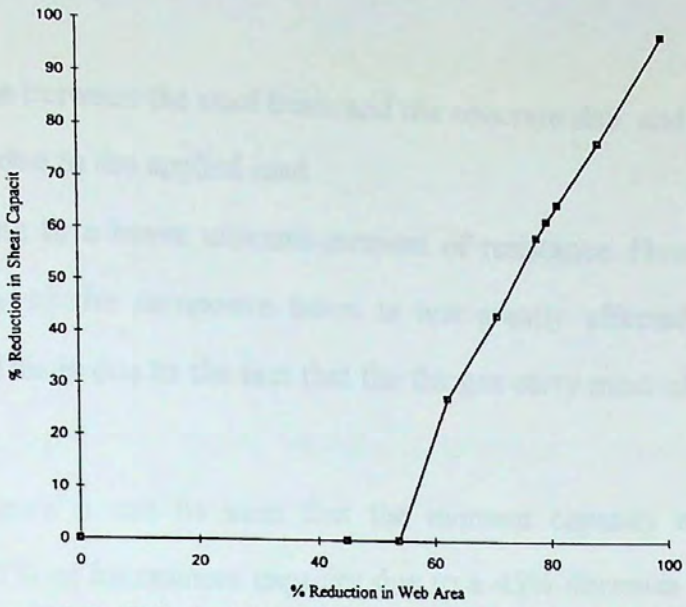

Figure 4.8- Effect of Reduction of Web Area on Shear Capacity of Composite Beams (M/V=0)

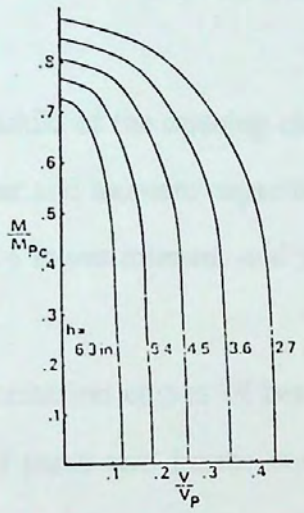

Figure 4.9- Interaction Diagrams for Beams with Various Opening Heights as Predicted by Todd et al(24)

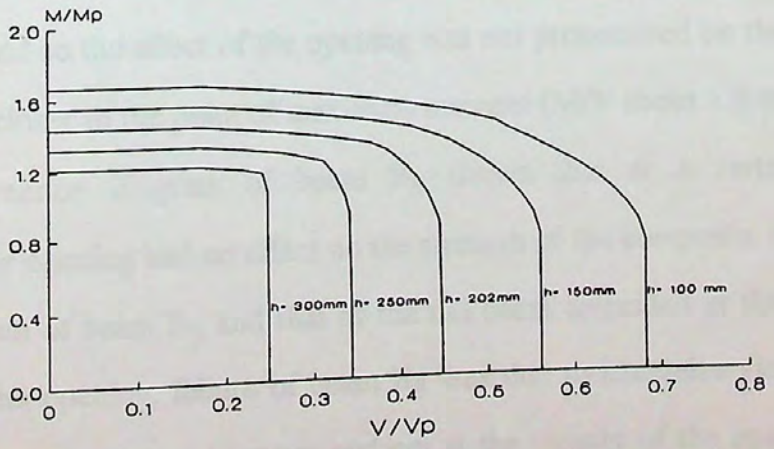

Figure 4.10- Interaction Diagrams for Beams with Various Opening Heights as Predicted by Fahmy(10)

i. the interaction between the steel beam and the concrete slab, and

ii. the moment due to the applied load

is reduced, leading to a lower ultimate moment of resistance. However, the ultimate moment capacity of the composite beam is not greatly affected by changing the opening height. This is due to the fact that the flanges carry most of the normal forces in the steel beam.

In the figure it can be seen that the moment capacity of beam B_6 has a reduction of 21.6% of its moment capacity due to a 45% decrease in web area, when compared to moment capacity of the full beam. A difference in web area of 43.7% between B_6 and B_{13} caused a mere 25% loss in the moment capacity of the composite beam.

As "M/V" ratio at the middle of the opening changes between ∞ and zero, the effect of the opening on the shear and moment capacities varies. Beams with openings of bigger heights proved to have lower moment and shear capacities at all values of M/V.

When comparing the interaction curves of beams B_6 and B_7 , it can be seen that the interaction diagrams of these two beams coincided when shear failure was governing the behavior of the beam. As the location of the opening was brought closer to the point of maximum moment in the two beams, beam B_6 showed to have a higher moment capacity than that of beam B_7. This is because beam B_6 had a smaller opening than that of B_7, and so the effect of the opening was not pronounced on the beam until the opening was closer to the point of maximum moment (M/V about 1.9 m).

The interaction diagram of beam B_8 shows that at a certain location (M/V=1.21 m) the opening had no effect on the strength of the composite beam, as the interaction diagram of beam B_8 and that of the full beam coincided at this point. For this location of the opening, failure of beam B_8 was due to excessive yielding of the panel at the point of maximum moment, and not at the vicinity of the opening. Based on the results in figure 4.7, it may be concluded that for this M/V ratio reduction of the web area upto 62.5% does not have a significant effect on the capacity of the

composite beam. At any other location the opening reduced the capacity of beam B_8 to carry loads.

On inspecting the interaction diagram of beam B_{13} and comparing it with that of the full beam, it can be seen that the loss in its ultimate moment capacity was 41.4% at M/V=∞. When compared with the loss in its shear capacity at M/V=0, which was 77.8%, the significance of changing the opening height can be seen to affect the shear capacity more than the moment capacity at these extreme locations for the reasons discussed previously.

The interaction diagrams show good agreement with the interaction diagrams presented by Todd et al[24]. Their curves are presented in figure 4.9. The same pattern is observed in both sets of interaction diagrams. The decrease in shear capacity of the composite beams due to the increase in opening height was also because of the decrease in net web area as the opening height increases, as, according to their model, the shear was resisted solely by the web of the steel beam. Also, according to Todd et al[24], the moment a composite beam can sustain is related to the opening height; moment capacity decreases as the opening height increases. This is caused by the decrease in net steel cross-section associated with the increase in opening height. This explains why beams with smaller opening heights had higher moment capacities.

The interaction diagrams were also compared with the interaction diagrams presented by Fahmy[10], which are presented in figure 4.10. The ultimate moment and shear capacities used to normalize the axes of the interaction diagrams presented by Fahmy were calculated for the steel section only. This explains why the ultimate moment capacity of some of the beams exceeded unity. As can be seen, figure 4.10 shows good agreement with figure 4.8. According to Fahmy[10], increasing the opening height caused a decrease in both the ultimate moment and shear capacities of the composite beams.

4.5.2. Effect of Varying the Opening Length:

The proposed program was used to plot the interaction diagrams of beam B_8 and beams B_{14} through B_{16}. These beams were composed of a steel beam W 310×28, and supporting a ribbed 10.0 cm thick slab, and the direction of the ribs was perpendicular to the longitudinal direction of the steel beam. The height of the corrugation was 2.5 cm. The openings in their webs were of a height of 18.2 cm. These beams were also over-connected in order to avoid connector failure, and were uniformly loaded. The characteristics of these beams are as presented in table 4.9.

Table 4.9. Characteristics of Beams to Study the Effect of Varying Opening Length.

Beam	Designation	Opening Height (cm)	Opening Length (cm)
B_{14}	W 310×28	18.2	15.2
B_{15}	W 310×28	18.2	30.5
B_8	W 310×28	18.2	45.7
B_{16}	W 310×28	18.2	61.0

The results of this study are presented in figure 4.11. As can be seen from the figure, both the ultimate moment and shear capacities of the composite beams decrease with increasing the opening length. However, at the two extreme M/V ratios, ∞ and zero, the ultimate shear capacity is more affected by increasing the opening length, as can be seen in figure 4.11.

When the opening is placed near the support (M/V = zero), increasing the opening length had a adverse effect on the ultimate shear capacity of the beam. The shear capacity decreases with increasing the opening length. This is due to the increase of Vierendeel moment caused by the increase in opening length.

When the opening is placed at the mid-span of the beam (M/V=∞), the ultimate moment capacity of the composite beams decreased with increasing the opening length. However, the ultimate capacity of composite beams is not as significantly

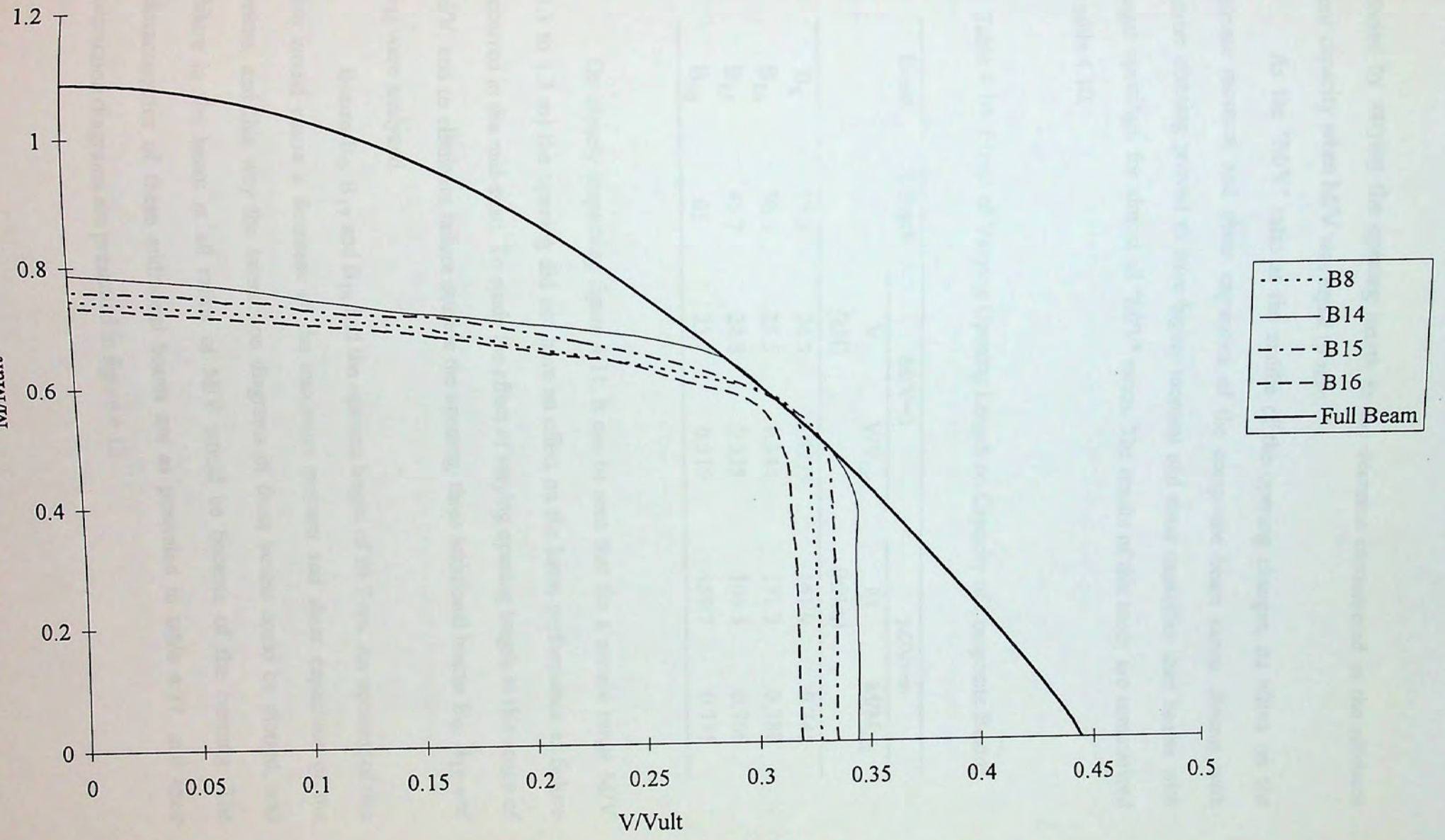

Figure 4.11- Effect of Varying Opening Length
(Opening Height = 18.2 cm)

affected by varying the opening length as the decrease encountered in the ultimate shear capacity when M/V was equal to zero.

As the "M/V" ratio at the middle of the opening changes, its effect on the ultimate moment and shear capacities of the composite beam varies. Beams with shorter opening proved to have higher moment and shear capacities than beams with longer openings, for almost all "M/V" ratios. The results of this study are summarized in table 4.10.

Table 4.10. Effect of Varying Opening Length on Capacity of Composite Beams.

Beam	Length	M/V=0		M/V=∞	
		V (kN)	V/V_{ult}	M (kNm)	M/M_{ult}
B_8	15.2	24.3	0.3275	161.9	0.745
B_{14}	30.5	25.5	0.344	171.3	0.788
B_{15}	45.7	24.8	0.335	166.5	0.766
B_{16}	61	23.7	0.319	159.7	0.735

On closely inspecting figure 4.11, it can be seen that for a certain range M/V (1.1 to 1.3 m) the opening did not have an effect on the beam performance as failure occurred in the mid-span. To study the effect of varying opening length in this range of M/V, and to eliminate failure outside the opening, three additional beams B_9, B_{17} and B_{18} were analyzed.

Beams B_9, B_{17} and B_{18} had the opening height of 20.7 cm. An opening of this size would cause a decrease of the maximum moment and shear capacities of the beams, and this way the interaction diagrams of these beams could be plotted, and failure in the beam at all ratios of M/V would be because of the opening. The characteristics of these additional beams are as presented in table 4.11, and their interaction diagrams are presented in figure 4.12.

Table 4.11. Characteristics of Beams to study the effect of varying opening length (h=20.7 cm).

Beam	Designation	Opening Height (cm)	Opening Length (cm)
B_{17}	W 310×28	20.7	15.24
B_{18}	W 310×28	20.7	30.48
B_9	W 310×28	20.7	45.72

Interaction diagrams of beams B_9, B_{17} and B_{18} also show the difference in maximum shear capacity at the middle of the opening between the three beams, as well as the slight moment capacity difference. At all locations of the opening, failure occurred in the vicinity of the opening. When the opening was close to the supports, the mode of failure was the four-hinge mechanism. As the opening approached the point of maximum moment, the mode of failure became a three hinge failure mechanism.

The beam with the smallest opening length, B_{17}, showed a higher capacity than the other beams for all values of M/V, while the beam with the largest opening length, B_9, showed the lowest capacity at all locations the opening was placed.

The interaction diagrams shown in figures 4.11 and 4.12 were compared with the interaction diagrams showing the effect of varying opening length presented by Todd et al[24] and Fahmy[10] (fig. 4.13 and 4.14). Their beams also showed an increase in the shear capacity of the composite beam as the opening length decreases. This increase, according to their model, was due to the decrease in the Vierendeel moment as the opening length decreases. However, the interaction diagrams presented by Todd et al[24] indicate that beams of different opening lengths have the same ultimate moment capacity. This is because the model presented by Todd et al[24] based the calculations of the moment capacity solely on the cross-section of the beam at the opening.

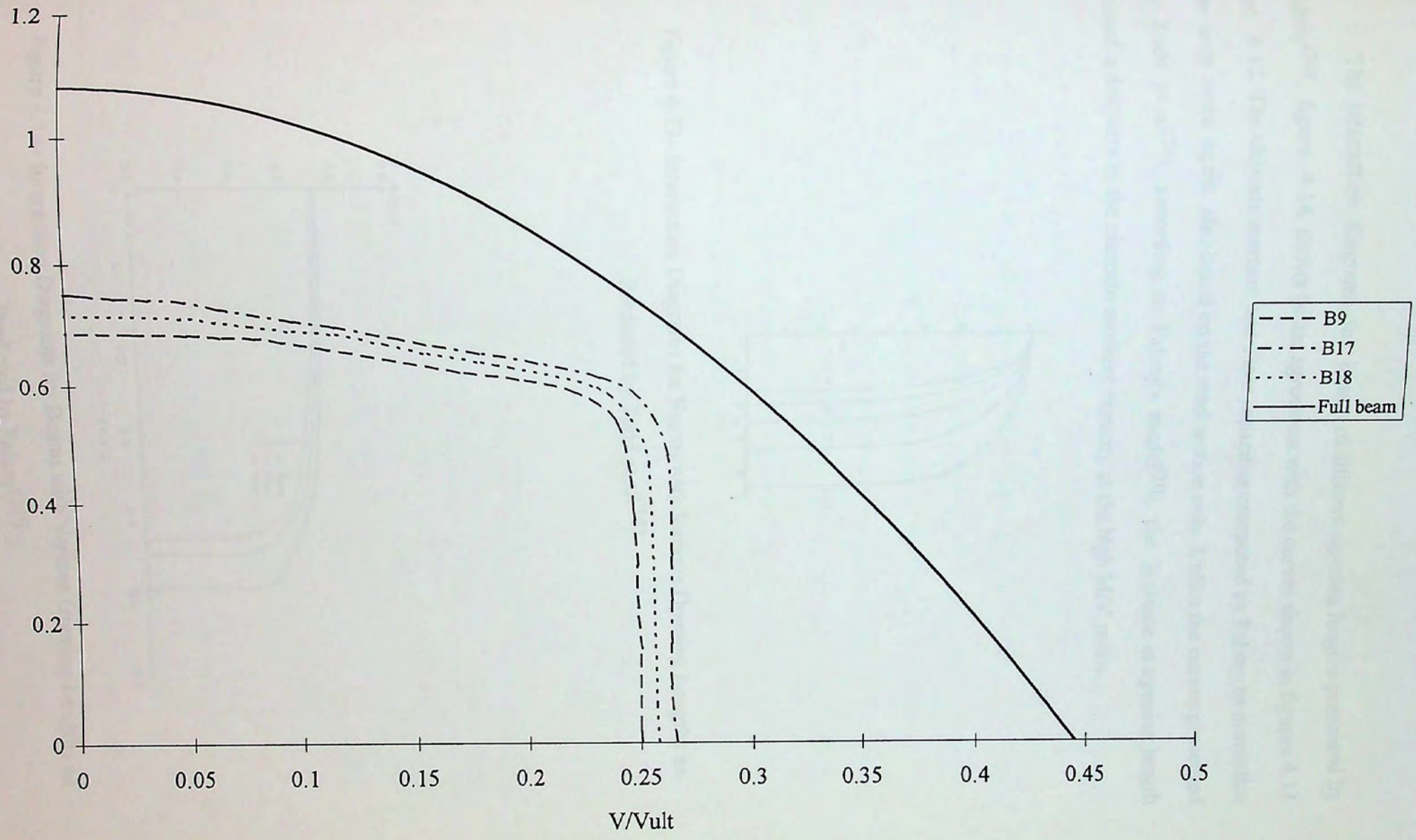

Figure 4.12- Effect of Varying Opening Length
(Opening Height = 20.7 cm)

The interaction diagrams for beams of different opening lengths presented by Fahmy[10], figure 4.14, shows better agreement with the curves shown in figures 4.11 and 4.12. The ultimate moment and shear capacities computed by Fahmy to normalize the axes were again also based on the steel section only. Unlike the curves presented by Todd et al[24], according to Fahmy's model[10], the increase in opening length caused a decrease in the ultimate moment capacity at the high M/V ratios.

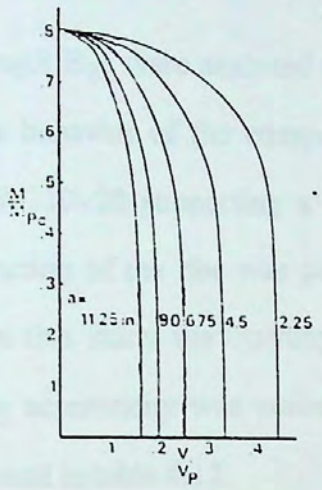

Figure 4.13- Interaction Diagrams for Beams with Various Opening Lengths as Predicted by Todd et al[24]

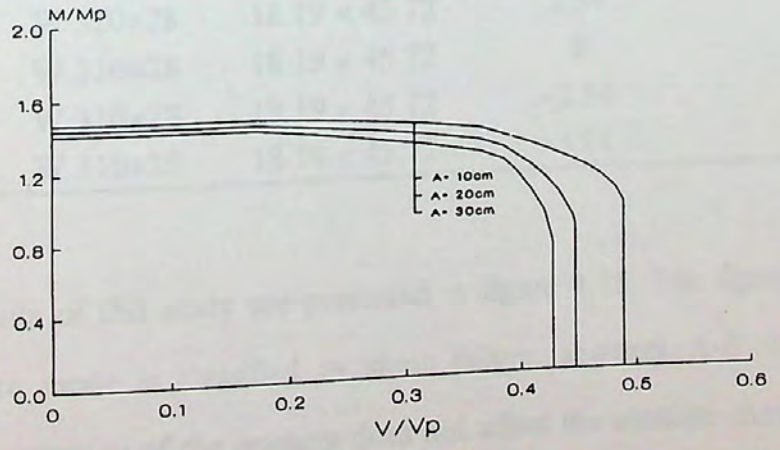

Figure 4.14- Interaction Diagrams for Beams with Various Opening Lengths as Predicted by Fahmy[10]

4.5.3. Effect of Varying the Opening Eccentricity:

The opening in the web of the steel beam can be either concentric or eccentric with regard to the steel beam depth. The opening is said to be 'concentric' when the mid-height of the opening coincides with the mid-depth of the steel beam, and eccentric if otherwise. Eccentricity of the opening can be either positive or negative; positive if the opening is closer to the top of the steel beam, and negative if closer to the bottom of the steel beam.

Beams B_8 and B_{19} through B_{22} were analyzed to study the effect of changing the opening eccentricity on the behavior of the composite beam. These beams were composed of a steel section W 310×28 supporting a 10.0 cm thick slab on 2.5 cm ribbed metal deck, and the direction of the ribs was perpendicular to the longitudinal direction of the steel beam. In this study the opening height and length were kept constant, and only the opening eccentricity was varied. Characteristics of beams B_8 and B_{19} through B_{22} are presented in table 4.12.

Table 4.12. Characteristics of Beams to Study the Effect of Varying Opening Eccentricity.

Beam	Designation	Opening Size (cm × cm)	Eccentricity (cm)	Eccentricity % of Beam Depth
B_{19}	W 310×28	18.19 × 45.72	3.81	12.3
B_{20}	W 310×28	18.19 × 45.72	2.54	8.2
B_8	W 310×28	18.19 × 45.72	0	0
B_{21}	W 310×28	18.19 × 45.72	-2.54	-8.2
B_{22}	W 310×28	18.19 × 45.72	-3.81	-12.3

The results of this study are presented in figure 4.15. The figure shows that when the failure mode is classified as shear failure, segment A-B on the curve, changing the eccentricity of the opening does not affect the ultimate shear capacity of the composite beam. At $M/V = \infty$, the opening eccentricity affects the ultimate moment capacity of the beam.

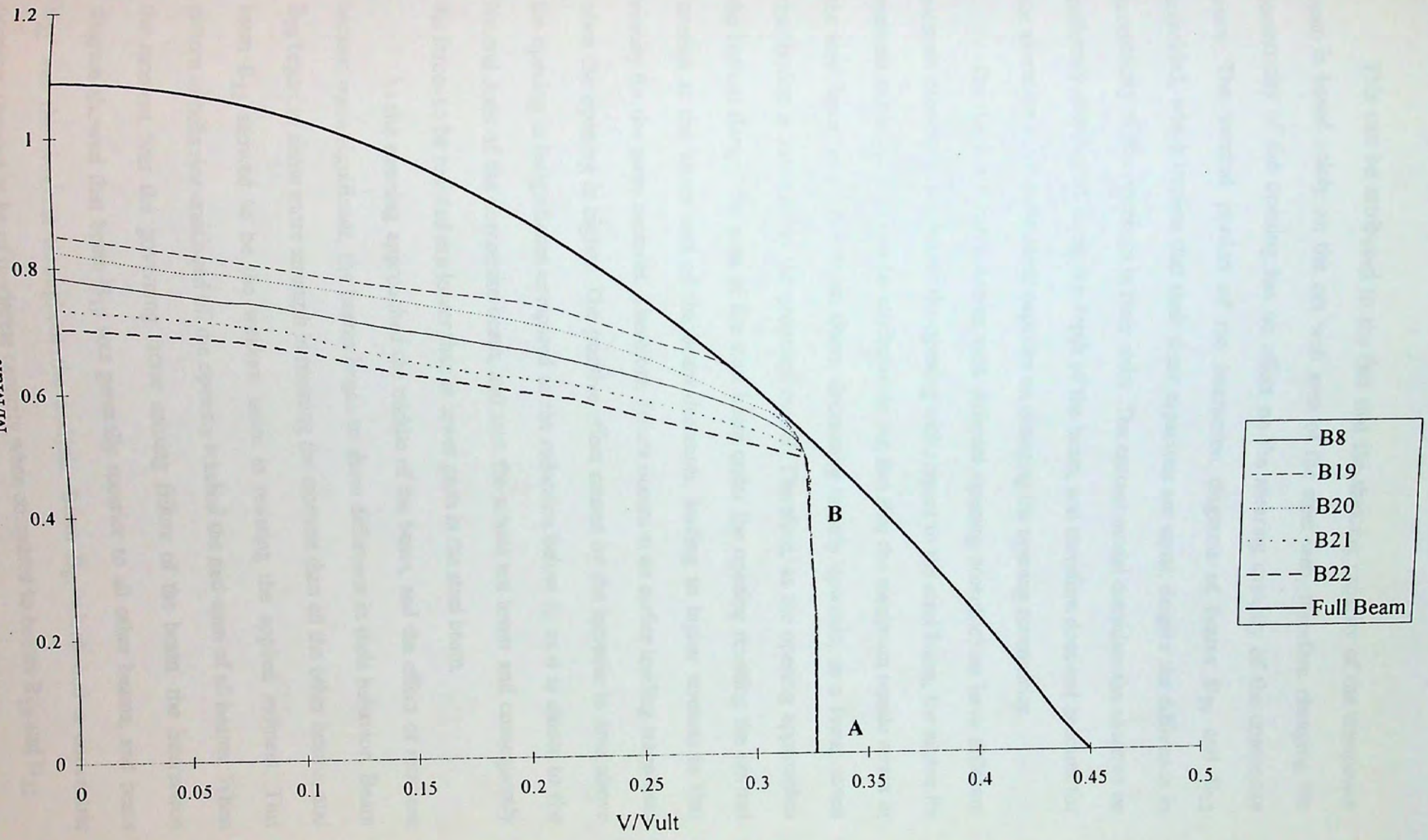

Figure 4.15- Effect of Varying Opening Eccentricity

This can be attributed to the fact that the shearing capacity of the composite beam is based solely on the net web area of the steel web, therefore changing the eccentricity of the opening has no effect on the shearing capacity of the composite beam. The vertical portion of the interaction diagrams of beams B_{19} and B_{22} coincided, which implies that their shear capacities are equal, despite the difference in eccentricity of the openings in their webs. The current model considers the shear to be uniformly-distributed along the depth of the beam, and therefore does not account for the alteration in ultimate shear capacity on changing the opening eccentricity.

On the other hand, beams with different opening eccentricities have different moment capacities; the higher the opening with respect to the steel beam, the higher its moment capacity. This can be attributed to the fact that the maximum tensile strain in the steel beam is at its bottom fibers, decreasing linearly upwards, as a linear strain distribution is assumed in the proposed model. Therefore, as the opening approaches the bottom flange, the area of the steel beam under the opening resisting the normal stresses at the lower end of the beam decreases, leading to higher stresses in that vicinity for the same moment. Therefore, failure occurs at an earlier loading stage than when the opening is higher. The positive effect caused by the increase in area above the opening is insignificant compared to the reduction below it, as it is closer to the Neutral Axis of the composite beam, and thus the strains are lower and consequently the forces to be resisted are lower than at lower parts in the steel beam.

As the opening approached the middle of the beam, and the effect of moment became more significant, the beams began to show difference in their behavior. Beam B_{19} began to show more strength in resisting the moment than all the other beams, and beam B_{22} showed to be the weakest beam in resisting the applied moment. This pattern of behavior continued till the opening reached the mid-span of all beams. When the moment was the governing factor causing failure of the beam, the interaction diagram showed that beam B_{19} was generally superior to all other beams, and beam B_{22} was the weakest throughout the analysis. Beam B_8, which had a concentric opening, showed to be of moderate capacity when compared to beams B_{19} and B_{22}.

Beam B_{19} showed approximately 8.3% increase in ultimate moment capacity, when compared to beam B_8, which had a concentric opening. Also, the ultimate moment of beam B_{22} was found to be approximately 10.2% lower than that of beam B_8. Also, beam B_{20}, which had an opening of 2.5 cm eccentricity, showed a 5.1% increase in ultimate moment capacity when compared to beam B_8, while beam B_{21}, which had an opening eccentricity of –2.5 cm, showed a decrease in ultimate moment capacity of 6.4% than that of beam B_8. These results are summarized in table 4.13.

The increase in ultimate moment capacity as the opening is approaches the top of the beam, for high M/V ratios, is attributed to the increase in arm of the moment caused by the force of interaction. As the opening approaches the top of the beam, a larger portion of the normal tensile stresses is resisted by the bottom tee, and therefore the arm of the moment; Z; increases, causing an increase in the moment of resistance of the section of the beam at the opening.

The modes of failure of all beams were generally similar. The four hinge failure mechanism was the governing mode of failure in all beams for low M/V locations of the opening. As the opening approached the mid-span of the beam, the three-hinge failure mechanism became the governing mode of failure. For higher M/V locations of the opening, the two hinge-failure became the governing mode of failure. The formation of the plastic hinges initiated at earlier loading stages for beams with negative opening eccentricity.

Table 4.13. Variation of ultimate moment capacity with eccentricity.

Beam	Eccentricity (cm)	Eccentricity % of Beam Depth	% of Ultimate Moment Capacity of Concentric Opening
B_{19}	3.81	12.3	108.3
B_{20}	2.54	8.2	105.1
B_8	0	0	100
B_{21}	-2.54	-8.2	93.6
B_{22}	-3.81	-12.3	89.8

Also, the interaction diagrams shown in figure 4.15 show that the interaction curves of beams B_{19} and B_{20} were closer to each other than those of beams B_{20} and B_8. This is because the difference in opening eccentricity between beams B_{19} and B_{20} was only 4.1 %, while the opening eccentricity difference between beams B_{20} and B_8 was 8.2 %. This implies that the change in ultimate moment capacities is proportional to the degree of eccentricity. The same is also observed in the interaction diagrams of beams B_{21} and B_{22}.

The interaction diagrams plotted with the aid of the presented model were compared to those presented by Todd et al[24]. Their curves are presented in figure 4.16. The interaction diagrams plotted by the their model show good agreement with the interaction diagrams shown in figure 4.15 as far as moment capacity at $M/V = \infty$ is concerned. However, in their diagrams, beams of different opening eccentricities had different shear capacities at M/V = zero; beams with larger absolute eccentricities showed higher resistance to shear.

The interaction diagrams of Fahmy[10] for beams with different opening eccentricities are presented in figure 4.17. Fahmy's curves[10] are also in agreement with those presented by Todd et al[24]. At M/V = zero, the increase in positive eccentricity caused the beam to have a lower ultimate shear capacity, but a higher ultimate moment capacity.

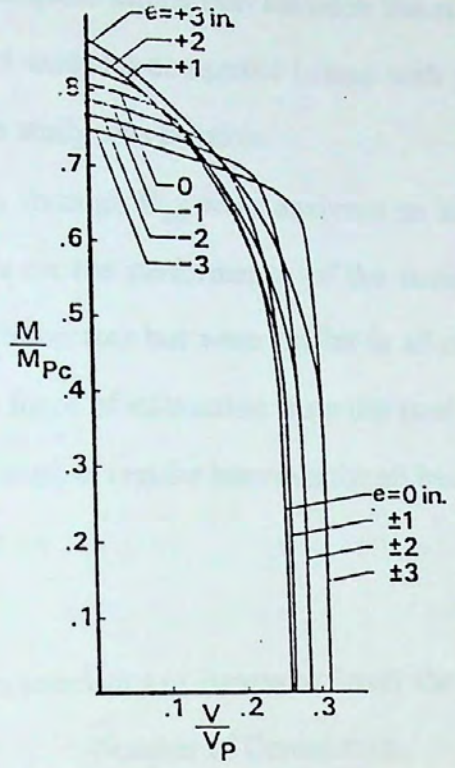

Figure 4.16- Interaction Diagrams for Beams with Various Opening Eccentricities as Predicted by Todd et al(24)

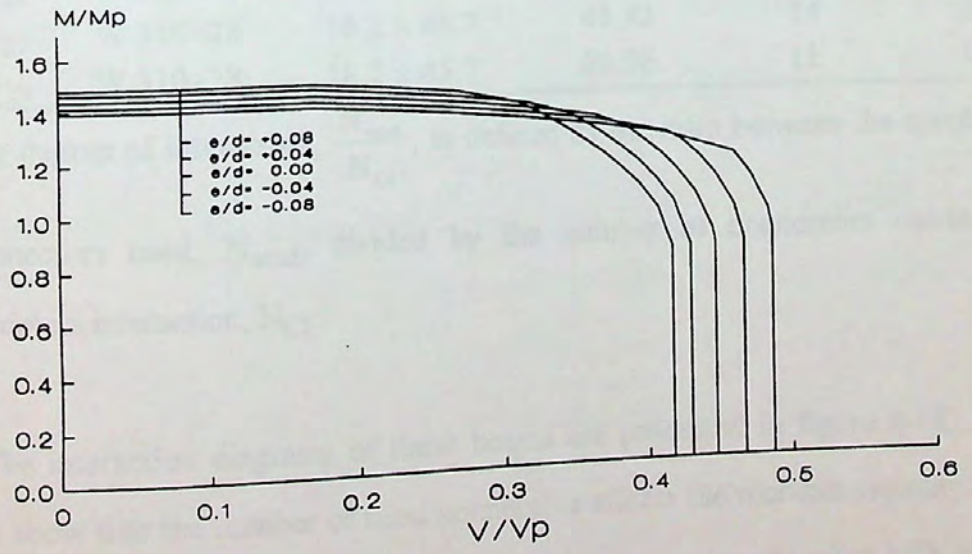

Figure 4.17- Interaction Diagrams for Beams with Various Opening Eccentricities as Predicted by Fahmy(10)

4.5.4. Effect of Varying the Number of Connectors:

This study could not be carried out by neither Todd et al[24] nor Fahmy[10], as they had both assumed complete interaction between the steel beam and the concrete slab. As the current model analyzes composite beams with partial interaction between the slab and the beam, this study was possible.

Beams B_8 and B_{23} through B_{26} were analyzed to study the effect of changing the number of connectors on the performance of the composite beam. These beams had different number of connectors but were similar in all other aspects. Headed studs were used to transmit the force of interaction from the steel beam to the concrete slab. Shear connectors were placed at regular intervals for all beams. Details of these beams are as presented in table 4.14.

Table 4.14. Characteristics of Beams to Study the Effect of Varying Number of Connectors.

Beam	Designation	Opening Size (cm × cm)	Spacing (cm)	Number of Connectors	Degree of Interaction
B_8	W 310×28	18.2 × 45.7	15.24	42	1.31
B_{23}	W 310×28	18.2 × 45.7	20.32	32	1.0
B_{24}	W 310×28	18.2 × 45.7	30.48	21	0.69
B_{25}	W 310×28	18.2 × 45.7	45.72	14	0.43
B_{26}	W 310×28	18.2 × 45.7	60.96	11	0.33

The degree of interaction, $\frac{N_{used}}{N_{CI}}$, is defined as the ratio between the number of connectors used, N_{used}, divided by the number of connectors needed for complete interaction, N_{CI}.

The interaction diagrams of these beams are presented in figure 4.18. These diagrams show that the number of used connectors affects the moment capacity of the beam when M/V=∞, but has no effect on its ultimate shear capacity when M/V = zero. This is because the current model bases the calculation of the shear strength of the

composite beam on the web net area only, and is not affected by the numbers of connectors used.

On the other hand, for M/V=∞, the number of connectors affects the ultimate moment capacity of the composite beam. This is because the force of interaction developed depends on the number of connectors used in the shear span. Any increase in the number of connectors increases the force that can be transmitted by the connectors from the beam to the slab. Beams B_8 and B_{23} had enough number of connectors to achieve full interaction. Beams B_{24}, B_{25} and B_{26} were under-connected. The interaction diagrams of beams B_8 and B_{23} almost coincided for a wide range of values of M/V at the opening. This is because complete interaction was possible for the case of both beams. However, for M/V ranging between 0.61 and 1.9 m, beam B_{23} showed a reduced moment and shear capacity. This could be because the number of connectors used between the support and the low moment-end of the opening were insufficient for the beam to develop its ultimate shear and moment capacities at the location of the opening. For this range of M/V at the opening, beam B_{23} failed due to failure of connectors between the support and the low-moment end of the opening. When enough connectors were used between the support and the low-moment end of the opening, the beam achieved its ultimate capacity, and the interaction diagrams of beams B_8 and B_{23} coincided for a wide range of M/V, and then deviated as M/V approached ∞. For M/V=∞, the ultimate moment capacity of beam B_8 was higher than that of B_{23}.

However, the ultimate moment capacity of beam B_8 wasn't significantly higher than that of beam B_{23}. By doubling the number of connectors used, the increase in moment capacity was approximately 7.0%. This could be because beams had a sufficient number of connectors to develop complete interaction. As the number of connectors in beam B_{23} was sufficient to transmit the load in the beam to the slab, the

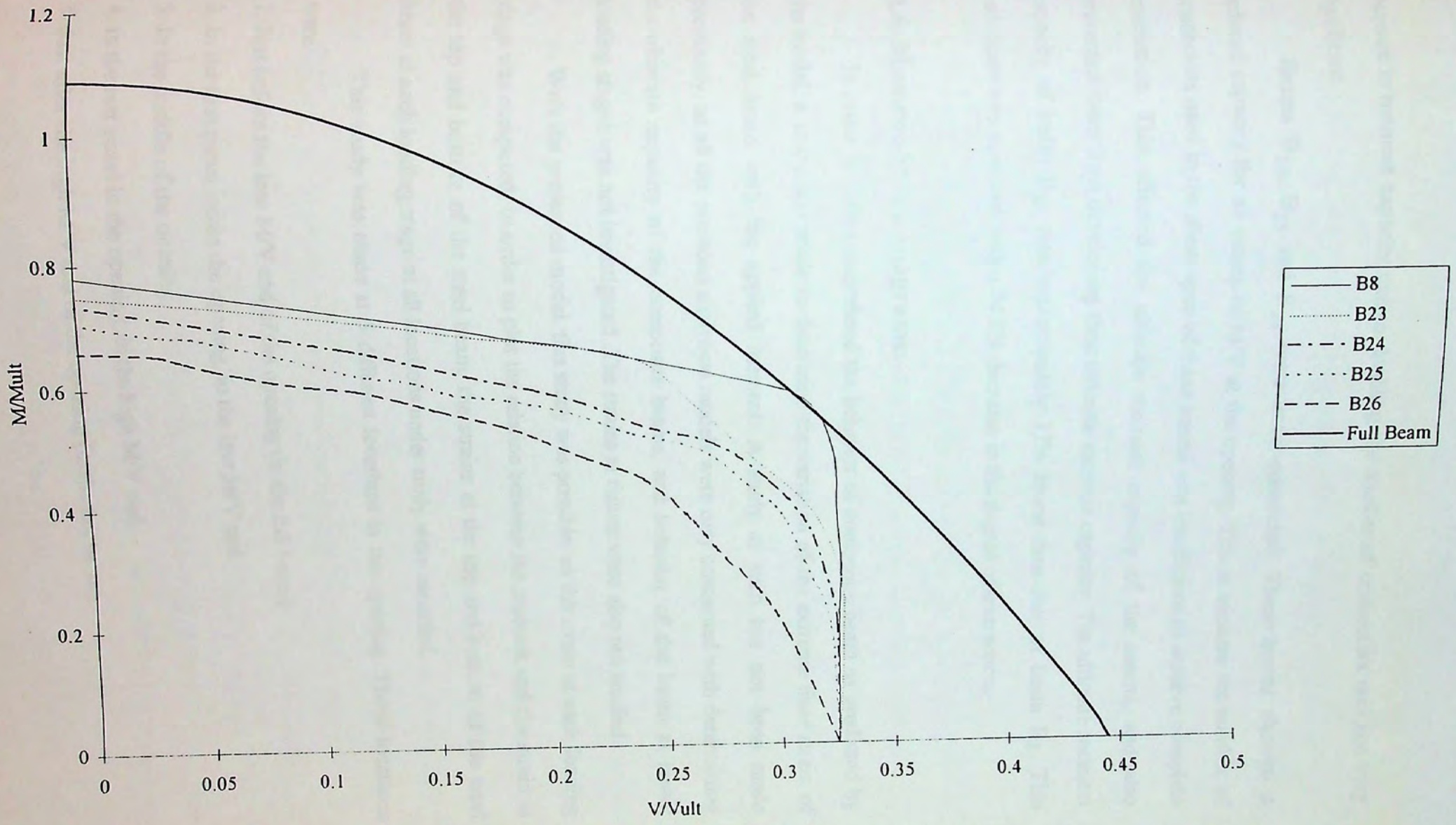

Figure 4.18- Effect of Varying Number of Connectors

increase in moment capacity due to doubling the number of connectors was not very significant.

Beams B_{24}, B_{25} and B_{26} were under-connected. These beams showed a reduced capacity for all values of M/V at the opening. This is because the number of connectors used in the shear span of these beams was insufficient to achieve complete interaction. This affected the ultimate moment capacity of the beams, and also prevented them from developing their ultimate moment capacity. The ultimate moment capacity of beam B_{26} was approximately 17% lower than that of beam B_8. This reduction was achieved with a 74.8% decrease in the degree of interaction.

4.6. Moment-Strain Diagrams:

In order to fully comprehend the behavior of composite beam as predicted by the model, a study was made to determine the variation of the extreme fiber strain of the steel beam with the applied moment. A study as such has not been made previously, as all the previous analytical models were only concerned with determining the ultimate capacity of the composite beams, and behavior of the beam at lower loading stages was not investigated. The strains at failure were also not studied.

With the presented model, this study was possible, as the strain at each loading stage was computed. In order to plot the relation between the moment and the strain at the top and bottom of the steel beam, the strains at the top and bottom of the steel beam at each loading stage at all locations under study were recorded.

This study was made at 5 different locations in the opening. These locations were:

1. Just before the low M/V end of the opening (in the full beam).
2. In the first panel inside the opening, in the low M/V end.
3. In the middle of the opening.
4. In the last panel in the opening, in the high M/V end.
5. Just after the high M/V end of the opening (in the full beam).

Figure 4.19 shows the moment-strain relation for a W 310×28 steel beam with a 18.2 cm × 45.7 cm web opening. The slab characteristics were the same as beam B_8. The opening was located at the middle of the span of the beam, and was concentric with regard to the beam depth. Figure 4.19(a) shows the variation of the strain with the applied moment just before the opening, while figures 4.19(b) and 4.19(c) show the variation of the strain with the moment at the beginning and middle of the opening, respectively. As the opening was located at the middle of the span of the beam, the strains at the end of the opening and just after it are identical to those at the beginning of the opening and just before it, respectively.

As can be seen from figure 4.19(a), the bottom fiber strain increased linearly with the increase in the applied moment in the elastic stages. Once the beam yields at any panel along the span, the moment-strain relation deviates from the linear relation. The compressive strain at the top of the beam was increased till a certain limit, and then began to decrease, while the strain at the bottom of the beam continued to increase throughout all loading stages, but at a lower rate. This is caused by the increase in the moment applied on the section, which also causes an increase in the moment due to interaction. This causes an increase in the interaction force which results in an increase in the net tensile forces in the steel beam. As the bottom fibers in the steel beam in that panel yield, they can resist no more tensile forces, and so the excess forces are resisted by the unyielded region of the steel beam. This results in a decrease in the compressive forces at the top of the steel beam. As the applied moment is further increased, another decrease in the compressive forces at the top of steel beam is necessary to accommodate for the increase in net tensile forces in the steel beam. On the other hand, the strain at the bottom fibers continues to increase with the increase in the applied moment. From figure 4.19(a), it can also be seen that the absolute strain at the bottom of the steel beam was higher than the absolute strain at the top of the steel beam at all loading stages. This indicates that the Neutral Axis of the beam was always closer to the top of the beam. This is expected in composite beams. Also, the Neutral Axis was continually raised towards the top of the beam in the inelastic loading stages

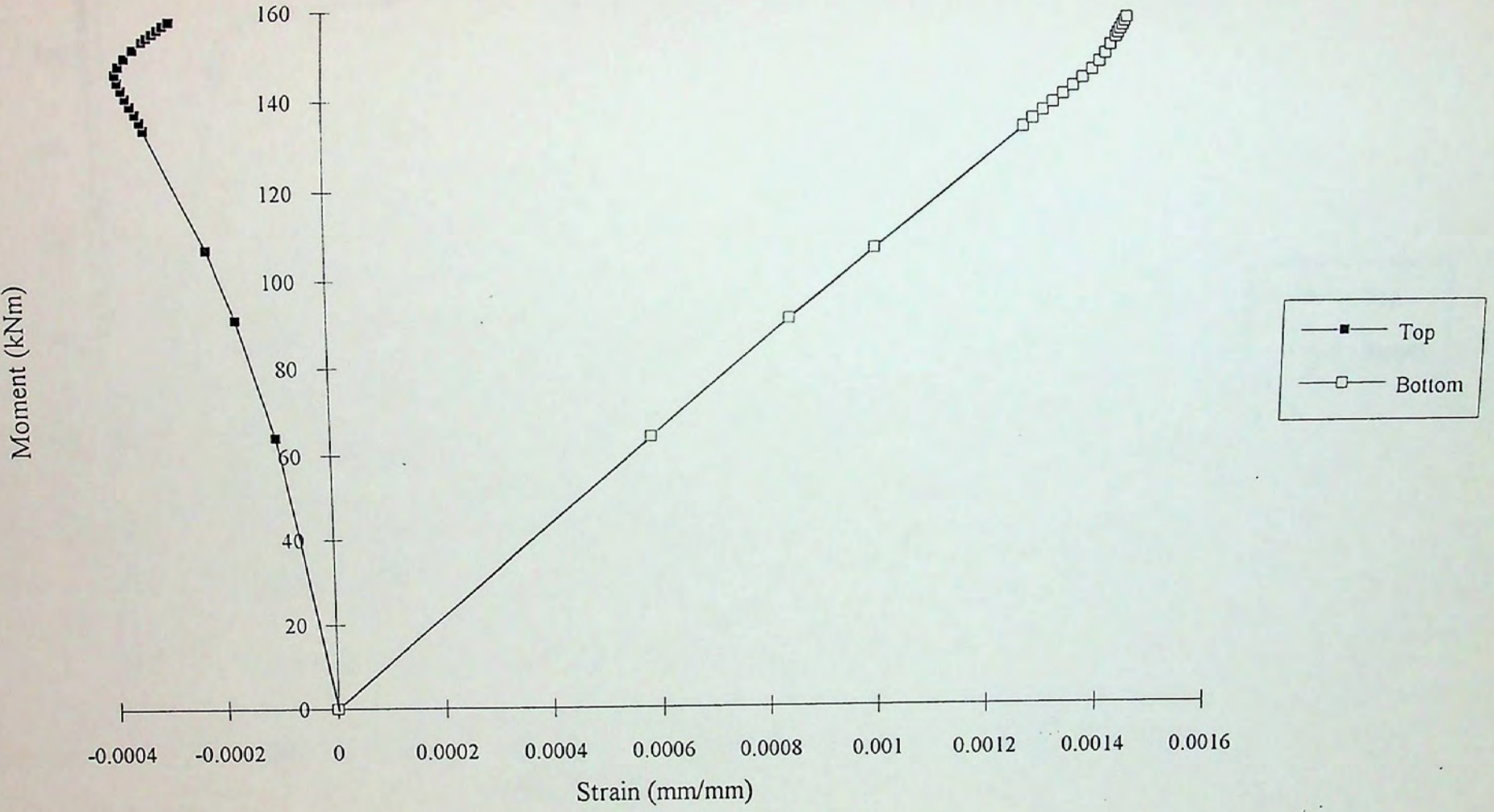

Figure 4.19(a)- Variation of Strain with Moment (Just Before Opening)

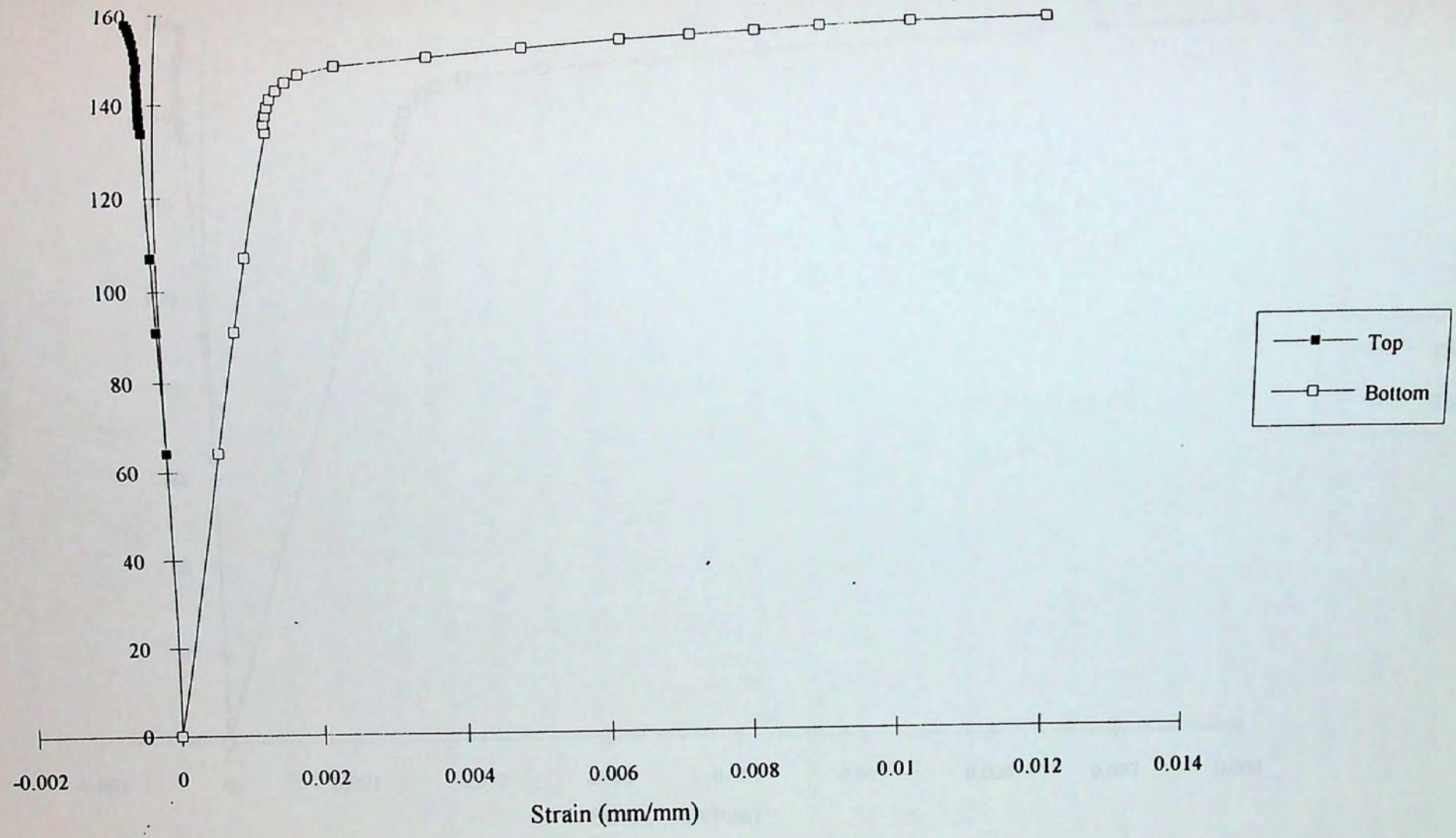

Figure 4.19(b)- Variation of Strain with Moment (Beginning of Opening)

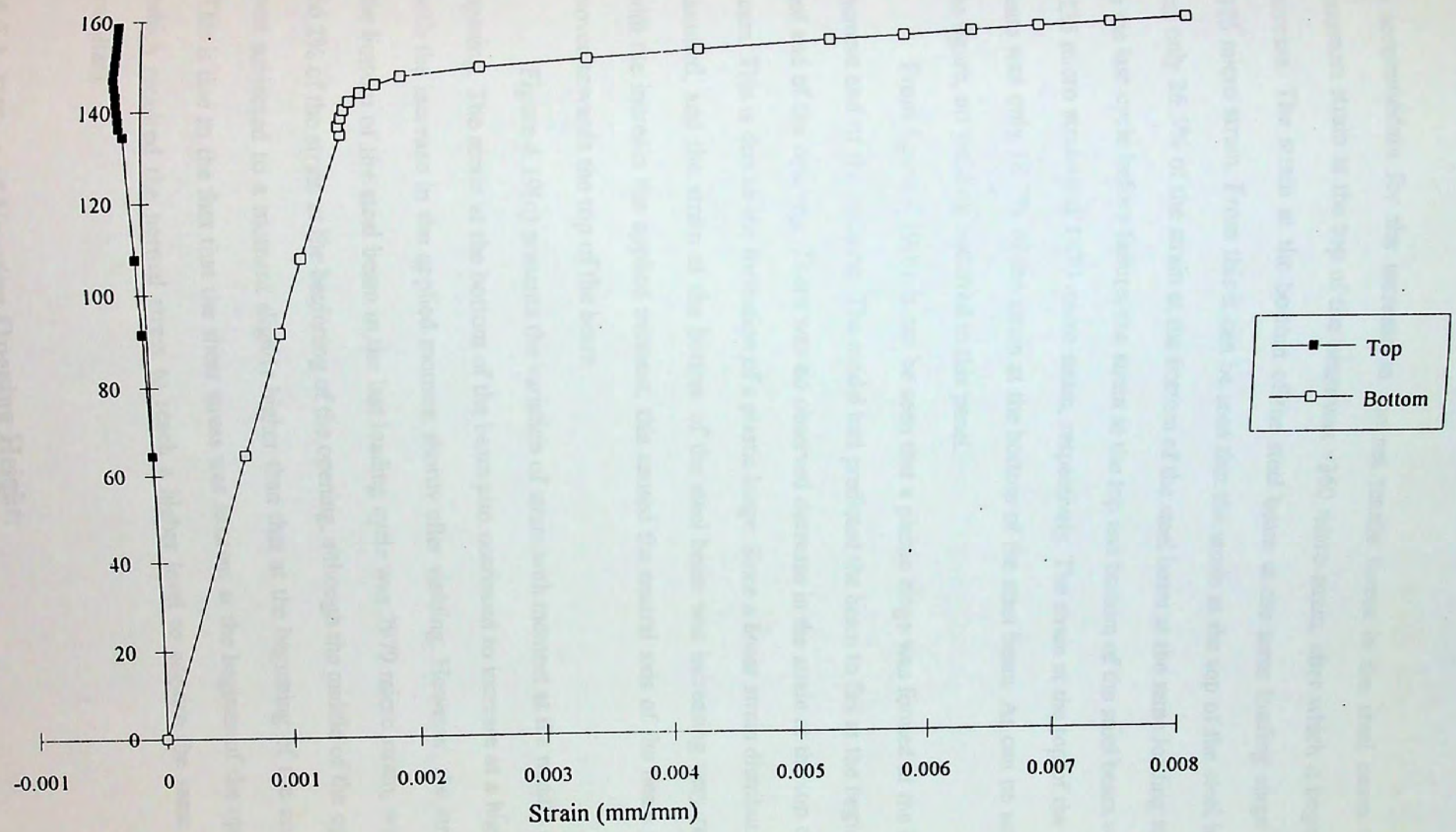

Figure 4.19(c)- Variation of Strain with Moment (Middle of Opening)

to accommodate for the increase in the net tensile forces in the steel beam. The maximum strain at the top of the beam was –360 micro strain, after which it began to decrease. The strain at the bottom of the steel beam at the same loading stage was 1375 micro strain. From this it can be seen that the strain at the top of the steel beam was only 26.5% of the strain at the bottom of the steel beam at the same loading stage. In the last cycle before failure, the strain at the top and bottom of the steel beam were –235 micro strain and 1470 micro strain, respectively. The strain at the top of the steel beam was only 18.7% of the strain at the bottom of the steel beam. As can be seen in the figure, no yielding occurred in this panel.

From figure 4.19(b), it can be seen that a plastic hinge was formed at the high-moment end of the opening. The model had predicted the beam to fail at the beginning and end of the opening. There was no observed decrease in the strain at the top of the beam. This is due to the formation of a plastic hinge. Since a linear strain distribution is assumed, and the strain at the bottom of the steel beam was increasing very rapidly with the increain the applied moment, this caused the neutral axis of the beam to be moved towards the top of the beam.

Figure 4.19(c) presents the variation of strain with moment at the middle of the opening. The strain at the bottom of the beam also continued to increase at a high rate with the increase in the applied moment shortly after yielding. However, the strain at the bottom of the steel beam in the last loading cycle was 7979 micro strain, which is 66.2% of the strain at the beginning of the opening, although the middle of the opening was subjected to a moment slightly higher than that at the beginning of the opening. This is due to the fact that the shear stress was existent at the beginninof the opening, which required the normal stress to reach a higher level to acquire the same stress resultant.

4.6.1. Effect of Varying Opening Height:

A study was made to determine the effect of varying opening height on the variation of the strain at the top and bottom of the steel beam with the applied

moment. This study is presented in figures 4.20, (a) through (e). The beams under study were W 460×68 steel beams supporting a 10 cm-thick solid slab, and its effective breadth was 1.22 m. The span of the beams was 6.4 m. The connectors used had 1.9 cm diameter and 7.6 cm height. Four identical beams, B_{27}, B_{28}, B_{29} and B_{30}, that had openings of identical lengths and different heights were analyzed by the model. The characteristics of these beams are presented in table 4.15. M/V at all the openings was 1.85 m.

Table 4.15. Beams to Study the Effect of Varying Opening Height.

Beam	Designation	Beam Depth (cm)	Opening Height (cm)	Opening Length (cm)
B_{27}	W 460×68	52.5	40.6	62.9
B_{28}	W 460×68	52.5	35.6	62.9
B_{29}	W 460×68	52.5	30.6	62.9
B_{30}	W 460×68	52.5	25.4	62.9

The model predicted that beam B_{27} would fail due to dominant shearing force at the low M/V end of the opening. Beams B_{28} and B_{29} and B_{30} were predicted to fail due to the formation of four plastic hinges at the both ends of the opening.

Figure 4.20(a) shows the variation of strain with the applied moment at a location just before the low M/V end of the opening, in the solid part of the beam. As can be seen from the figure, beam B_{27}, which had the largest opening height, was the first beam to yield. This is due to the high shear stresses, caused by the small net web area in the adjacent panel in the opening. The high shear stresses caused beam B_{27} to

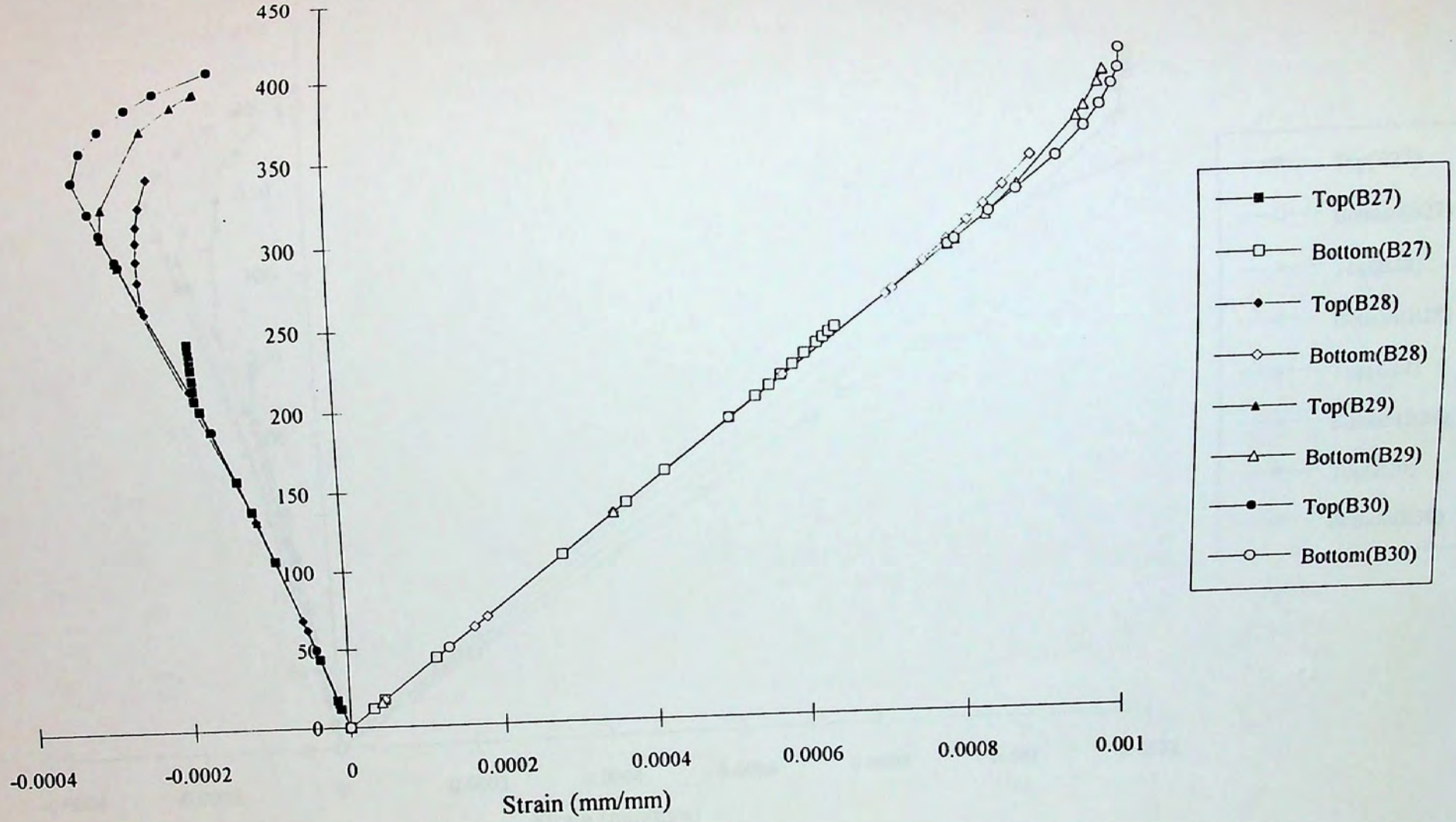

Figure 4.20(a)- Effect of Varying Opening Height (Just Before Opening)

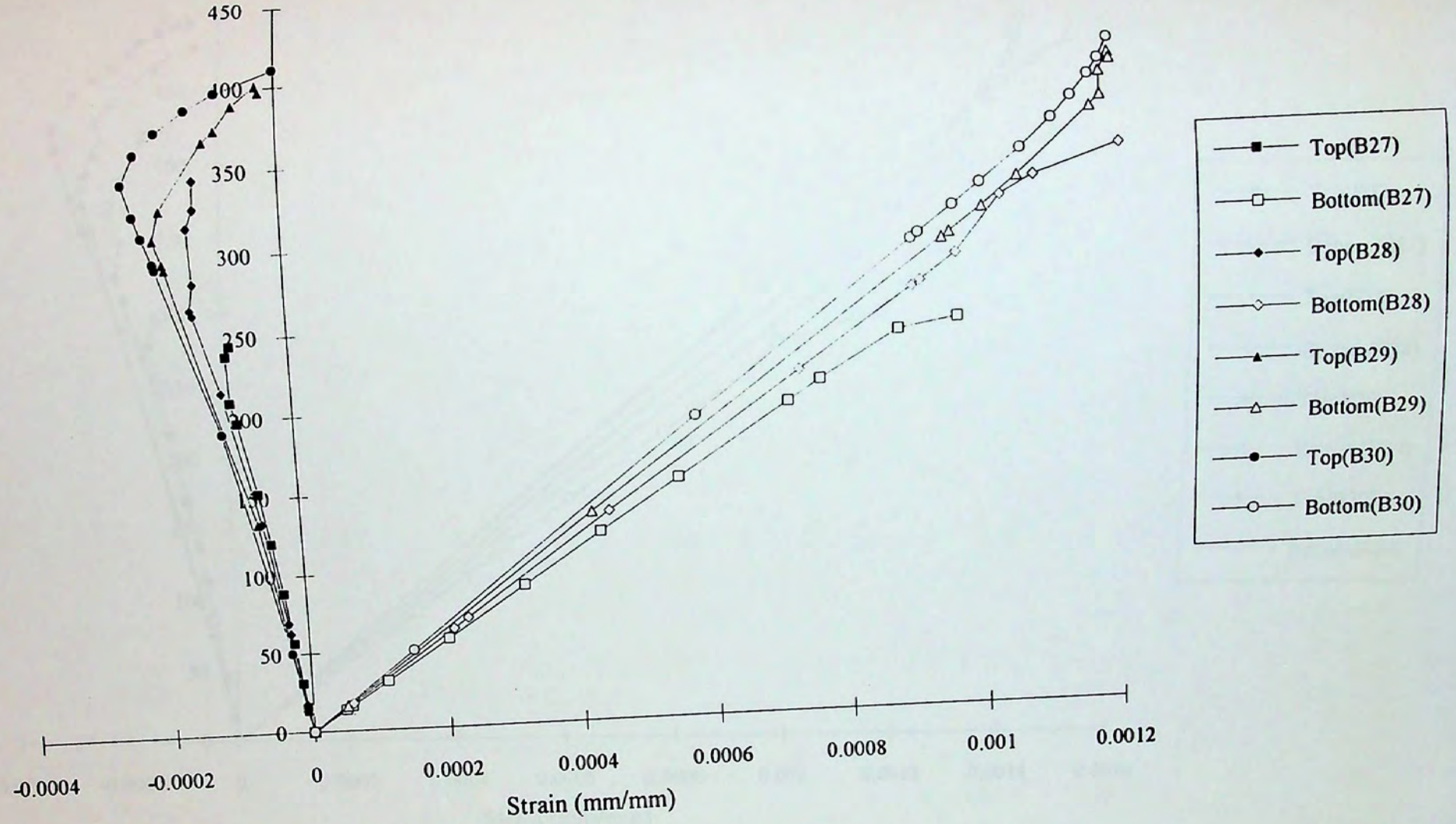

Figure 4.20(b)- Effect of Varying Opening Height (Beginning of Opening)

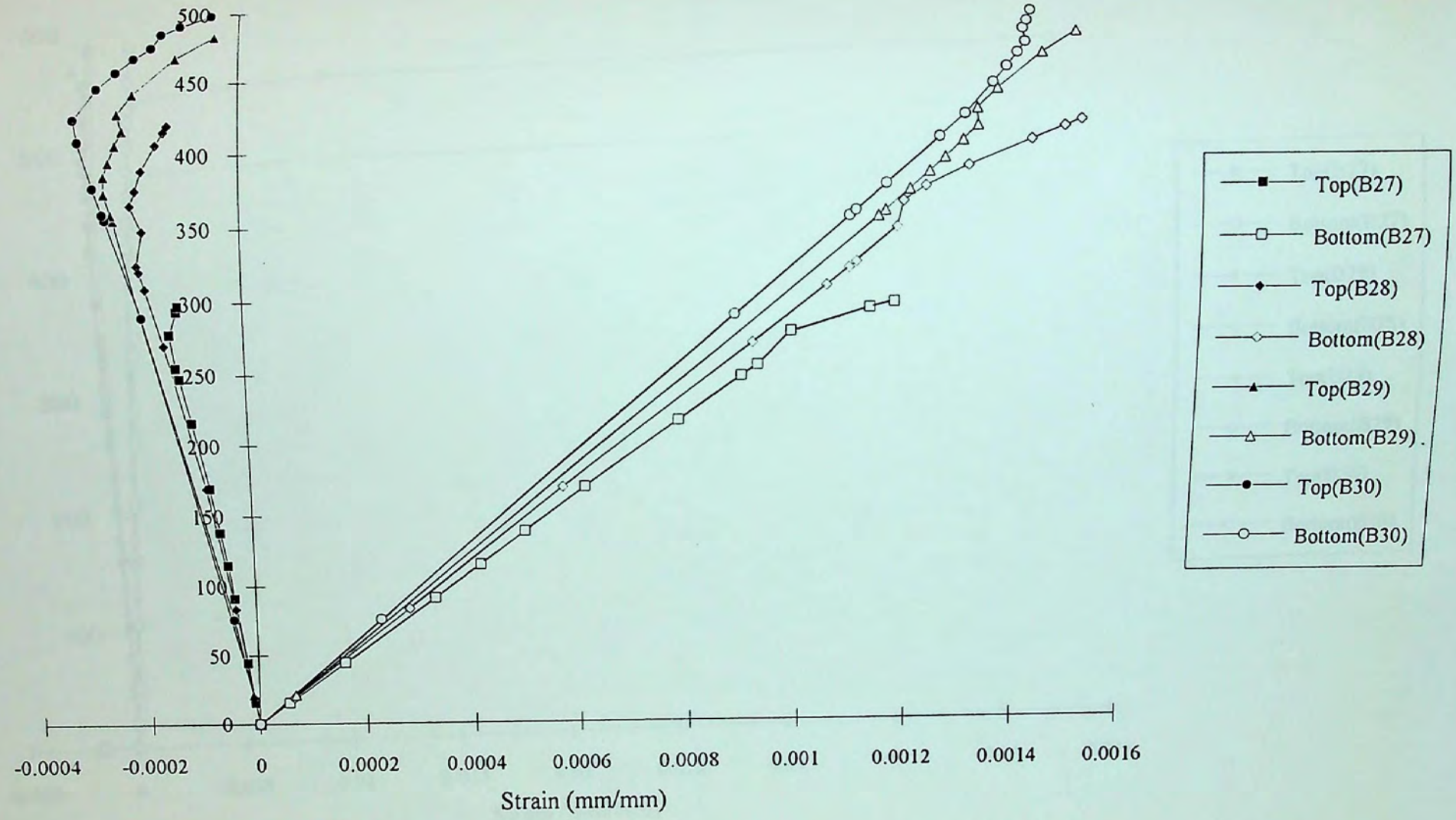

Figure 4.20(c)- Effect of Varying Opening Height (Middle of Opening)

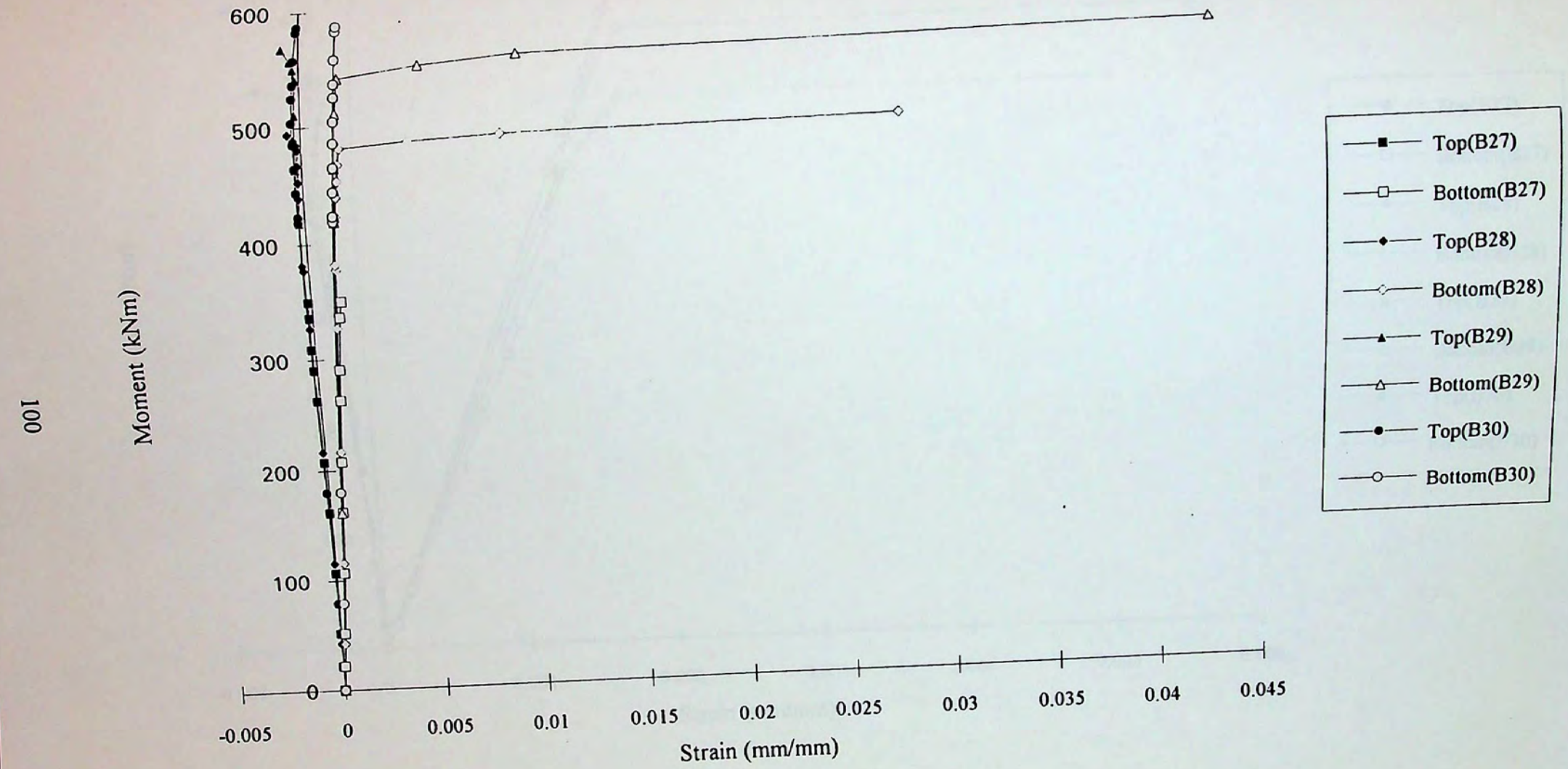

Figure 4.20(d.1)- Effect of Varying Opening Height (End of Opening)

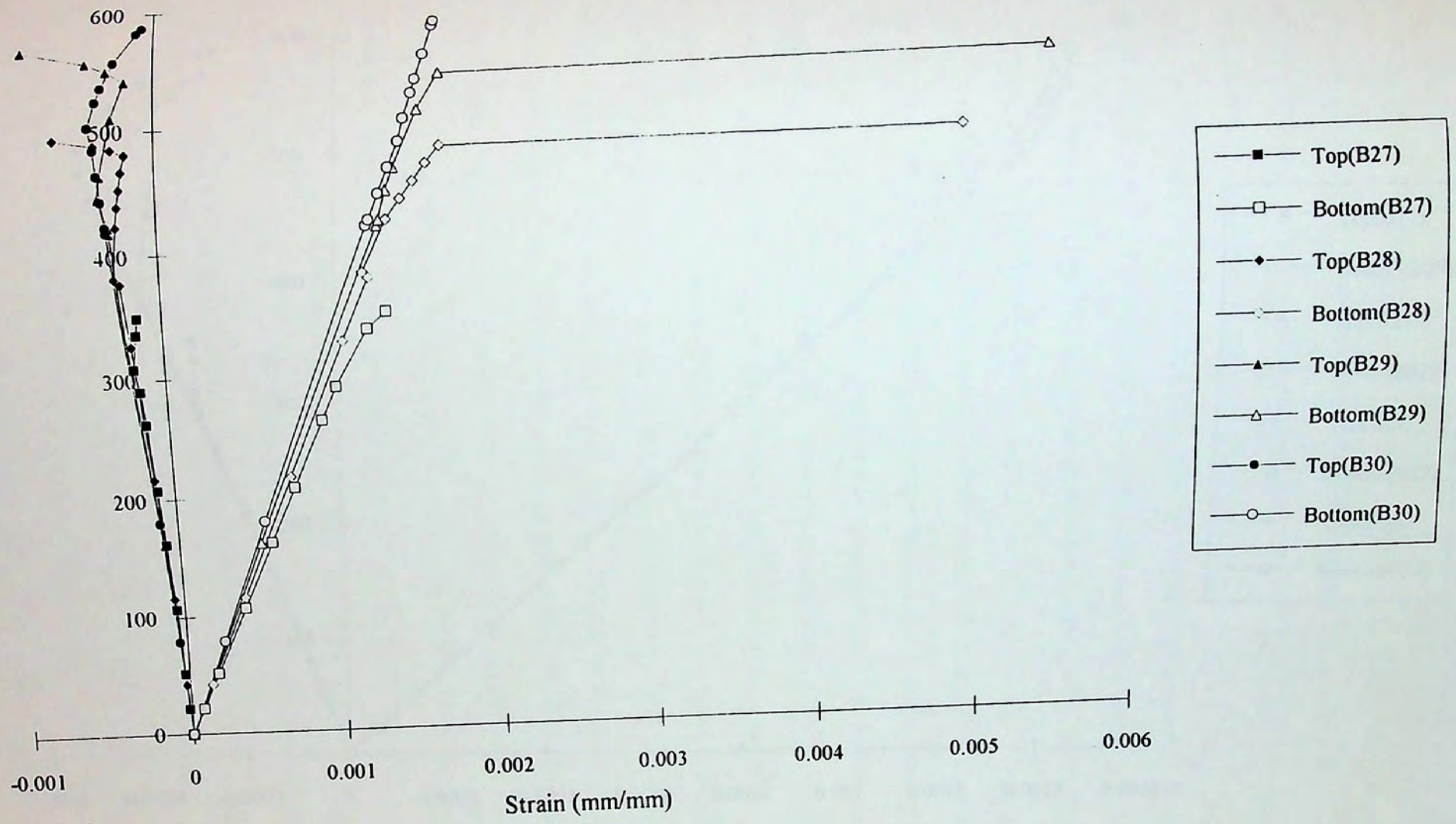

Figure 4.20(d.2)- Effect of Varying Opening Height (End of Opening Opening)

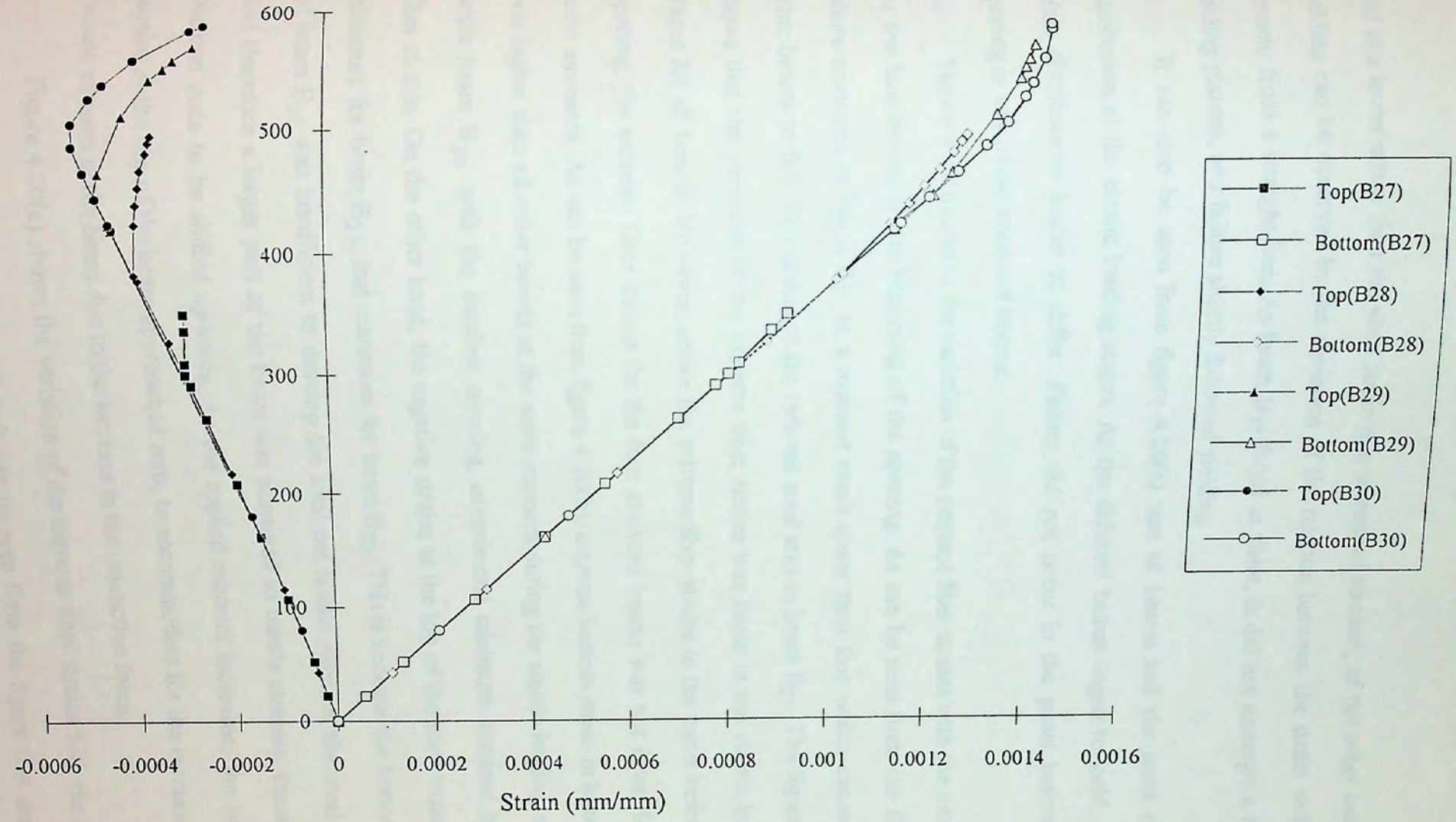

Figure 4.20(e)- Effect of Varying Opening Height (Just After Opening)

yield at a lower strain than the yield strain due to normal stresses, of the other beams. Yielding can be observed by the deviation of the relation between the strain and the moment from a straight line. As beam B_{27} failed in shear, it did not undergo a large yielding plateau, and failure shortly followed yielding.

It can also be seen from figure 4.20(a) that all beams had the same strain distribution at the elastic loading stages. As the different beams began to yield, their strain distributions began to differ. Failure did not occur in the panel before the opening in any of the analyzed beams.

Figure 4.20(b) shows the variation of the extreme fiber strains with the moment for the four beams at the beginning of the opening. As can be seen from the figure, failure occurred in beam B_{27} at a moment much lower than that which caused the other beams to fail. This is due to the reduced steel area in beam B_{27}. The figure also shows that the variation of the extreme fiber strains was linear in the elastic loading stages for all beams. However, unlike the extreme fiber strains in the panel before the opening, the extreme fiber strains for the four analyzed beams was not equal for the same moments. As can be seen from figure 4.20(b), extreme bottom strain in beam B_{27} was higher than all other beams at the same moment during the elastic loading stages, while beam B_{30}, with the smallest opening, experienced minimum extreme bottom fiber strains. On the other hand, the negative strains at the top of the steel beam were minimum for beam B_{27}, and maximum for beam B_{30}. This is because the bottom part of beam B_{27} was insufficient to develop the total net tensile stress in the steel beam, and therefore a larger part of the beam was subjected to tensile stresses, causing the Neutral Axis to be shifted upwards. As the applied moment increased, the negative strains at the top of the beam approached zero, to accommodate for the increase in net tensile stresses in the beam due to the increase in the interaction force.

Figure 4.20(c) shows the variation of the extreme fiber strains with the applied moment at the middle of the opening. It can be seen from the figure that the strain distribution followed a similar behavior to that at the beginning of the opening; for the same applied moment in the elastic loading stages, extreme fiber strains at the bottom

of the beam were highest in beam B_{27}, which had the biggest opening, and minimum for beam B_{30}, which had the smallest opening.

Figure 4.20 (d.1) shows the variation of the extreme fiber strains with the applied moment at the high M/V end of the opening. As can be seen, the strains at the bottom of beams b_{28} and B_{29} reached excessively high values, indicating the formation of a plastic hinge. In order to be able to study the behavior of the beam at that location, a more microscopic investigation of the diagram was required.

In figure 4.20 (d.2), the excessively high values for strain at the bottom fiber were not plotted in order to obtain a clearer view of the behavior of the beams. As can be seen from the figure, plastic hinges were formed in beams B_{28} and B_{29}, and excessively high values for strain were computed. Beam B_{27}, which failed in shear at the low-moment end of the opening didn't show any signs of excessive yielding. Beam B_{30} failed at the high-moment end, but the strains were not excessively large as in beams B_{28} and B_{29}. The large stub length in the beam prevented the hinge from developing.

Figure 4.20 (e) shows the variation of extreme fiber strains with the applied moment. As can be seen from the figure, all beams suffered the same strain distribution in the elastic loading stages. Once yielding occurred, each beam behaved differently.

4.6.2. Effect of Varying Opening Eccentricity:

Beams B_{31} through B_{33}, which were identical in all aspects except the opening eccentricity with regard to the beam depth, were analyzed by the model. These beams were W 460×68 steel beams supporting a 10 cm-thick solid slab, and its effective breadth was 1.22 m. The span of the beams was 6.4 m. The connectors used had 1.9 cm diameter and 7.6 cm height. The opening in beam B_{32} was concentric along the beam depth, while those of beams B_{31} and B_{33} had openings of positive and negative eccentricities, respectively. The effect of varying the opening eccentricity on the variation of extreme fiber strains with the applied moment is presented in figures 4.21 (a) through (e).

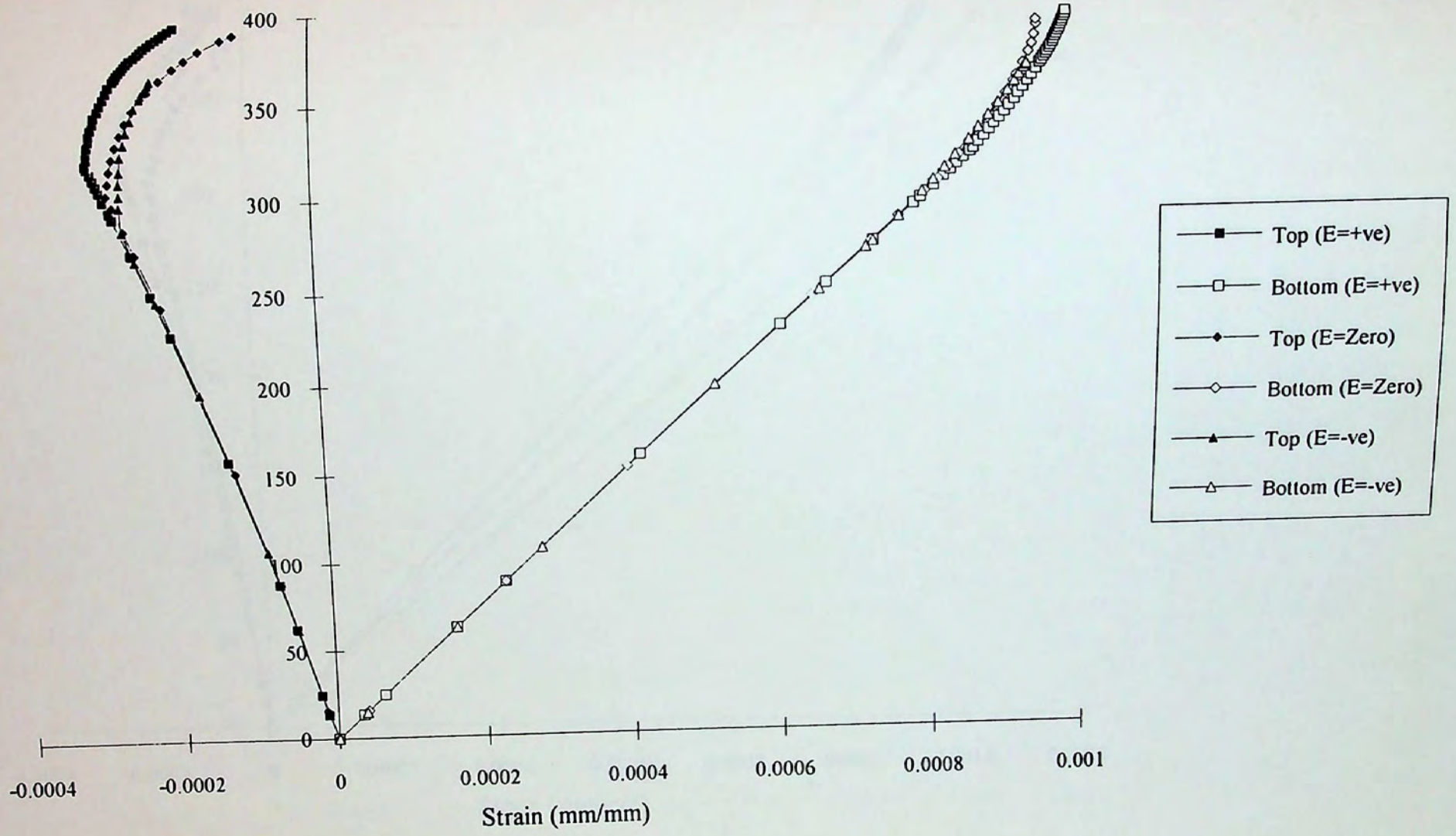

Figure 4.21(a)- Effect of Varying Opening Eccentricity (Just Before Opening)

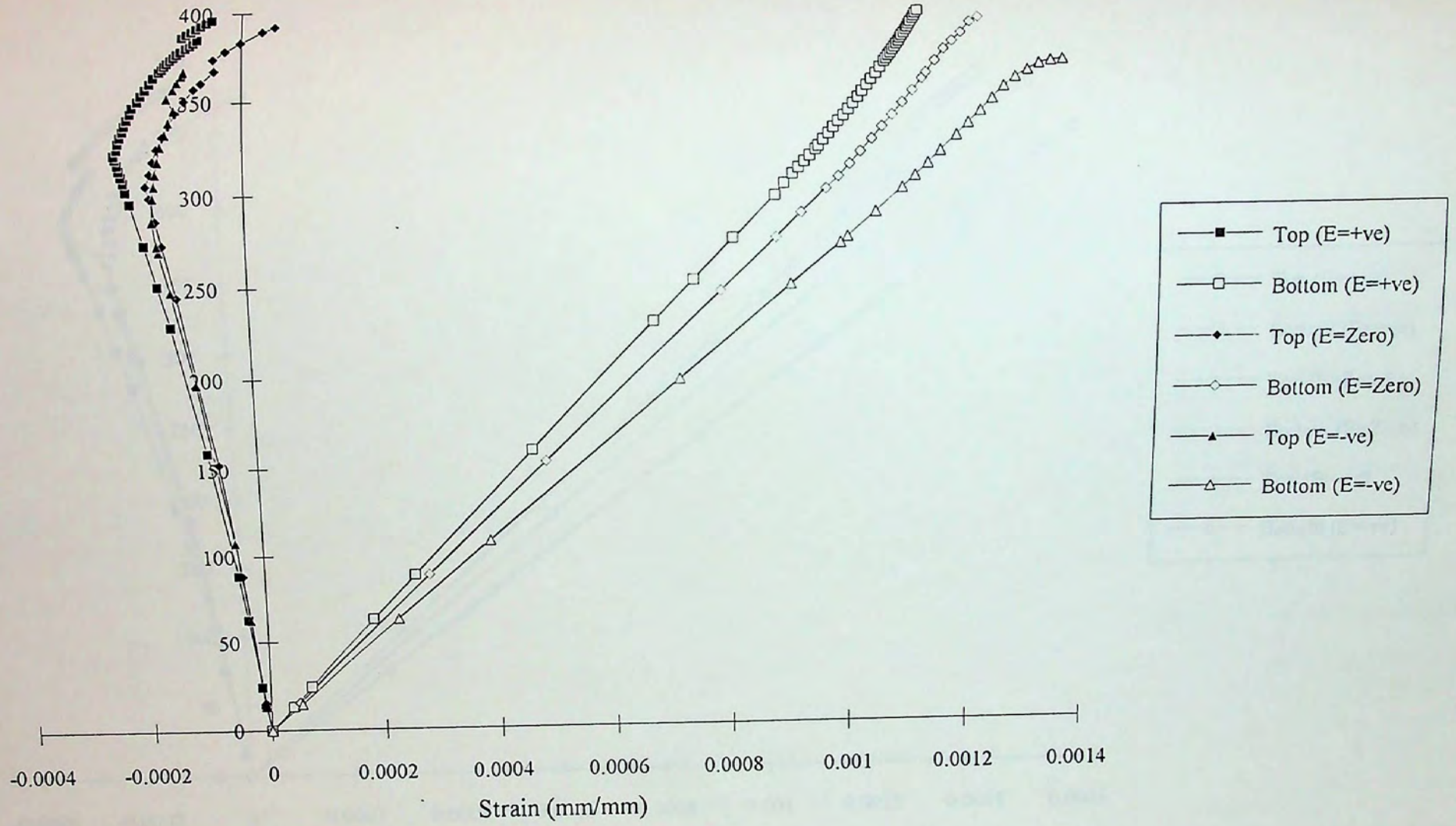

Figure 4.21(b)- Effect of Varying Opening Eccentricity (Beginning of Opening)

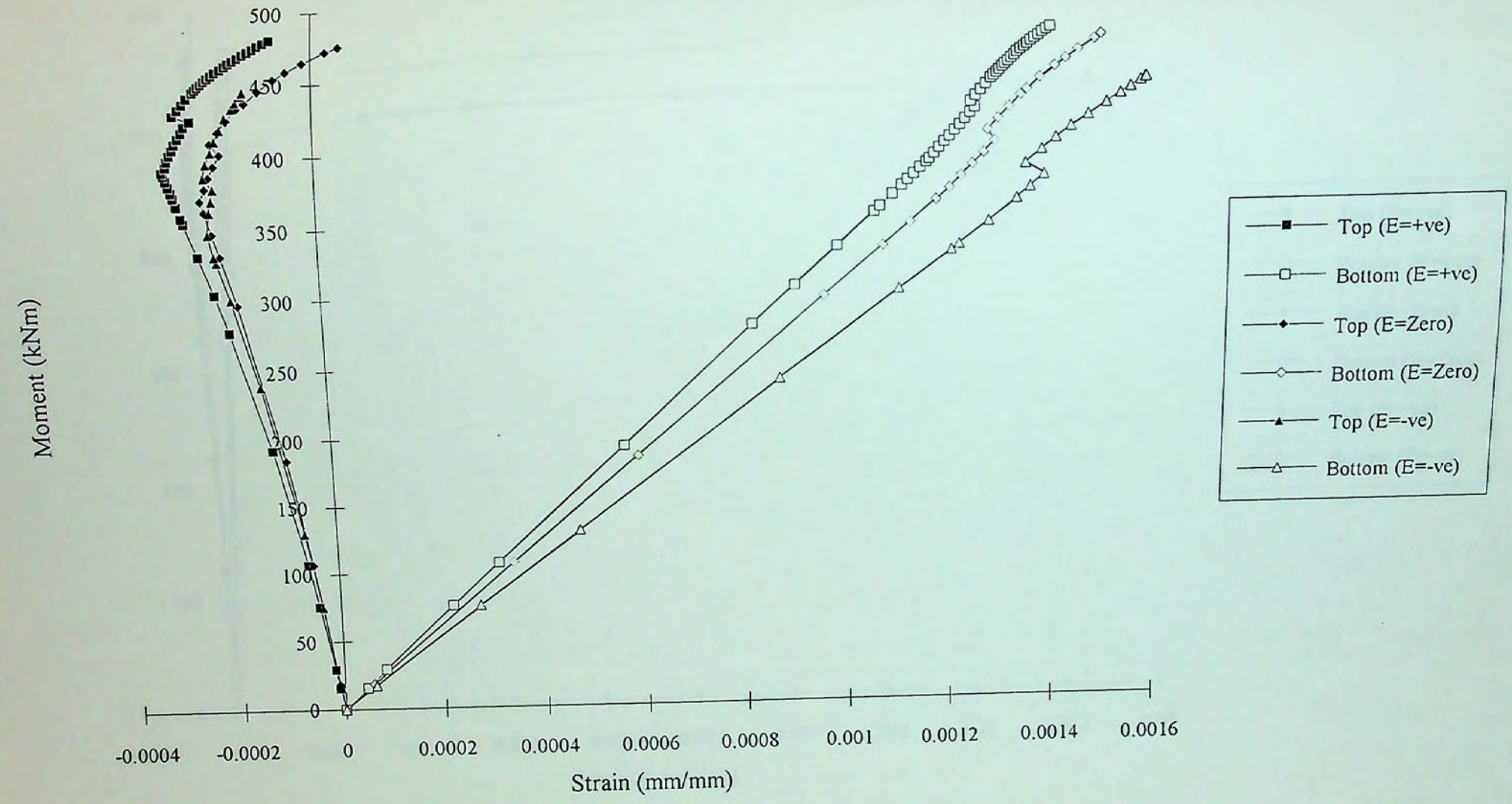

Figure 4.21(c)- Effect of Varying Opening Eccentricity(Middle of Opening)

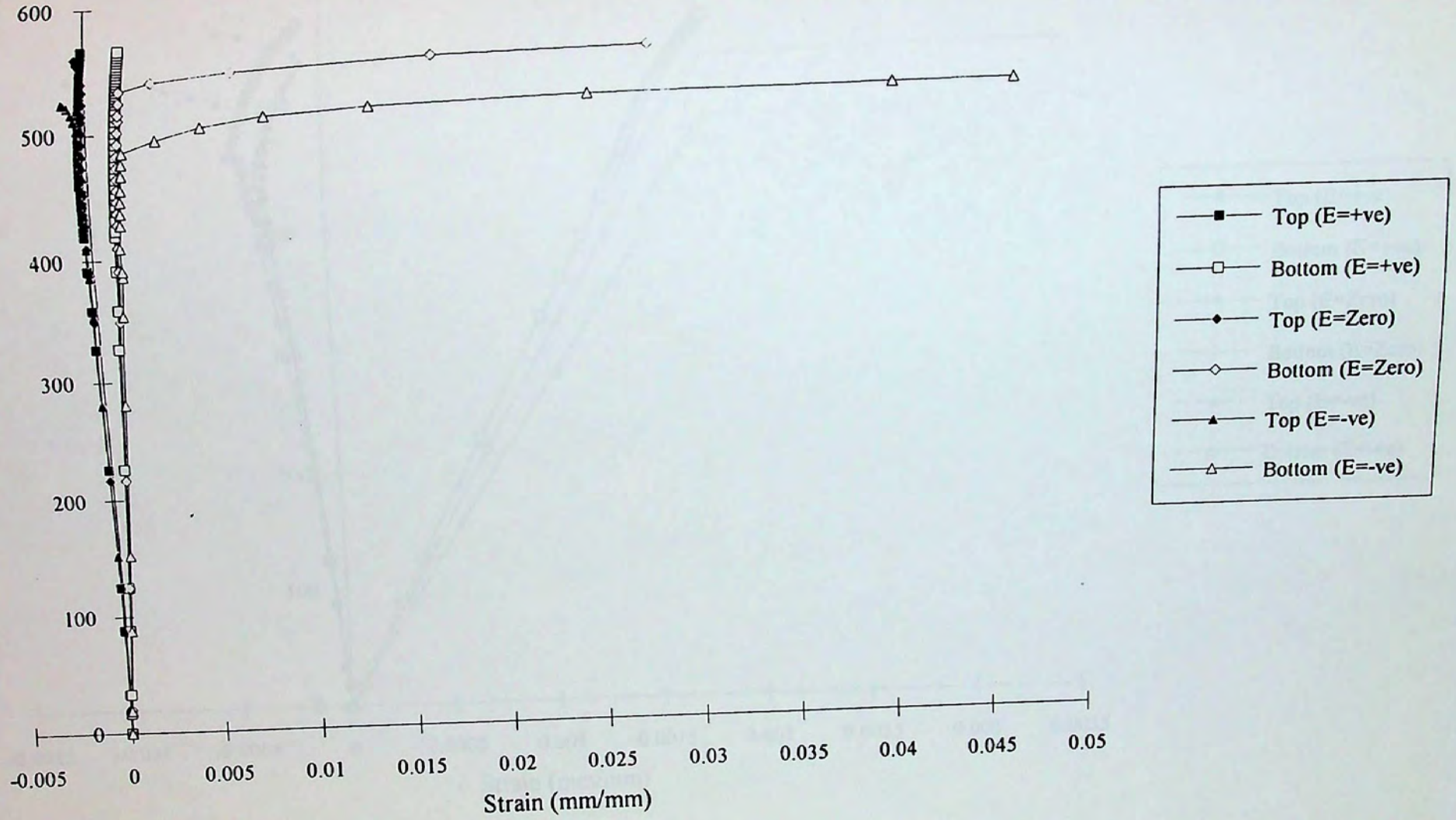

Figure 4.21(d.1)- Effect of Varying Opening Eccentricity (End of Opening)

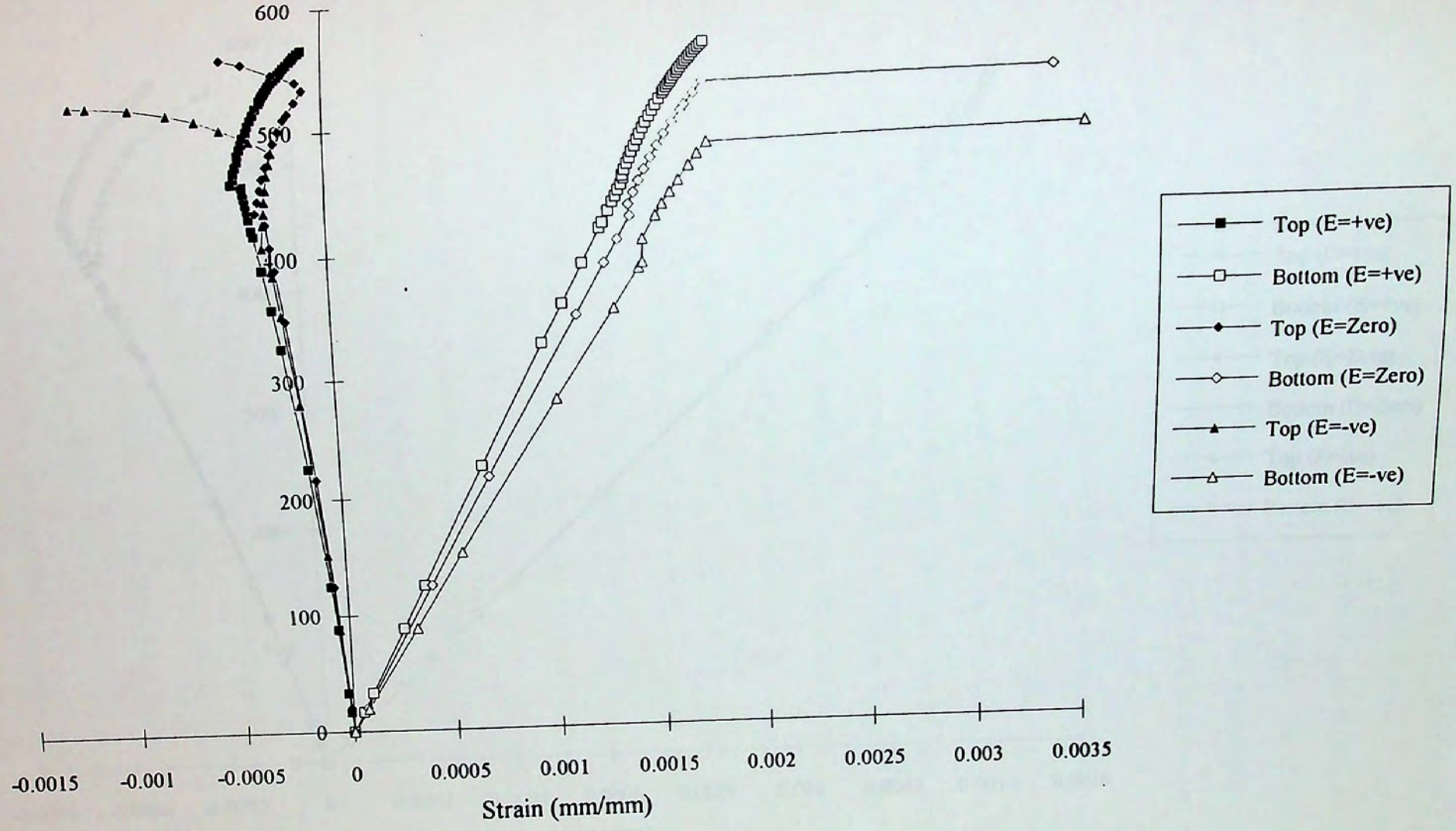

Figure 4.21(d.2)- Effect of Varying Opening Eccentricity (End of Opening Opening)

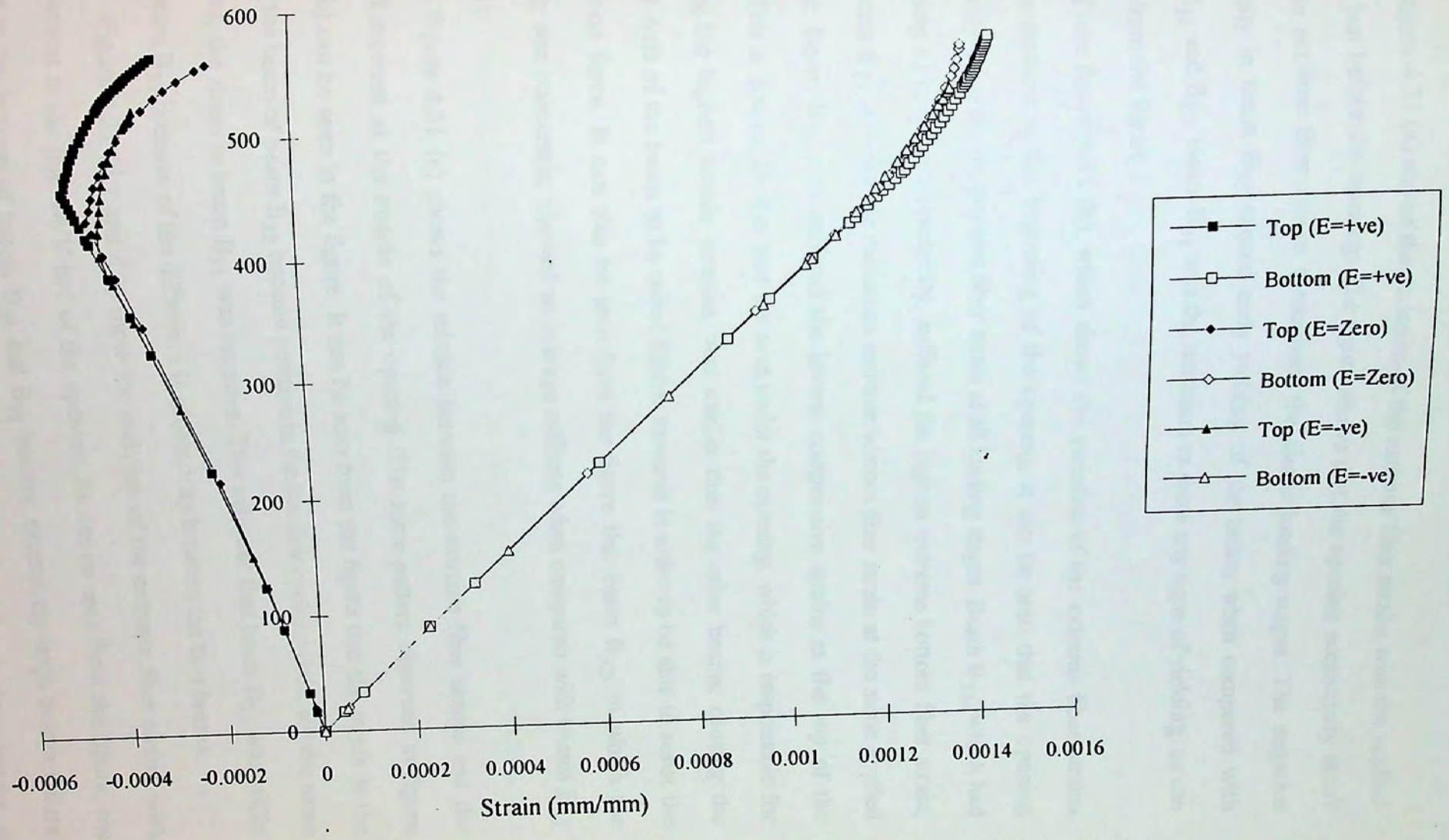

Figure 4.21(e)- Effect of Varying Opening Eccentricity (Just After Opening)

Figure 4.21 (a) shows the variation of the extreme fiber strains with the applied moment just before the opening. The figure shows that the opening eccentricity didn't affect the extreme fiber strains throughout the elastic loading stages. The negative eccentricity in beam B_{33} caused early yielding of the beam, when compared with beams B_{31} and B_{32}. Beam B_{31} was the last beam to show any signs of yielding, as can be seen from the figure.

From figure 4.21 (b), which shows the variation of the extreme fiber strains with the moment at the beginning of the opening, it can be seen that the opening eccentricity affected the extreme fiber strain at all loading stages. Beam B_{33}, which had an opening of negative eccentricity, suffered the highest extreme bottom fiber strain, while beam B_{31} suffered the minimum extreme bottom fiber strain at the same applied moment. Beam B_{33} also suffered the lowest compressive strains at the top of the beam. This is due to the fact that the area under the opening, which is responsible for resisting the highest tensile stresses, was smaller than the other beams, causing the Neutral Axis of the beam to be raised further upwards in order to be able to resist the interaction force. It can also be seen from the figure that beam B_{32}, in which the opening was concentric, showed an average stiffness when compared with beams B_{31} and B_{33}.

Figure 4.21 (c) shows the relation between the extreme fiber strains and the applied moment at the middle of the opening. The same pattern observed in figure 4.21 (b) can be seen in the figure. It can be seen from the figure that the stress at the top of the beam of beam B_{32} became positive in the last few cycles, while, for the same moment, the stress in beam B_{31} was negative. This indicates that beam B_{31} was stiffer than beam B_{32} because of the difference in eccentricity between the two beams.

Figure 4.21 (d.1 and d.2) show the variation of the extreme fiber strains with the moment at the high M/V end of the opening. As can be seen from the figure, the strains at the bottom of beams B_{32} and B_{33} became excessively large before failure. Plastic hinges were formed at the high moment ends of the opening in these beams, as well as at the bottom of the beam in the low-moment end. The plastic hinge formed at

the low-moment end was formed due to the combined effect of the normal and shear stresses, but the shear stresses were more dominant. This is why the strains at the low-moment end didn't grow exceedingly large. Plastic hinges were formed in the steel section above and below the opening at the high-moment end of the opening. A three-hinge failure mechanism was therefore the cause of failure of beams B_{32} and B_{33}.

Figure 4.21 (e) shows the variation of strain with the applied moment just after the high-moment end of the opening. As can be seen, the strain distribution was similar for all beams in the elastic loading stages. After yielding, the beams behaved differently.

4.6.3. Effect of Varying Degree of Interaction:

A study to determine the impact of varying the number of connectors in the shear span was carried out. Two beams, B_{34} and B_{35}, were identical in all aspects, but had a different number of connectors. These beams were W 310×28 steel beams supporting a 10 cm-thick solid slab, and its effective breadth was 1.22 m. The span of the beams was 6.4 m. The connectors used had 1.9 cm diameter and 7.6 cm height. The Opening was placed at the mid-span of the beam. Beam B_{34} had enough connectors to achieve complete interaction between the steel beam and the concrete slab, while beam B_{35} was under-connected. Figures 22 (a) through 22 (c) show the variation of extreme fiber strain with the applied moment at three different locations along the opening.

Figure 4.22 (a) shows the variation of extreme fiber strain with the applied moment just before the opening. As can be seen from the figure, beams B_{34} and B_{35} did not have the same strain distribution before the opening. This is because of the different force of interaction developed due to the difference in number of connectors used in the shear span in each beam. The figure also shows that at the high loading stages, the whole depth of the steel beam of B_{34} was subjected to tensile forces, while the top flange of beam B_{35} was still subjected to compressive forces.

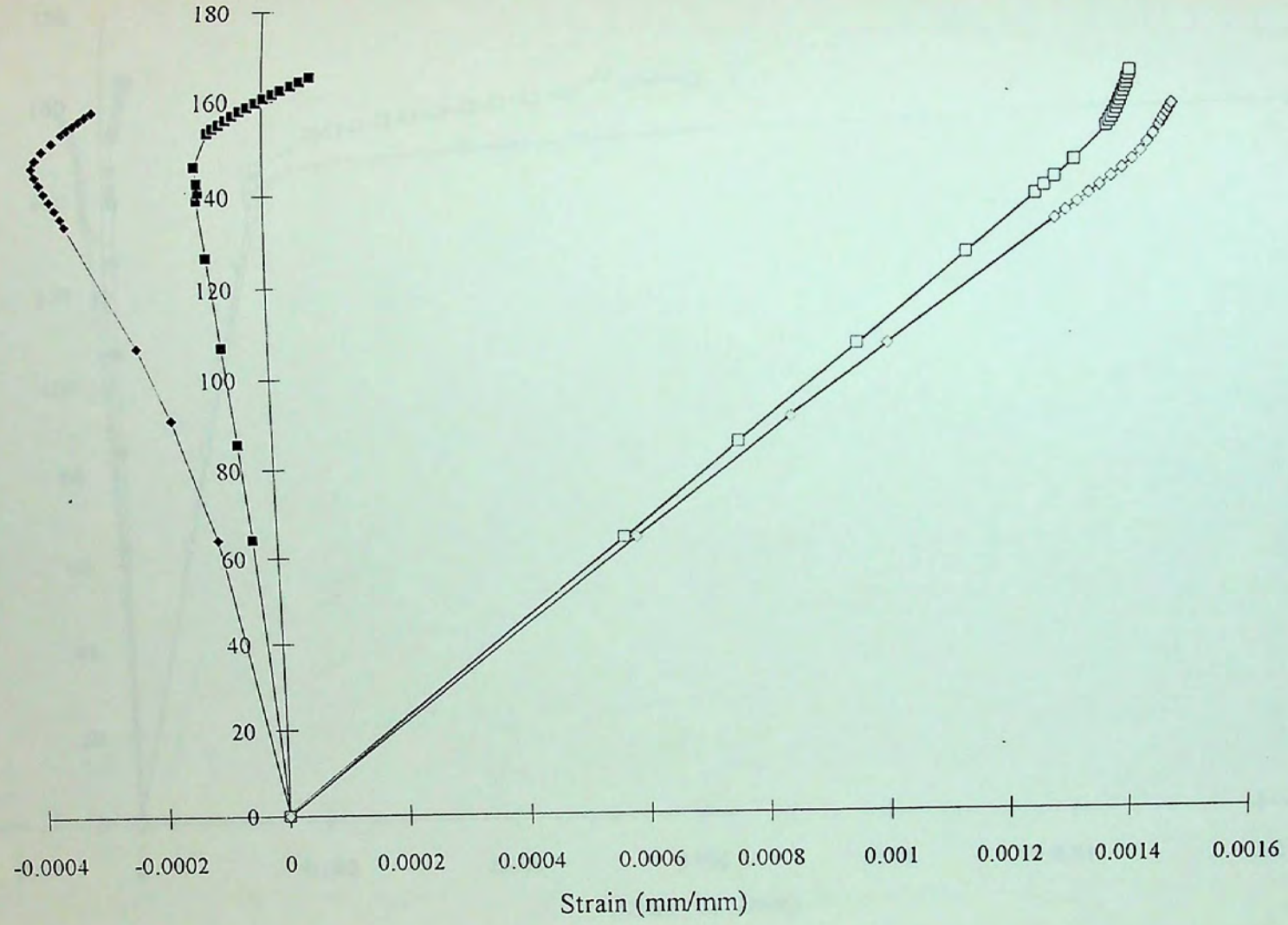

Figure 4.22(a)- Effect of Varying Degree of Interaction (Just Before Opening)

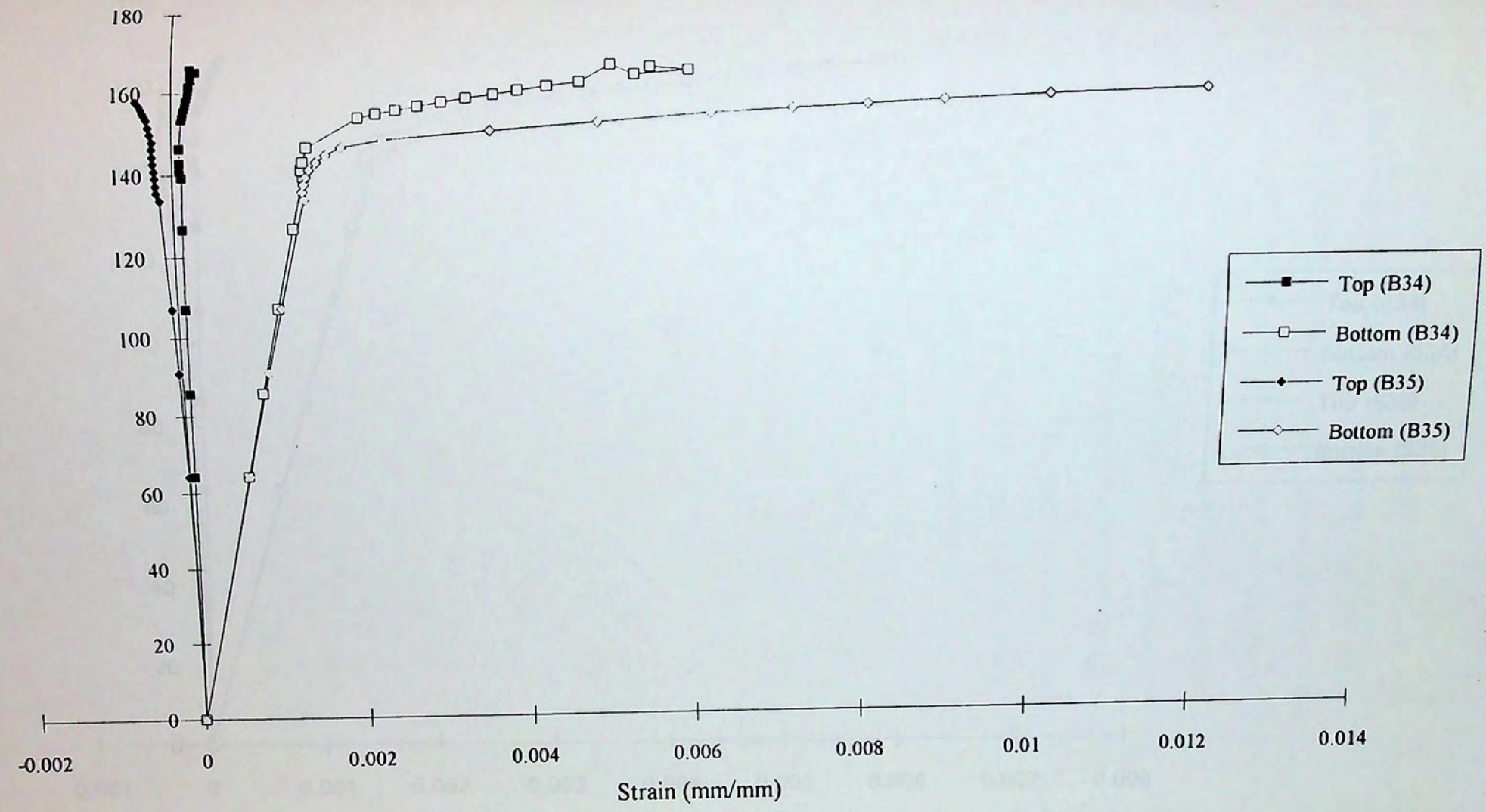

Figure 4.22(b)- Effect of Varying Degree of Interaction (Beginning of Opening)

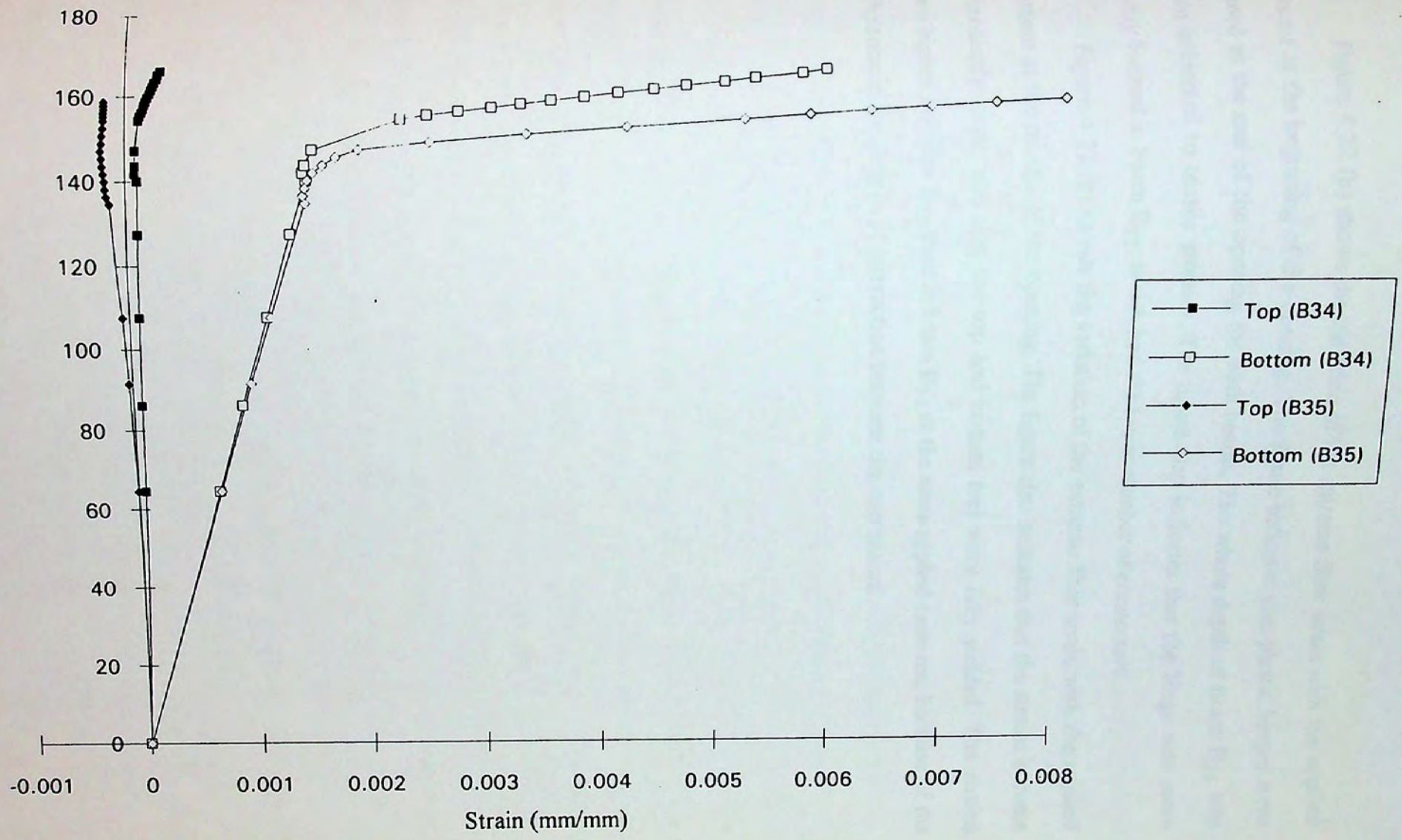

Figure 4.22(c)- Effect of Varying Degree of Interaction (Middle of Opening)

Figure 4.22 (b) shows the variation of the extreme fiber strain with the applied moment at the beginning of the opening. The figure indicates that plastic hinges were formed at the end of the opening for both beams. The whole depth of beam B_{34} was again subjected to tensile stresses. The figure also indicates that the hinge was more readily formed in beam B_{35}, which had the lower number of connectors.

Figure 4.22 (c) shows the variation of the extreme fiber strain with the applied moment at the middle of the opening. The figure also indicates that the strains became exceedingly large, and that the top and bottom tees were fully yielded. The strains were higher in beam B_{35} than in beam B_{34} at the same applied moment, because of the difference in the degree of interaction between the two beams.

CHAPTER 5
SUMMARY AND CONCLUSIONS

5.1. SUMMARY:

The finite difference method was used to construct a model to analyze the behavior of single span steel-concrete composite beams with web openings. The model accounts for partial interaction between the steel beam and the concrete slab, and can analyze steel beams supporting either ribbed or solid concrete slabs. Connection between the beam and the slab is provided by shear connections, placed at discrete locations along the span of the beam. Vertical shear along the opening length could be varying. The participation of the slab in resisting the vertical shear forces is taken into consideration, and the shear stress is considered to be uniform throughout the depth of the steel beam web. The vertical shear is divided between the beam and the slab according to their respective shear strength. Von-Mises yield criterion is adapted to determine the strength of the steel beam in resisting the equivalent stress resulting from the combined normal and shear stresses. The flange of the steel beam was not considered to resist any vertical shear. Linear strain distribution was assumed throughout the depth of the steel beam. Local buckling and instability failures were not considered in the model, and strain hardening of the steel was neglected. The model can analyze beams subjected to single or two-point-loading systems, or uniform loading.

The predictions of the model were compared with experimental results conducted by other investigators (4) (12), and were found to be in close agreement, with a tendency to being consistently conservative. The model factor was found to vary between 1.05 and 1.17. The conservatism of the model could be due to neglecting the participation of the flange in resisting vertical shear, and not considering strain hardening of the steel.

Having verified the validity of the model, it was used to plot the interaction diagrams of various composite beams. The interaction diagram plotted with the use

of the model was plotted by recording the ultimate moments and shear at the middle of the opening for all locations of the opening, and plotting them. Strains at failure were recorded, and the modes of failure of the beam for various locations of the opening along the span of the beam were also noted.

A parametric study was conducted to investigate the impact of changing some of the variables on the overall performance of the composite beam. The variables under study were the opening height, opening length, eccentricity of the opening with respect to the depth of the beam, and the number of connectors used in the shear span. 35 beams with various geometric properties were analyzed by the model, and their interaction diagrams were plotted and compared.

Eight beams (B_6 through B_{13}) were analyzed to determine the effect of varying the opening height on the behavior of composite beams with web openings. These beams were identical in all aspects except the opening height. Both the ultimate moment and shear capacities were found to be affected by varying the opening height; both the ultimate moment and shear capacities were found to decrease with increasing the opening height. The ultimate moment capacity for pure moment conditions was less affected by varying the opening height than the ultimate shear capacity for pure shear conditions. However, the ultimate shear capacity for pure shear conditions, for the analyzed beams, was found to be unaffected by increasing the opening height, if the reduction in web area was less than 54%.

Seven beams were analyzed to determine the impact of changing the opening length on the behavior of composite beams (beams B_8, B_9, and B_{14} through B_{18}). Both the ultimate moment and shear capacities were affected by varying the opening length; both the ultimate moment capacity for pure moment conditions and the ultimate shear capacity for pure shear conditions were higher for beams with shorter web openings. The impact of changing the opening length was more pronounced on the ultimate shear strength for pure shear conditions than for the ultimate moment capacity for pure moment conditions.

Five beams with different opening eccentricities with respect to the depth of the beam were analyzed to determine the impact of varying the opening eccentricity on the strength of composite beams (beams B_8 and B_{19} through B_{22}). Varying the eccentricity of the opening with regard to the beam depth was found to affect the ultimate moment capacity for pure moment conditions, and had no effect on the ultimate shear capacity for pure shear conditions. Beams in which the opening was closer to the top of the beam showed to have higher moment capacities for pure moment conditions. The ultimate shear strength for pure shear was not affected by varying the opening eccentricity because a uniform shear stress was assumed in the web of the steel beam.

The effect of varying the degree of interaction between the steel beam and the concrete slab was also investigated (beams B_8 and B_{23} through B_{26}). By increasing the number of connectors used in the shear span, the ultimate moment capacity for pure moment conditions increased. A reduction of 74.8% in the degree of interaction of B_8 caused a 17% loss in the ultimate moment capacity. The ultimate shear capacity of the beam was not affected for pure shear conditions.

Although web opening has a major effect on reducing the moment and shear capacity of the composite beams, the location of the opening may be selected such that the external moment and shear applied at the location of the opening will be less than the strength of the beam at this location, and failure occurs at the mid-span of the beam.

Variation of the extreme fiber strain with the applied moment was also investigated. The results of the study indicated that the Neutral Axis of the composite beam was continually raised as the applied moment increased, and that could result in the whole depth of the steel beam be subjected to tensile forces.

The effect of varying the opening height and eccentricity, and the number of connectors used on the strain-moment relation was also investigated. Formation of plastic hinges could be detected. The study showed that the plastic hinges were more readily formed in beams with larger opening heights, and with openings of negative

eccentricity. The number of connectors used was shown to significantly affect the strain distributions at all locations along the opening.

5.2. CONCLUSIONS:

Based on the results presented in this thesis, the following conclusions may be drawn:

1. The concrete slab contributes significantly to the shear and moment capacities of composite beams.
2. The height of the opening affects the ultimate strength of the composite beam; when the opening is placed in the low M/V region, the shear capacity of the composite beam decreases with the increase of opening height. When the opening is located at the mid-span of the beam, the ultimate moment capacity of the composite beam decreases with increasing the opening height. Between these two extreme locations, the % of reduction in both the ultimate moment and shear capacities vary with the change in M/V ratio.
3. The opening length also affects the capacity of the composite beam. At the low M/V region, the shear capacity of the composite beam decreases with increasing the opening length. At the mid-span of the beam, the ultimate moment capacity also decreases with increasing the opening length. Between these two extreme locations, the % of reduction in both the ultimate moment and shear capacities vary with the change in M/V ratio.
4. The effect of varying opening height or length on ultimate moment capacity for M/V=∞ is not as significant as their effect on ultimate shear capacity for M/V=0.
5. Eccentricity of the opening with regard to the beam depth does not affect the ultimate shear capacity of composite beams for low M/V locations of the opening. When the opening is placed in the pure-moment region of the beam, the ultimate moment capacity increases as the opening approaches the top of the beam. Between these two extreme locations, the percentage of reduction in both the ultimate moment and shear capacities vary with the change in M/V ratio.

6. Increasing the number of connectors in the shear span increases the ultimate moment capacity of the beam when the opening is placed at M/V=∞, but has no effect on the ultimate shear capacity when the opening is placed near the supports.
7. Based on geometric properties of the composite beam, reduction of the web are by opening up to corresponding limit has no effect on the ultimate shear capacity of the composite beam at M/V=0. For the analyzed beams, this percentage was 54%.
8. The composite beam can develop a large percentage of its ultimate moment capacity even with a low degree of interaction.
9. The Neutral Axis of the composite beam is continuously raised upwards. In some cases, the whole depth of the composite beam can be subjected to tensile stresses.

REFERENCES

1. Aglan, A.A. and Redwood, R.G.: **"Strain-Hardening Analysis Of Beams With Web-Rectangular Holes"**- The Arabian Journal for Science and Engineering, Vol. 12, No. 1, Sept. 1985. pp. 37-45.

2. Cho, S.H. and Redwood, R.G.: **"Slab Behavior In Composite Beams At Openings. I: Analysis"**- Journal of Structural Engineering, ASCE, Vol. 118, No. 9, Sept. 1992. pp. 2287-2303.

3. Cho, S.H. and Redwood, R.G.: **"Slab Behavior In Composite Beams At Openings. II: Tests And Verification"**- Journal of Structural Engineering, ASCE, Vol. 118, No. 9, Sept. 1992. pp. 2304-2322.

4. Clawson, W.C. and Darwin, D.: **"Tests Of Composite Beams With Web Openings"**- Journal of the Structural Division, ASCE, Vol. 108, No. ST1, Jan. 1982. pp. 145-162.

5. Clawson, W.C. and Darwin, D.: **"Strength Of Composite Beams At Web Openings"**- Journal of the Structural Division, ASCE, Vol. 108, No. ST3, March 1982. pp. 623-641.

6. Darwin, D. and Donahey, R.C.: **"LRFD For Composite Beams With Web Openings"**- Journal of Structural Engineering, ASCE, Vol. 114, No. 3, March 1988. pp. 535-552.

7. Darwin, D. and Lucas, W.K.: **"LRFD For Steel And Composite Beams With Web Openings"**- Journal of Structural Engineering, ASCE, Vol. 116, No. 6, June 1990. pp. 1579-1593.

8. Donahey, R.C.: **"Deflections Of Composite Beams With Web Openings"**- Proceedings of Structures Congress, Aug. 1987, (Building Structures), ASCE, New York, USA. pp. 404-417.

9. Donahey, R.C. and Darwin, D.: **"Web Openings In Composite Beams With Ribbed Slabs"**- Journal of Structural Engineering, ASCE, Vol. 114, No. 3, March 1988. pp. 518-534.

10. Fahmy, E.H.: **"Strength Of Composite Beams With Web Openings"**- Proceedings of 1988 Annual Conference of CSCE, Vol. 1, Calgary, Alberta, Canada, May 1988.

11. Fahmy, E.H.: **"Analysis Of Steel Beams With Rectangular Web Openings"**- Proceedings of 1989 Annual Conference of CSCE, Vol. 1, St. John's, Newfoundland, June 1989.

12. Lawson, R.M.: **"Design for Openings in the Webs of Composite Beams"**- SCI/CIRIA publication, SCI-P-068, 1987.

13. Lawson, R.M. and Chung, K.F. and Price, A.M.: **"Tests On Composite Beams With Large Web Openings To Justify Existing Design Methods"**- Journal of The Structural Engineer, Vol. 70, No. 1, Jan. 1992. pp. 1-7.

14. Ma. K.P.: **"Inelastic Analysis Of Composite Beams With Partial Connection"**- M.Sc. thesis, McMaster University, Hamilton, Ontario, Canada, Oct. 1973.

15. Redwood, R.G.: **"Design Of Beams With Web Holes"**- Publication by the Canadian Steel Industries Construction Council, Jan. 1974.

16. Redwood, R.G. and Cho, S.H.: **"Design Of Steel and Composite Beams With Web Openings"**- Journal of Constructional Steel Research, Vol. 25, 1993. pp. 23-41.

17. Redwood, R.G. and Poumbouras, G.: **"Analysis Of Composite Beams With Web Openings"**- Journal of Structural Engineering, ASCE, Vol. 110, No. 9, Sept. 1984. pp. 1949-1958.

18. Redwood, R.G. and Shrivastava, S.C.: **"Design Recommendations For Steel Beams With Web Holes"**- Canadian Journal of Civil Engineering, Vol. 7, Aug. 1980. pp. 642-650.

19. Redwood, R.G. and Wong, P.K.: **"Web Holes In Composite Beams With Steel Deck"**- Proceedings of Eighth Canadian Structural Engineering Conference, Canadian Steel Construction Council, Willowdale, Ontario, Canada, 1982.

20. Robinson, H.: **"Tests On Composite Beams With Cellular Deck"**- Journal of the Structural Division, ASCE, Vol. 93, No. ST4, Aug. 1967. pp. 139-164.

21. Robinson, H.: **"Composite Beams Incorporating Cellular Steel Decking"**- Journal of the Structural Division, ASCE, Vol. 95, No. ST3, March 1969. pp. 355-380.

22. Robinson, H. and Wallace, I.W.: **"Composite Beams with 1-½ Inch Metal Deck And Partial And Full Connection"**- The Engineering Journal, CSCE, Vol. 16, No. A-8, Sept. 1973. pp. I-VIII.

23. Thiruvengadam, T.R.: **"A Method For Inelastic Analysis Of Single Span Composite Beams"**- Ph.D. thesis, University of Illinois, Urbana, Illinois, USA, 1969.

24. Todd, D.M. and Cooper, P.B.: **"Strength Of Composite Beams With Web Openings"**- Journal of the Structural Division, ASCE, Vol. 106, No. ST2, Feb. 1980. pp. 431-444.

25. Wright, H.D. and Francis, R.W.: **"Tests On Composite Beams With Low Levels Of Shear Connection"**- Journal of The Structural Engineer, Vol. 68, No. 15, Aug. 1990. pp. 293-298.

APPENDIX A

FLOW CHART OF THE PROGRAM

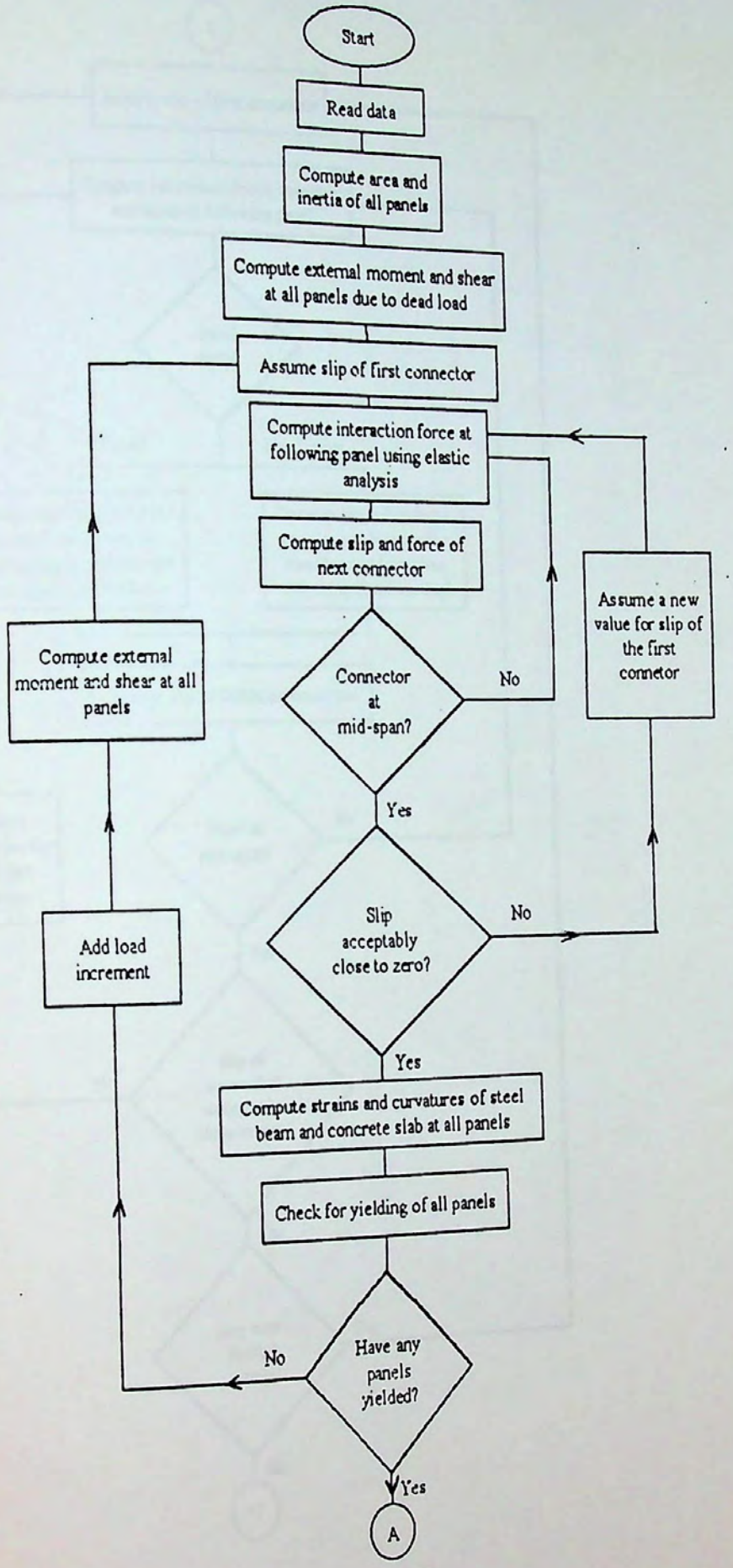
Start
Read data
Compute area and inertia of all panels
Compute external moment and shear at all panels due to dead load
Assume slip of first connector
Compute interaction force at following panel using elastic analysis
Compute slip and force of next connector
Connector at mid-span?
No
Yes
Assume a new value for slip of the first connetor
Slip acceptably close to zero?
No
Yes
Add load increment
Compute external moment and shear at all panels
Compute strains and curvatures of steel beam and concrete slab at all panels
Check for yielding of all panels
Have any panels yielded?
No
Yes
A

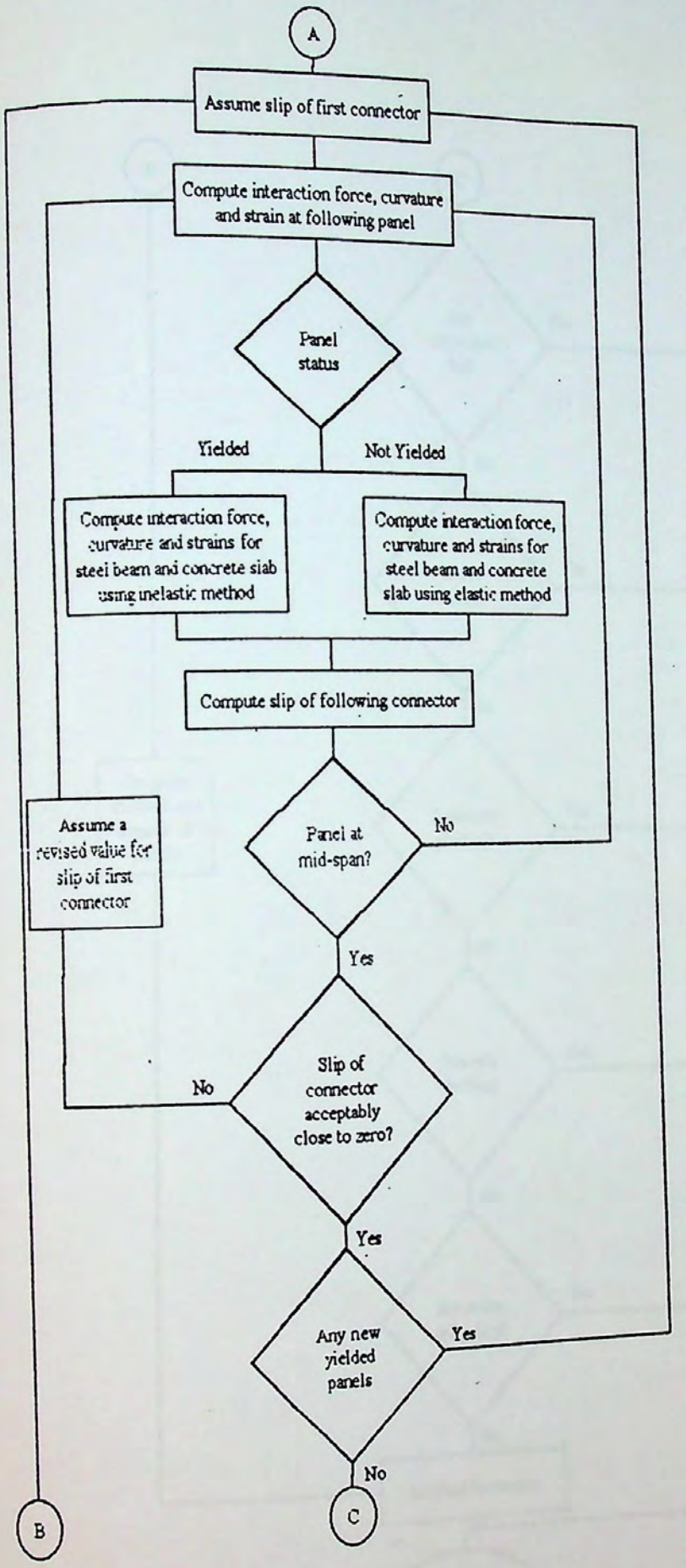
A
Assume slip of first connector
Compute interaction force, curvature and strain at following panel
Panel status
Yielded
Not Yielded
Compute interaction force, curvature and strains for steel beam and concrete slab using inelastic method
Compute interaction force, curvature and strains for steel beam and concrete slab using elastic method
Compute slip of following connector
Assume a revised value for slip of first connector
Panel at mid-span?
No
Yes
Slip of connector acceptably close to zero?
No
Yes
Any new yielded panels
Yes
No
B
C

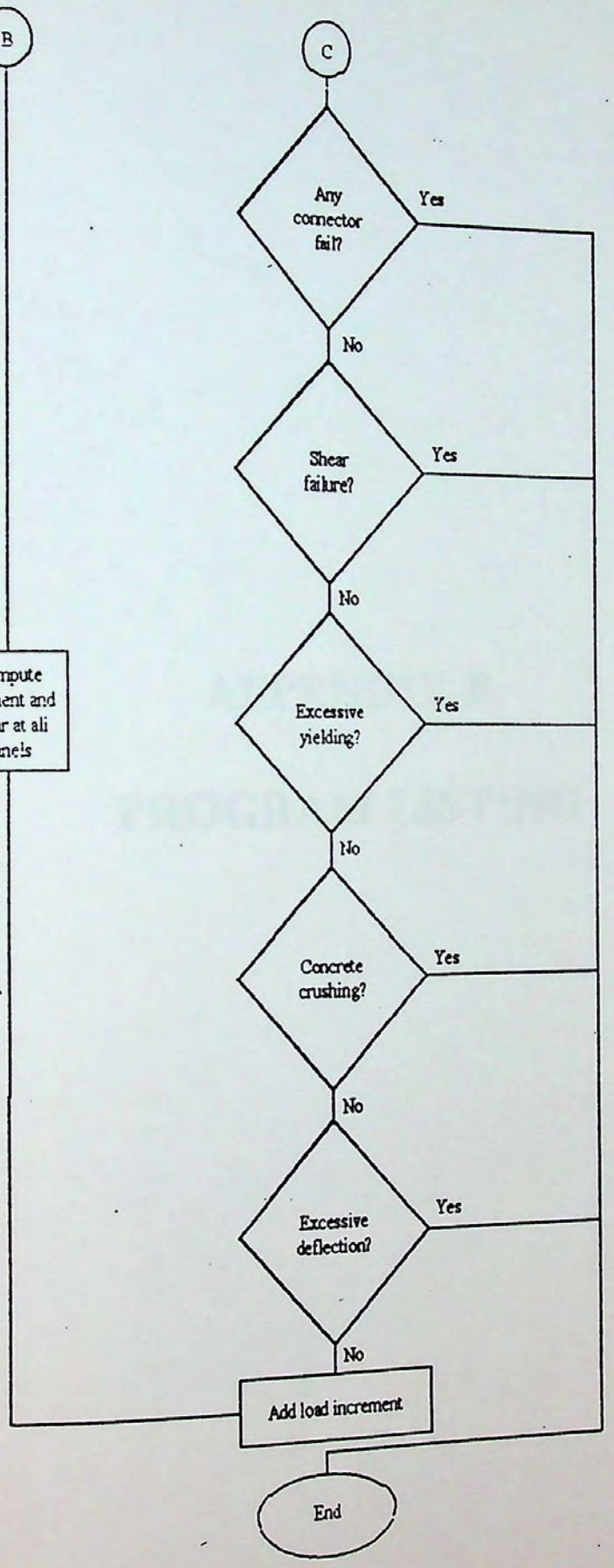
B
Compute moment and shear at all panels
C
Any connector fail?
Yes
No
Shear failure?
Yes
No
Excessive yielding?
Yes
No
Concrete crushing?
Yes
No
Excessive deflection?
Yes
No
Add load increment
End

APPENDIX B

PROGRAM LISTING

```
C                    ***************************
C                    * START OF THE PROGRAM *
C                    ***************************
C
C
      CHARACTER *16 FILENAME
      DIMENSION TITLE(20)
      DIMENSION AWEB(50),SHEARD(50),SHEAR(50),STWT(50),LIN(50)
      DIMENSION DEF(51),BMDL(51),Q(51),SL(51),CURD(51),AREA(51)
      DIMENSION GC(50,4),GS(50,4),GSL(50,4),GST(50,4)
      DIMENSION LABAL(50),TOTBM(50),EAC(6),STWB(50)
      DIMENSION ANTEG(50),HB(50),FAC(6),FAC2(6),SHFAC(50)
      DIMENSION INELA(50),CURS(50),CURB(50),TRSL(3)
      DIMENSION XX1(51),ZK(51),X(51),A(3,50),B(50),A1(100)
      DIMENSION STSB1(50),KOUT(50),TAREA(101),STOT(50),STOB(50),ITYP(50
      COMMON/BL1/WM(4)
      COMMON/BL2/FS(50),CS1
      COMMON/BL3/BMM(50)
      COMMON/BL4/BMS(50),BMB(50),BIT(50),TW,TF,BF,DS,BS,AB(50),DC
      COMMON/BL5/STSY,STRSY,STRPY,STRWY,STRFY,FB,STFY,ES,EBP,EX
      COMMON/BL6/FB(50)
      COMMON/BL7/CUR1(50)
      COMMON/BL8/CURB1(50)
      COMMON/BL9/CURS1(50)
      COMMON/BL10/AS(50),SI(50),SEI(50),EAB(50),EIB(50),Z(50),CS(50)
      COMMON/BL11/BET(50),ALP(50),BB(50),SS(50)
      COMMON/BL12/DN(50)
      COMMON/BL14/BM(50)
      COMMON/BL13/DBT(50),CBD(50),CB(50)
      COMMON/BL16/CURD1(50)
      COMMON/BL17/STST(50),STBB(50)
      COMMON/BL18/STSB(50)
      COMMON/BL19/STBT(50)
      COMMON/BL20/CUR(50)
      COMMON/BL21/BH(165),DDB(165),DFA(165),HARST,NFC,NFD,NW,NPL,PCUT
      COMMON/BL23/CURT(50),STBBT(50),STSTT(50)
      COMMON/BL24/BMBE(50),BMSL(50),BMFD(50)
      COMMON/BL25/MA,JM,NH,KER,KEM2
      COMMON/BL26/STC(50),CUC(50)
      COMMON/BL27/KKCC,MERM,MMM
      COMMON/BL28/GSNH,ERST,SCAL1,SCAL2
      COMMON/BL29/UU,VV,XL,XR,MER1,MER2,SAS(80),SLM(80),LAG
      COMMON/BL30/XX(50),XOL,XOR,NOT,NO,NOB,TAW(50),MSHEAR
      WRITE (*,4000)
 4000 FORMAT(1X,'ENTER INPUT FILE NAME',/)
      READ(*,4001) FILENAME
 4001 FORMAT(A16)
      OPEN(3,FILE=FILENAME,STATUS='OLD')
      WRITE (*,4002)
 4002 FORMAT(1X,'ENTER OUTPUT FILE NAME',/)
      READ (*,4001) FILENAME
      OPEN(6,FILE=FILENAME,STATUS='NEW')
```

```
C                    ****************************
C                    * DATA OF COMPOSITE BEAM *
C                    ****************************
C     READ(3,5300) TITLE
5300  FORMAT(20A4)
      WRITE(6,5301) TITLE
5301  FORMAT(1X,20A4,///)
      READ(3,*) DB,TW,TF,BF,BI
      READ(3,*) DS,BS,ZL
      READ(3,*) XOL,XOR,DOT,DOB,SLFAC
      WRITE(6,50)DB,TW,TF,BF,BI,DS,BS,ZL
      WRITE(6,50)XOL,XOR,DOT,DOB,SLFAC
      READ(3,*) U,SD4,DC,DL
      READ(3,*) HARST,RPE,SLMAX,DFMAX
      WRITE(6,50) U,SD4,DC,DL,HARST,RPE,SLMAX,DFMAX
      READ(3,*) STRSY,STRPY,STRWY,STRFY
      READ(3,*) STSTF,STSBF,STBTF,STBBF
      WRITE(6,50)STRSY,STRPY,STRWY,STRFY,STSTF,STSBF,STBTF,STBBF
      READ(3,*) ES,EB,EX
      WRITE(6,2)ES,EB,EX
      READ (3,*) DW1,DW2,DW3,DW4,DW5,DW6,DW7
      WRITE(6,85) DW1,DW2,DW3,DW4,DW5,DW6,DW7
      READ (3,*) W,WW3,WW4,WW5,WW6,WW7,WW8
      WRITE(6,85) W,WW3,WW4,WW5,WW6,WW7,WW8
      READ (3,*) N,NSHOR,LOAD,NFU,NFD,NPL,NOT,NO,NOB
      WRITE(6,1) N,NSHOR,LOAD,NFU,NFD,NPL,NOT,NO,NOB
      READ(3,*) WPL,TPL,PCUT
      WRITE(6,9)WPL,TPL,PCUT
49    FORMAT(6F10.4)
50    FORMAT(8F15.5)
2     FORMAT(3F10.0)
31    FORMAT(7F10.2)
85    FORMAT(7F15.2)
1     FORMAT(9I5)
9     FORMAT(3F10.5)
      READ(3,*) G2,G3,Q2,Q3,SLIN
      WRITE(6,1000)G2,G3,Q2,Q3,SLIN
1000  FORMAT(5F10.4)
      READ(3,*) NCE,NC,ER12,ER10,ACURA,TRYLD
      WRITE(6,237)NCE,NC,ER12,ER10,ACURA,TRYLD
237   FORMAT(2I10,4F10.6)
      READ(3,*)(FAC(I),I=1,3)
      READ(3,*)(FAC2(I),I=1,3)
      READ(3,*) (EAC(I),I=1,3)
238   FORMAT(3F10.5)
      DO 7776 I=1,3
      FAC(I+3)=2.-FAC(I)
      FAC2(I+3)=2.-FAC2(I)
      EAC(I+3)=2.-EAC(I)
7776  WRITE(6,7755) I,FAC(I),FAC2(I),EAC(I)
7755  FORMAT(' NO',I2,5X,'FAC',F9.5,5X,'FAC2',F9.5,5X,'EAC ',F9.5)
      READ(3,*) ERIN,CFST,FRACT,EACL,EACS,FALA,NCHA
      WRITE(6,79)ERIN,CFST,FRACT,EACL,EACS,FALA,NCHA
79    FORMAT(6F10.7,I10)
      READ(3,*) ERST,FANEG
7     WRITE(6,7)ERST,FANEG
      FORMAT(2F10.6)
```

```
C                ****************************************
C                * INITIAL VALUES OF CONTROL FACTORS *
C                ****************************************
C
      K=0
      MA=0
      JMK=0
      KKCC=0
      KER=0
      KSCH=0
      KM=0
      KN=0
      FACTOR=1.
      KMUL=0
      SCAL1=1.0
      SCAL2=10.0
      KEM2=0
      KNEG=0

C     AB1=2.*TF*BF+TW*(DB-2.*TF)
      STSY=STRSY/ES
      STBY=STRPY/EB
      STFY=STRFY/EB
      EBP=RPE*EB
      write(*,*)rpe,ebp
C                ********************************
C                * DIVISION OF THE STEEL BEAM *
C                ********************************
C
      NW=NOT+NO+NOB
      NN=NFU+NW+NFD+NPL
      DO 131 KL=1,NN
      DDB(KL)=TF/FLOAT(NFU)
      IF(KL.GT.NFU) DDB(KL)=(DOT-TF)/FLOAT(NOT)
      IF(KL.GT.(NFU+NOT)) DDB(KL)=(DOB-DOT)/FLOAT(NO)
      IF(KL.GT.(NFU+NOT+NO)) DDB(KL)=(DB-DOB-TF)/FLOAT(NOB)
      IF(KL.GT.(NFU+NW)) DDB(KL)=TF/FLOAT(NFD)
      IF(KL.GT.(NFU+NW+NFD)) DDB(KL)=TPL/FLOAT(NPL)
      BH(KL)=BF
      IF(KL.GT.NFU) BH(KL)=TW
      IF(KL.GT.(NFU+NW)) BH(KL)=BF
      IF(KL.GT.(NFU+NW+NFD))BH(KL)=WPL
  131 CONTINUE
      DFA(1)=DDB(1)
      DO 132 I=2,NN
  132 DFA(I)=DFA(I-1)+DDB(I)
  140 CONTINUE
C                ******************************
C                * LOAD-SLIP CHARACTERISTICS *
C                ******************************
      BV=(G2*Q2*Q3-G3*Q3*Q2)/(G2*Q3-G3*Q2)
      CV=(BV*G2*Q2-BV*BV*G2)/Q2
      AV=CV/BV
      DO 1100 I=1,30
      SL(I)=FLOAT(I)/200.
      Q(I)=(CV/(SL(I)-AV))+BV
 1100 WRITE(6,6005)SL(I),Q(I)
 6005 FORMAT(' SLIP AND FORCES',F7.4,F13.2)
```

```
C                ****************************************
C                * CONNECTORS SPACINGS AND COORDINATES *
C                ****************************************
C       NH=(N-1)/2
        NH1=NH+1
        READ(3,*) (SS(I),I=1,NH)
        WRITE(6,23) (SS(I),I=1,NH)
 32     FORMAT(14F5.1)
 23     FORMAT(' CONNECTOR SPACING',22F6.2)
 63     IF(JMK.LT.3) GO TO 54
        READ(3,*) N,NLA
        WRITE(6,35)N,NLA
 35     FORMAT(' NO OF TOTAL CONN.AFTER INTRODUCING PSEUDO ONES',I3,5X,
     1'NO OF PSEUDO CONN.',I3)
        IF(NLA.EQ.0) GO TO 999
        NH=(N-1)/2
        NH1=NH+1
        READ(3,*) (SS(I),I=1,NH)
 64     FORMAT(' NEW CONNECTOR SPACING',22F7.2)
        READ(3,*) (LABAL(I),I=1,NLA)
        WRITE(6,75) (LABAL(I),I=1,NLA)
 75     FORMAT(' PSEUDO CONNECTOR',40I3)
 61     FORMAT(2I5)
 999    W=WST
 54     JM=0
        XX(1)=SD4+.5*SS(1)
        DO 3 I=2,NH
 3      XX(I)=XX(I-1)+.5*(SS(I-1)+SS(I))
        X(1)=SD4
        DO 36 I=2,NH1
        X(I)=X(I-1)+SS(I-1)
 36     write(*,*)X(I)
C
        QIN=(CV/(SLIN-AV))+BV
        DO 1002 I=1,NH1
 1002   ZK(I)=QIN/SLIN
C                ********************************
C                * AREA AND MOMENT OF INERTIA *
C                ********************************
        DO 58 I=1,NH
        INELA(I)=0
        ITYP(I)=1
 58     DN(I)=DS
        AREAP=TPL*WPL
        ABO=AB1-TW*(DOB-DOT)
        AB1P=AB1+AREAP
        ABOP=ABO+AREAP
        YCMO=(AB1*0.5*DB-(TW*(DOB-DOT)*(DB-(DOT+DOB)/2.)))/ABO
        YCMP=(AB1*(0.5*DB+TPL)+AREAP*0.5*TPL)/(AB1P)
        YCMOP=(AB1*(0.5*DB+TPL)+AREAP*0.5*TPL-(TW*(DOB-DOT)*(DB+TPL-(DOT+
     1DOB)/2.)))/ABOP
        BPIO=BI+AB1*((0.5*DB-YCMO)**2)-(TW*(DOB-DOT)**3/12.+TW*(DOB-DOT)*
     1(DB-(DOT+DOB)/2.-YCMO)**2)
        BPIP=BI+AB1*((0.5*DB-(YCMP-TPL))**2)+(WPL*(TPL**3))/12.
     1+AREAP*((YCMP-0.5*TPL)**2)
```

```
      BPIOP=BI+AB1*((0.5*DB-YCMOP+TPL)**2)+(WPL*(TPL**3))/12.
     1+AREAP*((YCMOP-0.5*TPL)**2)-(TW*(DOB-DOT)**3/12.+TW*(DOB-DOT)*
     1(DB-(DOT+DOB)/2.-YCMOP+TPL)**2)
      DO 360 I=1,NH
      IF(XX(I).GE.XOL.AND.XX(I).LE.XOR) GO TO 3333
      IF(XX(I).GE.PCUT) GO TO 3335
      AB(I)=AB1
      BIT(I)=BI
      DBT(I)=DB
      CB(I)=0.5*DB
      CBD(I)=0.5*DB
      AWEB(I)=TW*(DB-2.*TF)
      GO TO 360
 3333 IF(XX(I).GE.PCUT) GO TO 3334
      AB(I)=ABO
      BIT(I)=BPIO
      DBT(I)=DB
      CB(I)=DB-YCMO
      CBD(I)=YCMO
      AWEB(I)=TW*(DB-(DOB-DOT)-2.*TF)
      GO TO 360
 3334 AB(I)=ABOP
      BIT(I)=BPIOP
      DBT(I)=DB+TPL
      CB(I)=DB+TPL-YCMOP
      CBD(I)=YCMOP
      AWEB(I)=TW*(DB-(DOB-DOT)-2.*TF)
      GO TO 360
 3335 AB(I)=AB1P
      BIT(I)=BPIP
      CBD(I)=YCMP
      CB(I)=DB+TPL-YCMP
      DBT(I)=DB+TPL
      AWEB(I)=TW*(DB-2.*TF)
  360 CONTINUE
      do 5555 i=1,nh
      write (6,*) i,x(i),bit(i),xol,xor
 5555 continue
C     ***************************************************************
C     * COMPUTATION OF THE SHEAR FACTOR FOR THE COMPOSITE BEAM *
C     ***************************************************************
      WRITE(6,*)'@£@£@£@ I     AWEB(I)    SHFAC @£@£@£'
      DO 761 I=1,NH
      SHFAC(I)=(AWEB(I)*STRWY/SQRT(3.))/(AWEB(I)*STRWY/SQRT(3.)
     1+10.5*SQRT(STRSY)*DS*DS)
      WRITE(6,*)I,AWEB(I),SHFAC(I)
  761 CONTINUE
C     ***************************************
C     * COMPUTATION OF B.M. DUE TO D.L. *
C     ***************************************
      TDL2=.5*DL*ZL
      DO 22 I=1,NH
      SHEARD(I)=TDL2-DL*XX(I)
   22 BMDL(I)=TDL2*XX(I)-DL*XX(I)*XX(I)*.5
   99 CONTINUE
      BMDLM=TDL2*(0.5*ZL)-DL*((ZL*0.5)**2)*0.5
      WRITE(6,7001)BMDLM
 7001 FORMAT( ' MID-SPAN B.M. DUE TO D.L. ',F12.2)
```

```
C                ****************************************
C                * COMPUTATION OF THE EFFECT OF D.L. *
C                ****************************************
C     IF(NSHOR.GT.0) GO TO 43
      CURVATURE DUE TO D.L. WILL BE ZERO IF THE BEAM IS SHORED.
C     DO 44 I=1,NH
      CURD(I)=0.
 44   GO TO 45
      DO 46 I=1,NH
 43   CURD(I)=BMDL(I)/(EB*BIT(I))
 46   DO 48 I=1,NH
      BMDL(I)=0.
 48   CONTINUE
           ************************************************************
C          * COMPUTATION OF THE EFFECT OF D.L. ON THE UNSHORED BEAM *
C          ************************************************************
C
 45   IF(JMK.EQ.3.AND.JM.EQ.0) GO TO 300
      GO TO 301
 300  IF(NSHOR-1) 301,302,302
 302  W=0.
      BMLL=0.
      BMMSP=BMDLM
      DO 304 I=1,NH
      CUR(I)=CURD(I)
      CURB(I)=CURD(I)
      STBT(I)=-CURB(I)*CB(I)
 304  STBB(I)=CURB(I)*CBD(I)
      WRITE(6,303)
 303  FORMAT(/////,' AT THIS LOADING THE D.L. EFFECT IS COMPUTED')
C      WRITE(6,311)
C 311  FORMAT(1HO,/,6X,'X',8X,'STBT',10X,'STBB',/)
C      WRITE(6,312)  (XX(I),STBT(I),STBB(I),I=1,NH)
C 312  FORMAT(1HO,F8.2,2E16.8)
 311  CONTINUE
 312  CONTINUE
      GO TO 305
 301  CONTINUE
C     ************************************************************************
C     * LOADING INCREMENT AND INITIAL VALUE OF OTHER CONTROL FACTORS .*
C     * VALUES OF MER1 & MER2 ARE SET ARBIRRARILY TO DIFFER FROM MERM *
C     ************************************************************************
      MMM=1
      WST=W
      DELW=DW1
 18   CONTINUE
      KN=0
      KM=0
      MERM=0
      MER1=100
      MER2=100
      CURP=0.
      LAG=0
      JM=JM+1
```

```
      JMK=JMK+1
      IF(TRYLD.EQ.1.) GO TO 8000
      IF(K.NE.0)    DELW=DW2
      IF(W.GE.WW3) DELW=DW3
      IF(W.GE.WW4) DELW=DW4
      IF(W.GE.WW5) DELW=DW5
      IF(W.GE.WW6) DELW=DW6
      IF(W.GE.WW7) DELW=DW7
      GO TO 77
 8000 DELW=1500.
      IF(K.NE.0) DELW=1500.
      IF(JMK.LE.6) GO TO 900
      IF(STBB(NH).GT.0.008)DELW=500.
      IF(STBB(NH).GT.0.02) DELW=250.
      IF(LOAD.EQ.3)DELW=(2./ZL)*DELW
      GO TO 77
  900 IF(LOAD.EQ.3)DELW=(2./ZL)*DELW
   77 W=W+DELW*FACTOR
      IF(JM.EQ.1.AND.NSHOR.EQ.0) W=0.
      IF(JM-4) 6100,6100,6101
 6100 WM(JM)=W
      GO TO 6102
 6101 DO 6103 I=1,3
 6103 WM(I)=WM(I+1)
  204 WM(4)=W
 6102 WRITE(6,34)W
   34 FORMAT(1HO,///,4H W =,F11.3)
      write(*,*)w
      MSHEAR=0
C                      **********************
C                      * B.M. CALCULATION *
C                      **********************
      REACL=W*0.5
      IF(LOAD.EQ.2) GO TO 102
      IF(LOAD.EQ.3) GO TO 1991
      DO 4 I=1,NH
      BM(I)=REACL*XX(I)+BMDL(I)
      SHEAR(I)=SHFAC(I)*REACL+SHEARD(I)
    4 CONTINUE
      BMLL=REACL*(ZL*0.5)
      GO TO 103
  102 DO 108 I=1,NH
      IF(XX(I).GT.U.AND.XX(I).LE.(ZL/2.)) BM(I)=BMDL(I)+REACL*U
      IF(XX(I).LE.U) SHEAR(I)=SHFAC(I)*REACL+SHEARD(I)
      IF(XX(I).GT.U) SHEAR(I)=SHEARD(I)
  108 IF(XX(I).LE.U)  BM(I)=BMDL(I)+REACL*XX(I)
      BMLL=REACL*U
      GO TO 103
 1991 REACL=W*ZL*.5
      DO 1992 I=1,NH
      BM(I)=BMDL(I)+REACL*XX(I)-.5*W*XX(I)*XX(I)
      SHEAR(I)=SHFAC(I)*(REACL-W*XX(I))+SHEARD(I)
 1992 CONTINUE
      BMLL=REACL*(.5*ZL)-.5*W*((.5*ZL)**2)
  103 DO 5 I=1,NH
      IF(NSHOR.EQ.0) TOTBM(I)=BM(I)
      IF(NSHOR.EQ.1) TOTBM(I)=BM(I)+(TDL2*XX(I)-DL*XX(I)*XX(I)*0.5)
    5 CONTINUE
      BMMSP=BMDLM+BMLL
```

```
C     ************************************************************************
C     * SOLVING THE FINITE DIFFERENCE EQUATION FOR THE FIRST TWO TRIAL *
C     *                              VALUES OF SLIP                            *
C     ************************************************************************
C     IF(JMK.GT.6) GO TO 8
      IF(JMK.GT.3) GO TO 2001
      NH2=2*NH
      NH21=NH2-1
      DO 9000 I=1,NH2
 9000 A1(I)=0.0
      DO 5101 I=1,NH
      CALL TERMS(I,EB,ES)
   92 FORMAT(F40.8)
      B(I)=-BB(I)
      A(2,I)=-(1./ZK(I)+1./ZK(I+1)+ALP(I)*SS(I))
      A(3,I)=1./ZK(I+1)
 5101 A(1,I)=1./ZK(I)
      A(1,1)=0.
      A(3,NH)=0.
      A(2,NH)=-(1./ZK(NH)+ALP(NH)*SS(NH))
      II=1
      DO 9900 I=1,NH21,2
      A1(I)=-A(2,II)
      IF(I.EQ.NH21) GO TO 9900
      A1(I+1)=-A(1,II+1)
      II=II+1
 9900 CONTINUE
      DET= 10.**(-7)
      CALL BAND(A1,B,NH,2,1,DET)
      Q(1)=B(1)
      DO 5105 I=2,NH
 5105 Q(1)=B(1)-B(1-1)
      Q(NH+1)=0.
      DO 5665 I=1,NH
 5665 SL(I)=Q(I)/ZK(I)
      SL(NH+1)=0.
      TRSL(JMK)=SL(1)
      IF(JMK.LT.3) GO TO 18
      IF(JMK.EQ.3) GO TO 63
C     ************************************************************************
C     * ST BAR, CUR BAR AND STSTT BAR ARE FOUND HERE BY EXTRAPOLATION *
C     ************************************************************************
    8 CALL EXTRA(1,GSL,SUML)
      WRITE(6,92) SUML
      GSL(1,4)=SUML
      DO 902 I=1,NH
      CALL EXTRA(I,GC,SUML)
      GC(I,4)=SUML
      CALL EXTRA(I,GS,SUML)
      GS(I,4)=SUML
      CALL EXTRA(I,GST,SUML)
      GST(I,4)=SUML
  902 CONTINUE
      GSNH=GS(NH,4)
      IF(GSNH.GE.CFST) GO TO 9250
```

```
      GO TO 851
 9250 DO 9253 I=1,6
 9253 FAC(I)=FAC2(I)
  851 SAS(MMM)=GSL(1,4)
      IF(MSHEAR.EQ.1) SAS(MMM)=SLFAC*SAS(MMM)
      WRITE(6,2858) SAS(MMM)
 2858 FORMAT(//,'  SLIP ASSUMED',F15.6)
C             ***************************************
C             * BEGINNING OF ELASTIC COMPUTATION *
C             ***************************************
C
      IF(K.NE.0) GO TO 70
 2001 IF(JMK.EQ.4) SAS(MMM)=TRSL(1)
      IF(JMK.EQ.5) SAS(MMM)=TRSL(2)
      IF(JMK.EQ.6) SAS(MMM)=GSL(1,2)+((GSL(1,2)-GSL(1,1))/(WM(2)-WM(1)))
     1*(WM(3)-WM(2))
 1624 SL(1)=SAS(MMM)
      I=1
      NLAB=1
  565 Q(I)=(CV/(SL(I)-AV))+BV
      IF(I.EQ.LABAL(NLAB)) GO TO 15
      GO TO 16
   15 NLAB=NLAB+1
      Q(I)=0.
   16 CALL TERMS(I,EB,ES)
      IF(I-1) 800,800,801
  801 B(I)=Q(I)+B(I-1)
      GO TO 802
  800 B(I)=Q(I)
  802 HB(I)=B(I)*ALP(I)*SS(I)+BB(I)
      SL(I+1)=SL(I)+HB(I)
      IF(B(I).LT.(-200000.)) GO TO 289
      IF(Q(I).LT.(-200000.)) GO TO 289
      GO TO 290
  289 SAS(MMM)=SAS(MMM)*FALA
      KSCH=KSCH+1
      WRITE(6,291)
  291 FORMAT('ORIGINAL SLIP ASSUMED IS TOO SMALL')
      GO TO 1624
  290 I=I+1
      IF(I.LT.NH1) GO TO 565
      SLM(MMM)=SL(NH1)
      IF(JM.LE.3.AND.ABS(SLM(MMM)).LE.ERIN) GO TO 57
      IF(ABS(SLM(MMM))-ER12) 57,57,2323
 2323 WRITE(6,1239) MMM,SAS(MMM),SLM(MMM)
      MMM=MMM+1
      IF(MMM.GT.NCE) GO TO 26
C             ***************************************************
C             * PREDICT THE VALUE OF SLIP FOR THE NEXT CYCLE *
C             ***************************************************
      IF(SLM(MMM-1).LE.(-.03)) SAS(MMM)=SAS(MMM-1)*EAC(1)
      IF(SLM(MMM-1).GT.(-.03).AND.SLM(MMM-1).LE.(-.001 ))
     1SAS(MMM)=SAS(MMM-1)*EAC(2)
      IF(SLM(MMM-1).GT.(-.001).AND.SLM(MMM-1).LE.0.)SAS(MMM)=
     1SAS(MMM-1)*EAC(3)
```

```
      IF(SLM(MMM-1).GE.(0.03 )) SAS(MMM)=SAS(MMM-1)*EAC(4)
      IF(SLM(MMM-1).LT.(0.03 ).AND.SLM(MMM-1).GE.(.001 ))
     1SAS(MMM)=SAS(MMM-1)*EAC(5)
      IF(SLM(MMM-1).LT..001 .AND.SLM(MMM-1).GE.0.) SAS(MMM)=
     1SAS(MMM-1)*EAC(6)
      IF(SLM(MMM-1).LE.(-.1)) SAS(MMM)=SAS(MMM-1)*EACL
      IF(SLM(MMM-1).GE.1.) SAS(MMM)=SAS(MMM-1)*EACS
      IF(MMM.LE.2) GO TO 1624
      CALL REGULA (MMM,MERM)
      IF(ABS(SAS(MMM-1)-SAS(MMM-2)).LE.0.0000003) SAS(MMM)=(XL+XR)*0.5
      GO TO 1624
   57 WRITE(6,1239)MMM,SAS(MMM),SLM(MMM)
      WRITE(6,1248)
      SREC=SAS(MMM)
      MMB=MMM-1
      MMM=1
      KSCH=0
      LAG=0
      IF(SL(NH1-2).LE.0.) GO TO 470
      GO TO 471
  470 KMUL=KMUL+1
      W=W-(DELW/FLOAT(KMUL+1))
      IF(KMUL.EQ.5) GO TO 26
      IF(JM.GT.4) GO TO 204
      WM(JM)=W
      GO TO 6102
  471 KMUL=0
C                 *********************************
C                 * END OF ELASTIC COMPUTATION *
C                 *********************************
      DO 14 I=1,NH
      CUR(I)=(BM(I)-B(I)*Z(I))/SEI(I)
      CURS(I)=CUR(I)
      CURB(I)=CUR(I)+CURD(I)
      STST(I)=-B(I)/(ES*AS(I))-CS(I)*CURS(I)
      STSB(I)=CURS(I)*DS+STST(I)
      STBT(I)=B(I)/(EB*AB(I))-CURB(I)*CB(I)
      STOT(I)=B(I)/(EB*AB(I))-CURB(I)*(CB(I)-DOT)
      STBB(I)=B(I)/(EB*AB(I))+CURB(I)*CBD(I)
      STOB(I)=B(I)/(EB*AB(I))+CURB(I)*(DOB-CB(I))
      STWT(I)=STBT(I)+CURB(I)*TF
      STWB(I)=STBT(I)+CURB(I)*(DB-TF)
      TAW(I)=SHEAR(I)/AWEB(I)
      DN(I)=-STST(I)/CUR(I)
      IF(DN(I).GT.DS.OR.DN(I).LT.0.) DN(I)=DS
   14 CONTINUE
      WRITE(6,330) (STBB(I),I=1,NH)
  330 FORMAT(   ' STBB',8F15.5)
C                 ************************************
C                 * CHECK FOR YIELDING OF THE PANELS *
C                 ************************************
      DO 8855 I=1,NH
      LIN(I)=0
 8855 CONTINUE
```

```
      DO 52 I=1,NH
      STY=STFY
      IF(XX(I).GE.PCUT) STY=STBY
      IF((3.*TAW(I)**2).GT.(STRWY**2)) GOTO 4045
      STRWY1=SQRT(STRWY**2-3.*(TAW(I)**2))
      WRITE(6,*) I,STRWY1
      IF(ABS(STST(I)).LE.STSY.AND.STBB(I).LE.STY) GO TO 5552
      GO TO 5554
 5552 STRWT=STWT(I)*EB
      STRWB=STWB(I)*EB
      IF(ABS(STRWT).LE.STRWY1.AND.ABS(STRWB).LE.STRWY1) GO TO 52
 5554 IF(K.EQ.0) GO TO 53
      DO 84 LL=1,K
      IF(INELA(LL).EQ.I) GO TO 52
   84 CONTINUE
   53 K=K+1
      LIN(I)=1
      ITYP(I)=2
      INELA(K)=I
   52 CONTINUE
      IF(K.EQ.0) GO TO 55
      SAS(MMM)=SREC
   70 L=1
C               ****************************************
C               * BEGINNING OF INELASTIC COMPUTATION *
C               ****************************************
      KOUT(L)=K
      WRITE(6,72) (FAC(I),I=1,6)
   72 FORMAT(/,' FAC',8F10.6,/)
      NE=NH-K
      NE1=NE+1
      KREPT=0
   73 SL(1)=SAS(MMM)
      WRITE(6,3151)MMM,SAS(MMM)
 3151 FORMAT(1X,      ' CYCLE NO ',I5,9X,'SLIP ASSUMED',F20.8)
      NLAB=1
C               ****************************************
C               * COMPUTATION OF THE ELASTIC PANELS *
C               ****************************************
      I=1
      GOTO 8222
  765 IF(LIN(I-1).EQ.1)GOTO 8989
 8222 Q(I)=(CV/(SL(I)-AV))+BV
      IF(I.EQ.LABAL(NLAB)) GO TO 56
      GO TO 67
   56 NLAB=NLAB+1
      Q(1)=0.
   67 IF(I.EQ.NH1) GOTO 1236
      CALL TERMS(I,EB,ES)
      IF(I-1) 700,700,701
  701 B(I)=Q(I)+B(I-1)
      GO TO 702
  700 B(I)=Q(I)
  702 HB(I)=B(I)*ALP(I)*SS(I)+BB(I)
      SL(I+1)=SL(1)+HB(I)
      IF(LIN(I).EQ.0)GOTO 7077
```

```
8989 II=I
     IF(LIN(II).EQ.1) GOTO 1235
     Q(II)=(CV/(SL(II)-AV))+BV
     IF(II.EQ.LABAL(NLAB)) GO TO 8228
     GO TO 677
8228 NLAB=NLAB+1
     Q(II)=0.
677  IF(II.EQ.NH1) GOTO 1236
     CALL TERMS(I,EB,ES)
     IF(II-1) 710,710,711
711  B(II)=Q(II)+B(II-1)
     GO TO 712
710  B(II)=Q(II)
712  HB(II)=B(II)*ALP(II)*SS(II)+BB(II)
     SL(II+1)=SL(II)+HB(II)
7077 ii=i
     CUR(II)=(BM(II)-B(II)*Z(II))/SEI(II)
     CURS(II)=CUR(II)
     CURB(II)=CUR(II)+CURD(II)
     STST(II)=-B(II)/(ES*AS(II))-CS(II)*CURS(II)
     STSB(II)=CURS(II)*DS+STST(II)
     STBT(II)=B(II)/(EB*AB(II))-CURB(II)*CB(II)
     STOT(II)=B(II)/(EB*AB(II))-CURB(II)*(CB(II)-DOT)
     STBB(II)=B(II)/(EB*AB(II))+CURB(II)*CBD(II)
     STOB(II)=B(II)/(EB*AB(II))+CURB(II)*(DOB-CB(II))
     TAW(II)=SHEAR(II)/AWEB(II)
     DN(II)=-STST(II)/CUR(II)
     IF(DN(II).GT.DS.OR.DN(II).LT.0.) DN(II)=DS
     I=I+1
     GOTO 765
C               ***************************************
C               * COMPUTATION OF THE INELASTIC PANELS *
C               ***************************************
1235 STSTT(II)=GST(II,4)
     STBBT(II)=GS(II,4)
     CURT(II)=GC(II,4)
     CURD1(II)=CURD(II)
     TAW(II)=SHEAR(II)/AWEB(II)
     BMREP=BM(II)
     IF(MERM.EQ.MER1.OR.MERM.EQ.MER2) GO TO 11
     GO TO 68
11   IF(ABS(SAS(MMM-1)-SAS(MMM-2)).GT.0.0000001) GO TO 68
     SCAL2=SCAL1
     SCAL1=SCAL1*0.5
     MSHEAR=0
68   CALL STRAIN(B,BM,CURD1,II)
     IF(MSHEAR.EQ.1) GOTO 4003
     BM(II)=BMREP
1247 FORMAT('$$$$$$$$$$$$$$$$$$$$$$$$$$$$$$$$$$$$$$$$$$$$',/)
     IF(KKCC.GT.4.AND.MMM.EQ.1) GO TO 201
     IF(KKCC.GT.4.AND.MMM.NE.1) GO TO 202
     GO TO 6106
201  IF(KM.EQ.6) GO TO 26
     W=(WM(3)+WM(4))*0.5
     IF(KREPT.EQ.1) GO TO 6
```

```
      IF(KM.EQ.1) GO TO 6
      FACTOR=0.75
      KM=KM+1
    6 WRITE(6,6112)
 6112 FORMAT(' THE LOADING INCREMENT IS CHANGED TO A SMALL VALUE--------
     1------------------------',//)
      GO TO 204
  202 IF(KN.EQ.NCHA) GO TO 26
      SAS(MMM)=SAS(MMM-1)+(SAS(MMM)-SAS(MMM-1))/5.
      KN=KN+1
      IF(KN.EQ.1) GO TO 4444
      DO 6111 I=1,6
      IF(I.LE.3) FAC(I)=(FAC(I)-1.)*FRACT+1.
      IF(I.GE.4) FAC(I)=2.-FAC(I-3)
      FAC2(I)=FAC(I)
 6111 CONTINUE
 4444 WRITE(6,6110)
 6110 FORMAT(' THE VALUE OF SLIP IS REASSUMED--------------------------
     1------------------------',//)
      GO TO 73
 6106 CUR(II)=CUR1(II)
      CURS(II)=CURS1(II)
      CURB(II)=CURB1(II)
      DN(II)=-STST(II)/CURS(II)
      IF(DN(II).GT.DS.OR.DN(II).LT.0.) DN(II)=DS
      STSB1(II)=STSB(II)+CUR1(II)*DC
      ANTEG(II)=(STBT(II)-STSB1(II))*SS(II)
      SL(II+1)=SL(II)+ANTEG(II)
      Q(II+1)=(CV/(SL(II+1)-AV))+BV
      IF((II+1).EQ.LABAL(NLAB)) GO TO 104
      GO TO 12
  104 NLAB=NLAB+1
      Q(II+1)=0.
   12 IF(II-NH) 1234,1236,1236
 1234 I=I+1
      B(I)=B(I-1)+Q(I)
      IF(B(II).GT.0.) GO TO 765
      KNEG=KNEG+1
      SAS(MMM)=SAS(MMM)*FANEG
      IF(KNEG.EQ.10) GO TO 26
      GO TO 73
 1236 ER11=0.
      IF(ABS(CURB(NH)-CURP).LE.(ACURA*CURB(NH))) ER11=1.
      CURP=CURB(NH)
      SLM(MMM)=SL(NH+1)
      IF(ABS(SLM(MMM)).LE.ER10.AND.ER11.EQ.1) GO TO 59
      WRITE(6,1239)MMM,SAS(MMM),SL(NH+1)
 1239 FORMAT(' CYCLE',I3,5X,'END SLIP ASSUMED',F12.8,6X,'MID-SPAN SLIP'
     1,F12.8)
      WRITE( 6,4333)                                                    ',
 4333 FORMAT('-----------------------------------------------------',/)
     1'-----------------------------------------------------',/)
      MMM=MMM+1
      KNEG=0
      IF(MMM.GT.NC) GO TO 26
```

```
C              ***********************************************
C              * PREDICT THE VALUE OF SLIP FOR NEXT CYCLE *
C              ***********************************************
C     IF(SLM(MMM-1).LE.(-.025)) SAS(MMM)=SAS(MMM-1)*FAC(1)
      IF(SLM(MMM-1).GT.(-.025).AND.SLM(MMM-1).LE.(-.002))
     1SAS(MMM)=SAS(MMM-1)*FAC(2)
      IF(SLM(MMM-1).GT.(-.002).AND.SLM(MMM-1).LE.0.) SAS(MMM)=
     1SAS(MMM-1)*FAC(3)
      IF(SLM(MMM-1).GE.(0.025)) SAS(MMM)=SAS(MMM-1)*FAC(4)
      IF(SLM(MMM-1).LT.(.025).AND.SLM(MMM-1).GE.(.002))
     1SAS(MMM)=SAS(MMM-1)*FAC(5)
      IF(SLM(MMM-1).LT.(.002).AND.SLM(MMM-1).GE.0.) SAS(MMM)=
     1SAS(MMM-1)*FAC(6)
      SASRE=SAS(MMM)
      IF(MMM.LE.2) GO TO 73
      CALL REGULA (MMM,MERM)
      IF(ABS(SAS(MMM-1)-SAS(MMM-2)).LE.0.0000003) SAS(MMM)=SASRE
      GO TO 73
   59 WRITE(6,1239) MMM,SAS(MMM),SL(NH+1)
      WRITE(6,1248)
 1248 FORMAT('$$$$$$$$$$ THIS IS THE LAST CYCLE $$$$$$$$$$')
      SREC=SAS(MMM)
      MMB=MMM-1
      MMM=1
      LAG=0
      CURP=0.
      MER2=100
      MERM=0
      MER1=100
      SCAL1=1.
      SCAL2=10.
C              ***********************************
C              * END OF INELASTIC COMPUTATION *
C              ***********************************
 4511 DO 433 I=1,NH
      CURT(I)=CURB(I)
      STBBT(I)=STBB(I)
      STSTT(I)=STST(I)
      STOT(I)=STBB(I)-CURB(I)*(DBT(I)-DOT)
      STOB(I)=STBB(I)-CURB(I)*(DBT(I)-DOB)
      STWT(I)=STBB(I)-CURB(I)*(DBT(I)-TF)
      STWB(I)=STBB(I)-CURB(I)*(DBT(I)-DB+TF)
      TAW(I)=SHEAR(I)/AWEB(I)
  433 CONTINUE
C     ***************************************************************************
C     *CHECK FOR YIELDING OF THE PANELS. IF NEW PANELS BECOME INELASTIC*
C     *                                                                *
C     *                    TREAT THEM INELASTICALLY                    *
C     ***************************************************************************
      KO=K
      DO 62 I=1,NH
      STY=STFY
```

```
      IF(XX(I).GE.PCUT) STY=STBY
      STRWY1=SQRT(STRWY**2-3.*(TAW(I)**2))
      WRITE(6,*) I,STRWY1
      IF(ABS(STST(I)).LE.STSY.AND.STBB(I).LE.STY) GO TO 6662
      GO TO 6664
 6662 STRWT=STWT(I)*EB
      STRWB=STWB(I)*EB
      IF(ABS(STRWT).LE.STRWY1.AND.ABS(STRWB).LE.STRWY1) GO TO 62
 6664 LIN(I)=1
      DO 66 LL=1,K
      IF(INELA(LL).EQ.I) GO TO 62
   66 CONTINUE
      K=K+1
      ITYP(I)=2
      INELA(K)=I
   62 CONTINUE
      L=L+1
      KOUT(L)=K
      KNEW=KOUT(L)-KO
      WRITE(6,2352)KNEW
 2352 FORMAT (1X,' NO OF NEW YIELDED PANELS IS ',I4)
      WRITE(6,1247)
      NE=NH-K
      NE1=NE+1
      MMM=1
      IF(KNEW.EQ.0) GO TO 55
      SAS(MMM)=SREC
      KREPT=1
      DO 74 I=1,NH
      GST(I,4)=STST(I)
      GC(I,4)=CURB(I)
   74 GS(I,4)=STBB(I)
      GO TO 73
   55 CONTINUE
      DO 76 I=1,NH
      CURT(I)=CURB(I)
      STBBT(I)=STBB(I)
      STSTT(I)=STST(I)
   76 CONTINUE
      DO 1110 I=1,MMB
      DSAS=SAS(I)-SREC
      RATS=SREC/SAS(I)
      WRITE(6,1117) I,DSAS,RATS,SAS(I),SLM(I)
 1117 FORMAT( ' NO',I3,5X,'SLIP DIFF',F9.7,5X,'RATIO',F10.8,5X,'SAS',
     1F11.8,5X,'MID-SPAN SLIP',F10.7)
 1110 CONTINUE
      MMM=1
      Q(NH1)=(CV/(SL(NH1)-AV))+BV
      DO 432 I=1,NH
      BMBE(I)=CURB(I)*EB*BIT(I)
      BMSL(I)=CURS(I)*ES*SI(I)
      BMFD(I)=BMBE(I)+BMSL(I)+B(I)*Z(I)
  432 CONTINUE
      DO 141 I=1,K
      IN1=INELA(I)
```

```
      BMBE(IN1)=BMB(IN1)
      BMSL(IN1)=BMS(IN1)
      BMFD(IN1)=BMM(IN1)
  141 CONTINUE
      DO 9951 I=1,NH
      IF(DN(I)-DS) 9950,9951,9950
 9950 WRITE(6,9952) I,DN(1)
 9952 FORMAT(    '   PANEL NO ',I3,5X,'DN',F10.3)
 9951 CONTINUE
C                 ************************************
C                 * COMPUTATION OF THE DEFLECTION *
C                 ************************************
  305 XX1(I)=.66666667*SD4
      AREA(1)=CUR(1)*.5*SD4
      TAREA(1)=AREA(1)
      DO 37 I=2,NH1
      XX1(I)=XX(I-1)
      AREA(I)=CUR(I-1)*SS(I-1)
   37 TAREA(I)=TAREA(I-1)+AREA(I)
      REACT=TAREA(NH1)
      DO 38 J=1,NH1
      DDIO=REACT*X(J)
      SUM=0.
      DO 39 I=1,NH1
      IF(XX1(I).GT.X(J)) GO TO 40
      SUM=SUM+AREA(I)*(X(J)-XX1(I))
   39 CONTINUE
   40 DEF(J)=DDIO-SUM
   38 CONTINUE
      WRITE(6,3001) W,BMLL
 3001 FORMAT(1X,///,' LIVE LOAD FORCE',F11.3,8X,'LIVE LOAD
     1MOMENT AT MID-SPAN',F13.0)
      WRITE(6,7008) BMMSP
 7008 FORMAT(' TOTAL B.M. AT MID-SPAN',F14.2)
      WRITE(6,41) (DEF(I),I=1,NH1)
   41 FORMAT(1HO,'DEF',13F9.5)
      IF(JM.EQ.0.AND.NSHOR.EQ.1) GO TO 301
      WRITE(6,412)
  412 FORMAT(1HO,/,6X,'X',8X,'Q',10X,'SL',/)
      WRITE(6,411)  (X(I),Q(I),SL(I),I=1,NH1)
  411 FORMAT(1HO,F8.2, F12.0,F12.7)
      WRITE(6,144)
  144 FORMAT(1HO,5X,'XX',13X,'STST',12X,'STSB',12X,'STBT',12X,
     1'STBB',12X,'CUR',13X,'CURB',12X,'CURS',12X,'F'/)
      WRITE(6,33)(XX(I),STST(I),STSB(I),STBT(I),STBB(I),CUR(I),
     1CURB(I),CURS(I),B(I),I=1,NH)
   33 FORMAT(1HO,F8.2,8E16.8)
      WRITE(6,7144)
 7144 FORMAT(1HO,5X,'STWT',13X,'STOT',12X,'STOB',12X,'STWB',12X,
     1'TAW',/)
      WRITE(6,60)(STWT(I),STOT(I),STOB(I),STWB(I),TAW(I),SHEAR(I)
     1,AWEB(I),I=1,NH)
   60 FORMAT(1HO,7E16.8)
      WRITE(6,1502)
 1502 FORMAT(1HO,6X,'XX',12X,'BMSL',12X,'BMBE',12X,'BMFD',12X,'TOTBM')
```

```
      WRITE(6,1501)(XX(I),BMSL(I),BMBE(I),BMFD(I),TOTBM(I),I=1,NH)
1501  FORMAT(1X, F8.2,4E16.8)
      IF(MH.EQ.1) GOTO 4046
      IF(MSHEAR.EQ.1) GOTO 4046
      MNM=1
7777  IF((3.*(TAW(MNM)**2)).GT.(STRWY**2))GOTO 4045
      MNM=MNM+1
      IF(MNM.LT.NH) GOTO 7777
      IF(K.EQ.0) GO TO 145
      WRITE(6,143) K,(INELA(L),L=1,K)
143   FORMAT(1HO,'NO. AND INELASTIC PANELS ',I6,18I4/)
      DO 4005 I=1,NH
4005  IF((3.*(TAW(I)**2)).GT.(STRWY**2))GOTO 26
C     ***************************************************************
C     *CHECK AGAINST EXCESSIVE YIELDING OF PANELS AND CONNECTOR FAILURE*
C     ***************************************************************
145   DO 93 I=1,NH
      IF(STBB(I).GE.STBBF .OR.ABS(STBT(I)).GE.STBTF ) GO TO 94
      IF(ABS(STST(I)).GE.STSTF.OR.STSB(I).GE.STSBF) GO TO 95
93    CONTINUE
      DO 90 I=1,NH1
      IF(ABS(SL(I)).GE.SLMAX) GO TO 91
      IF(DEF(I).GT.DFMAX) GO TO 5000
90    CONTINUE
      GO TO 100
91    WRITE(6,96)I
96    FORMAT('FAILURE OF CONNECTOR(S) NO ',I3)
      GO TO 26
94    WRITE(6,97) I,STBB(I),STBT(I)
97    FORMAT(1X,'EXCESSIVE YIELDING IN PANEL NO. ',I4,' STRAINS AR
     1E ',2E15.4)
      GO TO 26
95    WRITE(6,98) I,STST(I),STSB(I)
98    FORMAT(1X,' CONC CRUSHES IN PANEL NO. ',I4,' STRAINS ARE ',2E1
     15.4)
      GO TO 26
5000  WRITE(6,3000)
3000  FORMAT(' DEFLECTION EXCEEDS THE ALLOWABLE LIMIT')
      GO TO 26
100   IF(JM.GE.4) GO TO 6000
C     ***************************************************************
C     * RECORD THE VALUES USED IN EXTRAPOLATION IN THE NEXT CYCLE *
C     ***************************************************************
      DO 901 I=1,NH
      GS(I,JM)=STBBT(I)
      GC(I,JM)=CURT(I)
      GSL(I,JM)=SL(I)
901   GST(I,JM)=STSTT(I)
      GO TO 6104
6000  DO 6001 I=1,NH
      DO 6001 MJ=1,2
      GS(I,MJ)=GS(I,MJ+1)
      GC(I,MJ)=GC(I,MJ+1)
      GST(I,MJ)=GST(I,MJ+1)
6001  GSL(I,MJ)=GSL(I,MJ+1)
```

```
      DO 6003 I=1,NH
      GS(1,3)=STBBT(I)
      GC(1,3)=CURT(I)
      GSL(1,3)=SL(I)
 6003 GST(1,3)=STSTT(I)
      TS1=DS/2.0
      DO 9966 I= 1,NH
      CONSH=10.5*SQRT(STRSY)*DS*DS
      IF(DN(I).LT.TS1)CONSH=(1+ABS(B(I))/2000./BS/DS)
     1*SQRT(STRSY)*BS*DS
      IF(NSHOR.GT.0)GOTO 4020
      SHSLAB=(1-SHFAC(I))*((SHEAR(I)/SHFAC(I))-sheard(i))
      GOTO 4010
 4020 SHSLAB=(1-SHFAC(I))*((SHEAR(I)/SHFAC(I))-SHEARD(I))
 4010 IF(SHSLAB.LT.CONSH). GO TO 9966
      WRITE(6,9977) I,CONSH,SHSLAB
 9966 CONTINUE
 9977 FORMAT (1X,'SHEAR FAILURE IN SLAB IN PANEL',I5,5X,2E16.8)
      IF(SHSLAB.GE.CONSH) GO TO 26
 6104 IF (W.LE.WW8) GO TO 18
      GOTO 26
 4003 WRITE(6,4004)I
 4004 FORMAT(1X,' SHEAR FAILURE IN PANEL NO 'I3)
      IF((3.*(TAW(I)**2)).GT.(STRWY**2))GOTO 4045
      GOTO 4046
 4045 SEB=STRWY/SQRT(3.)
      SHEAR(I)=SEB*AWEB(I)
      WES=SHEAR(I)/(ZL/2.-XX(I))
      WRITE(6,*)SHEAR(I),XX(I),AWEB(I)
      WRITE(6,*)MSHEAR
      WRITE(6,*)WES
      W=WES-DL
      MH=1
      GOTO 6102
 4046 WRITE(6,143) K,(INELA(L),L=1,K)
 26   STOP
      END
C
C
      SUBROUTINE EXTRA(I,GYY,SUML)
C     ----------------------------
      DIMENSION GYY(50,4)
      COMMON/BL1/WM(4)
      SUML=0.0
      DO 7273 J=1,3
      PROL=GYY(I,J)
      DO 7283 L=1,3
      IF(J-L) 7293,7283,7293
 7293 PROL=PROL*((WM(4)-WM(L))/(WM(J)-WM(L)))
 7283 CONTINUE
 7273 SUML=SUML+PROL
      RETURN
      END
```

```
C     SUBROUTINE TERMS(I,EB,ES)
      ------------------------
C     COMMON/BL4/BMS(50),BMB(50),BIT(50),TW,TF,BF,DS,BS,AB(50),DC
      COMMON/BL10/AS(50),SI(50),SEI(50),EAB(50),EIB(50),Z(50),CS(50)
      COMMON/BL11/BET(50),ALP(50),BB(50),SS(50)
      COMMON/BL12/DN(50)
      COMMON/BL13/DBT(50),CBD(50),CB(50)
      COMMON/BL14/BM(50)
      AS(I)=DN(I)*BS
      CS(I)=.5*DN(I)
      Z(I)=(DS-CS(I))+CB(1)+DC
      SI(I)=BS*DN(I)**3./12.
      SEI(I)=EB*BIT(I)+ES*SI(I)
      EAB(I)=EB*AB(I)*ES*AS(I)/(EB*AB(I)+ES*AS(I))
      EIB(I)=SEI(I)+EAB(I)*Z(I)**2.
      BET(I)=Z(I)/SEI(I)
      ALP(I)=EIB(I)/(EAB(I)*SEI(I))
      BB(I)=-BET(I)*BM(I)*SS(I)
      RETURN
      END
C
      SUBROUTINE REGULA(MMM,MERM)
C     --------------------------
      COMMON/BL29/UU,VV,XL,XR,MER1,MER2,sas(80),SLM(80),LAG
      IF(LAG.LT.1) GO TO 2007
      IF(SLM(MMM-1)*VV) 2009,2009,2010
 2010 XL=SAS(MMM-1)
      VV=SLM(MMM-1)
      MER1=MMM-1
      GO TO 2005
 2009 XR=SAS(MMM-1)
      UU=SLM(MMM-1)
      MER2=MMM-1
      GO TO 2005
 2007 IF(SLM(MMM-1)*SLM(MMM-2)) 2002,2002,25
 2002 LAG=LAG+1
      IF(SLM(MMM-1)) 2003,2003,2004
 2003 VV=SLM(MMM-1)
      UU=SLM(MMM-2)
      XL=SAS(MMM-1)
      XR=SAS(MMM-2)
      MER1=MMM-1
      MER2=MMM-2
      GO TO 2005
 2004 UU=SLM(MMM-1)
      VV=SLM(MMM-2)
      XR=SAS(MMM-1)
      XL=SAS(MMM-2)
      MER2=MMM-1
      MER1=MMM-2
 2005 SAS(MMM)=(XL*UU-XR*VV)/(UU-VV)
      IF(MERM.EQ.MER1.OR.MERM.EQ.MER2)SAS(MMM)=(XL+XR)*0.5
   25 RETURN
      END
```

```
C
      SUBROUTINE STRAIN(FST,BMST,CURD1,I)
C     ------------------------------------
      DIMENSION FST(50),BMST(50),CURD1(50)
      COMMON/BL3/BMM(50)
      COMMON/BL4/BMS(50),BMB(50),BIT(50),TW,TF,BF,DS,BS,AB(50),DC
      COMMON/BL5/STSY,STRSY,STRPY,STRWY,STRFY,EB,STFY,ES,EBP,EX
      COMMON/BL6/FB(50)
      COMMON/BL7/CUR1(50)
      COMMON/BL8/CURB1(50)
      COMMON/BL9/CURS1(50)
      COMMON/BL13/DBT(50),CBD(50),CB(50)
      COMMON/BL17/STST(50),STBB(50)
      COMMON/BL18/STSB(50)
      COMMON/BL19/STBT(50)
      COMMON/BL20/CUR(50)
      COMMON/BL23/CURT(50),STBBT(50),STSTT(50)
      COMMON/BL25/MA,JM,NH,KER,KEM2
      COMMON/BL26/STC(50),CUC(50)
      COMMON/BL27/KKCC,MERM,MMM
      COMMON/BL28/GSNH,ERST,SCAL1,SCAL2
      COMMON/BL30/XX(50),XOL,XOR,NOT,NO,NOB,TAW(50),MSHEAR
      KER=0
      KKCC=0
      KK2=0
      CUR1(I)=CURT(I)
      STBB(I)=STBBT(I)
      BMST(I)=BMST(I)+CURD1(I)*EB*BIT(I)
      CURB1(I)=CUR1(I)
      WRITE(6,604) I,CUR1(I),STBB(I)
604   FORMAT( '  INELASTIC PANEL  NO',I2,5X,'CURVATURE BAR',E13.6,5X,'S
     1TRAIN BAR',E14.6)
      MSHEAR=0
      CALL FAMB(STBB,CURB1,I)
      IF(MSHEAR.EQ.1) GOTO 5
      CURS1(I)=CURB1(I)-CURD1(I)
      CALL STAMS(FB,CURS1,I)
      FB2=FB(I)
      BMB2=BMM(I)
      FB4=FB(I)
      BMB4=BMM(I)
      CUC(I)=0.1E-07
      STC(I)=0.1E-07
8012  NLK=0
      NLM=0
      NLL=0
      GO TO 2
7051  CUC(I)=0.1E-05
      STC(I)=0.1E-05
      NLK=1
      GO TO 2
7052  CUC(I)=0.1E-06
      STC(I)=0.1E-08
      NLL=1
      GO TO 2
```

```
7053 CUC(I)=0.1E-08
     STC(I)=0.1E-06
     NLM=1
2    IF(KK2.GE.2) GO TO 58
     GO TO 59
58   CUC(I)=0.5E-08
     STC(I)=0.5E-08
59   CURB1(I)=CUR1(I)+CUC(I)
     MSHEAR=0
     CALL FAMB(STBB,CURB1,I)
     IF(MSHEAR.EQ.1) GOTO 5
     CURS1(I)=CURB1(I)-CURD1(I)
     IF (FB(I).LE.0.) GO TO 8019
     MA=1
     CALL STAMS(FB,CURS1,I)
     MA=0
     IF(KEM2.EQ.1) GO TO 8019
     FBC=FB(I)
     BMBC=BMM(I)
     CURB1(I)=CUR1(I)
     IF(KKCC.EQ.0) GO TO 505
     WRITE(6,606) CUC(I),FBC,BMBC
606  FORMAT (' DEL CUR',E26.8,4X,'F DEL CUR',F25.6,4X,'M DELT CUR'
    1,F21.8)
505  STBB(I)=STBB(I)+STC(I)
     MSHEAR=0
     CALL FAMB(STBB,CURB1,I)
     IF(MSHEAR.EQ.1) GOTO 5
     CURS1(I)=CURB1(I)-CURD1(I)
     CALL STAMS(FB,CURS1,I)
     IF(KEM2.EQ.1) GO TO 8019
     FBST=FB(I)
     BMBST=BMM(I)
     IF(KKCC.EQ.0) GO TO 506
     WRITE(6,607)STC(I),STBB(I),FBST,BMBST
607  FORMAT(1HO,'DELT ST',1E22.5,4X,'STRAIN P',1E23.5,5X,'F DELT ST',
    1F22.1,6X,'M DEL ST',1E21.4)
506  DFDC=(FBC-FB2)/CUC(I)
     DMDC=(BMBC-BMB2)/CUC(I)
     DFDST=(FBST-FB2)/STC(I)
     DMDST=(BMBST-BMB2)/STC(I)
     IF(DFDST.LE.0..OR.DMDST.LE.0.) GO TO 3
     IF(DFDC.GE.0..OR.DMDC.GE.0.) GO TO 3
     DENO=DFDST*DMDC-DMDST*DFDC
     IF(DENO.NE.0..AND.DFDC.NE.0.) GO TO 7060
3    KER=1
8019 KKCC=KKCC+1
     KK2=1
     WRITE(6,8010) KKCC
8010 FORMAT(/////,'OOOOOOOOOOOOOOOOOOOOOOOOOOOOOOOOOKKCC IS ',I3,//)
     IF(KKCC.GT.4) GO TO 5
     CUR1(I)=CURT(I)
     STBB(I)=STBBT(I)
     FB2=FB4
     BMB2=BMB4
```

```
      IF(NLK.EQ.0) GO TO 7051
      IF(NLL.EQ.0) GO TO 7052
      IF(NLM.EQ.0) GO TO 7053
7060  STBB2N=(DMDC*(FST(I)-FB2)-DFDC*(BMST(I)-BMB2))/(DFDST*DMDC-D
     1FDC*DMDST)
      CURIN2=(FST(I)-FB2-DFDST*STBB2N)/DFDC
      IF(KKCC.EQ.0) GO TO 10
      WRITE(6,989)
989   FORMAT('                DFDC          ','                DMDC          ','
     1 DFDST                    DMDST                DELT ST                ','
     2'DELT CUR')
      WRITE(6,7) DFDC,DMDC,DFDST,DMDST,STBB2N,CURIN2
7     FORMAT(2X,6E20.8)
10    STBB(I)=STBB(I)-STC(I)+STBB2N
      CURI(I)=CURI(I)+CURIN2
      IF(KKCC.EQ.0) GO TO 122
      WRITE(6,960)STBB(I),CURI(I)
960   FORMAT('  STR  PRIME AND CURVATURE PRIME',2E14.5)
122   CONTINUE
      IF(STBB(I).GT.1..OR.CURI(I).GT.1.) GO TO 8019
      IF(STBB(I).GT.0..AND.CURI(I).GT.0.) GO TO 8
      GO TO 8019
8     CURB1(I)=CURI(I)
      MSHEAR=0
      CALL FAMB(STBB,CURB1,I)
      IF(MSHEAR.EQ.1) GOTO 5
      CURS1(I)=CURB1(I)-CURD1(I)
      CALL STAMS(FB,CURS1,I)
      IF(KEM2.EQ.1) GO TO 8019
      FB2=FB(I)
      BMB2=BMM(I)
      KK2=KK2+1
      ERFAC=ERST
      IF(GSNH.GE.0.008) ERFAC=ERST/4.
      IF(GSNH.GE.0.05) ERFAC=ERST/25.
      ERR1=ABS(FST(I))*ERFAC*SCAL1
      ERR2=ABS(BMST(I))*ERFAC*SCAL1
      IF(KKCC.EQ.0) GO TO 121
      WRITE(6,632) FST(I),FB2,BMST(I),BMB2
632   FORMAT('  FORCE ASSUMED IN THE PANEL',F12.1,5X,'F SOLVED
     1',F15.4,5X,'MOMT ASSUMED',F13.0,5X,'MSOL',F15.4)
121   CONTINUE
      IF(ABS(FST(I)-FB2).LE.ERR1.AND.ABS(BMST(I)-BMB2).LE.ERR2)
     1GO TO 4
      IF(KK2.GE.4) GO TO 4
      GO TO 2
4     CONTINUE
      WRITE(6,8187)KK2
8187  FORMAT(' KK2= 'I3)
      IF(KK2.EQ.4) MERM=MMM
      ERE1=ABS(FST(I))*ERFAC*SCAL2
      ERE2=ABS(BMST(I))*ERFAC*SCAL2
      IF(ABS(FST(I)-FB2).GT.ERE1.OR.ABS(BMST(I)-BMB2).GT.ERE2)
     1GO TO 8019
```

```
      STBBT(I)=STBB(I)
      STSTT(I)=STST(I)
      CURT(I)=CUR1(I)
      CUR1(I)=CURS1(I)
      WRITE(6,6) KK2,I
      FORMAT(2X,'((((((((((    KK2= ',I2,'    ))))))))))','PANEL NO',
    6 1I3,/)
      RETURN
    5 END

C     SUBROUTINE STAMS(FB,CURS1,I)
C     ----------------------------
      DIMENSION FB(50),CURS1(50),FB1(10)
      COMMON/BL2/FS(50),CS1
      COMMON/BL3/BMM(50)
      COMMON/BL4/BMS(50),BMB(50),BIT(50),TW,TF,BF,DS,BS,AB(50),DC
      COMMON/BL5/STSY,STRSY,STRPY,STRWY,STRFY,EB,STFY,ES,EBP,EX
      COMMON/BL13/DBT(50),CBD(50),CB(50)
      COMMON/BL17/STST(50),STBB(50)
      COMMON/BL18/STSB(50)
      COMMON/BL23/CURT(50),STBBT(50),STSTT(50)
      COMMON/BL25/MA,JM,NH,KER,KEM2
      COMMON/BL28/GSNH,ERST,SCAL1,SCAL2
      KEM2=0
      KC=0
      NNA=0
      NNB=0
      STST(I)=STSTT(I)
      CALL FAMS(STST,CURS1,I)
      FB1(1)=FS(I)
      DSTST=-5.0E-6
    6 CONTINUE
      DO 2 L=1,6
      IF(MA.EQ.1) DSTST=DSTST*(-1.0)
      STST(I)=STST(I)+DSTST
      CALL FAMS(STST,CURS1,I)
      FD1=FS(I)
      DFDE=(FD1-FB1(L))/DSTST
      IF(DFDE.NE.0.)GO TO 5
      STST(I)=STSTT(I)
      IF(NNA.EQ.1) GO TO 7
      DSTST=-1.0E-04
      NNA=1
      GO TO 6
    7 IF(NNB.EQ.1) GO TO 9
      DSTST=-5.0E-03
      NNB=1
      GO TO 6
    9 KEM2=1
      GO TO 4
    5 DSTST1=(FB(I)-ABS(FB1(L)))/DFDE
      STST(I)=STST(I)-DSTST1-DSTST
      CALL FAMS(STST,CURS1,I)
      ERCOE=0.0001
```

```
      IF(GSNH.GE.0.015) ERCOE=0.00001
      IF(GSNH.GE.0.045) ERCOE=0.000002
      ERR3=ABS(FB(I))*ERCOE
      IF(KER.GE.1) ERR3=ERR3*0.0001
      IF(MA.EQ.1) DSTST=DSTST*(-1.0)
      IF(ABS(FB(I)-ABS(FS(I))).LE.ERR3) GO TO 3
      FB1(L+1)=FS(I)
      CONTINUE
2     Z1=CS1+CB(I)
3     BMM(I)=BMB(I)+BMS(I)+FB(I)*Z1
      RETURN
4     END

C     SUBROUTINE FAMS(STST,CURS1,I)
C     -----------------------------
      DIMENSION STST(50),CURS1(50)
      COMMON/BL2/FS(50),CS1
      COMMON/BL4/BMS(50),BMB(50),BIT(50),TW,TF,BF,DS,BS,AB(50),DC
      COMMON/BL5/STSY,STRSY,STRPY,STRWY,STRFY,EB,STFY,ES,EBP,EX
      COMMON/BL18/STSB(50)
      STSB(I)=STST(I)+DS*CURS1(I)
      DNAS=ABS(STST(I))/CURS1(I)
      IF(DNAS.GE.DS) DNAS=DS
      CS1=DS-.5*DNAS+DC
      STBO=STST(I)+DNAS*CURS1(I)
      ZMABO=STBO*ES*(-1.)
      ZMAT=STST(I)*ES*(-1.)
      IF(ABS(STST(I)).GE.STSY) ZMAT=STRSY
      DEZMA=ZMAT-ZMABO
      H=(STSY-ABS(STBO))/CURS1(I)
      IF(H.GT.DNAS) H=DNAS
      F1=ZMAT*DNAS*BS
      F2=DEZMA*0.5*H*BS
      FS(I)=F2-F1
      YBA=(F1*DNAS*0.5-(F2*H)/3.)/(F1-F2)
      BMS(I)=(0.5*DNAS-YBA)*FS(I)
      RETURN
      END
C
      SUBROUTINE FAMB(STBB,CURB1,I)
C     -----------------------------
      DIMENSION STBB(50),CURB1(50),FBB(165),BMBB(165),TFBB(165),
     $TBMBB(165),STBD(165),STRBD(165)
      COMMON/BL4/BMS(50),BMB(50),BIT(50),TW,TF,BF,DS,BS,AB(50),DC
      COMMON/BL5/STSY,STRSY,STRPY,STRWY,STRFY,EB,STFY,ES,EBP,EX
      COMMON/BL6/FB(50)
      COMMON/BL13/DBT(50),CBD(50),CB(50)
      COMMON/BL19/STBT(50)
      COMMON/BL21/BH(165),DDB(165),DFA(165),HARST,NFU,NFD,NW,NPL,PCUT
      COMMON/BL30/XX(50),XOL,XOR,NOT,NO,NOB,TAW(50),MSHEAR
      IF(XX(I).LE.PCUT) NN=NFU+NW+NFD
      IF(XX(I).GT.PCUT) NN=NFU+NW+NFD+NPL
      STBT(I)=STBB(I)-CURB1(I)*DBT(I)
      STBD(1)=STBT(I)
      STRBD(1)=STBD(1)*EB
```

```
      IF(3*TAW(I)**2..GE.STRFY**2.)GOTO 4444
      IF(STBD(1).GE.STFY.AND.STBD(1).LE.HARST)
     1STRBD(1)=STFY*EB
      IF(STBD(1).GT.HARST)
     1STRBD(1)=STFY*EB+(STBD(1)-HARST)*EBP
      DO 4 KL=1,NN
      STRY=STRFY
      IF((KL+1).GT.NFU) STRY=SQRT(STRWY**2.-3.*(TAW(I)**2.))
      IF((KL+1).GT.(NFU+NW)) STRY=STRFY
      IF((KL+1).GT.(NFU+NW+NFD)) STRY=STRPY
      STBY=STRY/EB
      STBD(KL+1)=STBD(KL)+CURB1(I)*DDB(KL)
      STRBD(KL+1)=STBD(KL+1)*EB
      IF(ABS(STBD(KL+1)).GE.STBY.AND.ABS(STBD(KL+1)).LE.HARST)
     1STRBD(KL+1)=STRY*STBD(KL+1)/ABS(STBD(KL+1))
      IF(ABS(STBD(KL+1)).GT.HARST) STRBD(KL+1)=(STRY+(ABS(STBD(KL+1))-
     1HARST)*EBP)*STBD(KL+1)/ABS(STBD(KL+1))
      FBB(KL)=(STRBD(KL+1)+STRBD(KL))*.5*DDB(KL)*BH(KL)
      IF(XX(I).GT.XOL.AND.XX(I).LT.XOR) GO TO 10
      GO TO 20
   10 IF(KL.GT.(NFU+NOT).AND.KL.LT.(NFU+NOT+NO)) FBB(KL)=0.0
   20 BMBB(KL)=(DFA(KL)-DDB(KL)*.5)*FBB(KL)
      IF(KL.GT.1) GO TO 8
      TFBB(KL)=FBB(KL)
      TBMBB(KL)=BMBB(KL)
      GO TO 4
    8 TFBB(KL)=TFBB(KL-1)+FBB(KL)
      TBMBB(KL)=TBMBB(KL-1) +BMBB(KL)
    4 CONTINUE
      FB(I)=TFBB(NN)
      YYY=DBT(I)-(TBMBB(NN)/FB(I))
      BMB(I)=ABS(CBD(I)-YYY)*FB(I)
C      WRITE(6,4343)FB(I),BMB(I)
C4343 FORMAT(1X, 'FORCE IN PANEL= 'E20.8,' MOMENT IN PANEL=' E20.8)
      GOTO 4440
 4444 WRITE(*,*) 'SHEAR FAILURE'
      MSHEAR=1
      GOTO 4440
      WRITE(6,4441)KL
 4441 FORMAT(1X,'SHEAR FAILURE IN ELEMENT NO 'I4)
 4440 RETURN
      END
C
      SUBROUTINE BAND(A,B,N,M,LT,DET)
C     ------------------------------
      DIMENSION A(4000),B(250)
      MM=M-1
      NM=N*M
      NM1=NM-MM
      IF (LT.NE.1) GO TO 55
      MP=M+1
      KK=2
      FAC=DET
      A(1)=1./SQRT(A(1))
      BIGL=A(1)
```

```
      SML=A(1)
      A(2)=A(2)*A(1)
      A(MP)=1./SQRT(A(MP)-A(2)*A(2))
      IF(A(MP).GT.BIGL)BIGL=A(MP)
      IF(A(MP).LT.SML)SML=A(MP)
      MP=MP+M
      DO 62 J=MP,NM1,M
      JP=J-MM
      MZC=0
      IF(KK.GE.M) GO TO 1
      KK=KK+1
      II=1
      JC=1
      GO TO 2
1     KK=KK+M
      II=KK-MM
      JC=KK-MM
2     DO 65 I=KK,JP,MM
      IF(A(I).EQ.0.) GO TO 64
      GO TO 66
64    JC=JC+M
65    MZC=MZC+1
      ASUM1=0.
      GO TO 61
66    MMZC=MM*MZC
      II=II+MZC
      KM=KK+MMZC
      A(KM)=A(KM)*A(JC)
      IF(KM.GE.JP) GO TO 6
      KJ=KM+MM
      DO 5 I=KJ,JP,MM
      ASUM2=0.
      IM=I-MM
      II=II+1
      KI=II+MMZC
      DO 7 K=KM,IM,MM
      ASUM2=ASUM2+A(KI)*A(K)
7     KI=KI+MM
5     A(I)=(A(I)-ASUM2)*A(KI)
6     CONTINUE
      ASUM1=0.
      DO 4 K=KM,JP,MM
4     ASUM1=ASUM1+A(K)*A(K)
61    S=A(J)-ASUM1
      IF(S.LT.0.)DET=S
      IF(S.EQ.0.)DET=0.
      IF(S.GT.0.)GO TO 63
      NROW=(J+MM)/M
      WRITE(6,99) NROW
99    FORMAT(35HOERROR CONDITION ENCOUNTERED IN ROW ,I6)
      RETURN
63    A(J)=1./SQRT(S)
      IF(A(J).GT.BIGL)BIGL=A(J)
      IF(A(J).LT.SML)SML=A(J)
```

```
62    CONTINUE
      IF(SML.LE.FAC*BIGL)GO TO 54
      GO TO 53
54    DET=0.
      RETURN
53    DET=SML/BIGL
55    B(1)=B(1)*A(1)
      KK=1
      K1=1
      J=1
      DO 8 L=2,N
      BSUM1=0.
      LM=L-1
      J=J+M
      IF(KK.GE.M)GO TO 12
      KK=KK+1
      GO TO 13
12    KK=KK+M
      K1=K1+1
13    JK=KK
      DO 9 K=K1,LM
      BSUM1=BSUM1+A(JK)*B(K)
      JK=JK+MM
9     CONTINUE
8     B(L)=(B(L)-BSUM1)*A(J)
      B(N)=B(N)*A(NM1)
      NMM=NM1
      NN=N-1
      ND=N
      DO 10 L=1,NN
      BSUM2=0.
      NL=N-L
      NL1=N-L+1
      NMM=NMM-M
      NJ1=NMM
      IF(L.GE.M)ND=ND-1
      DO 11 K=NL1,ND
      NJ1=NJ1+1
      BSUM2=BSUM2+A(NJ1)*B(K)
11    CONTINUE
10    B(NL)=(B(NL)-BSUM2)*A(NMM)
      RETURN
      END
```

APPENDIX C

SAMPLE DATA FILE

```
BEAM 2N
20.95,.382,.506,8.03,1330.
4.72,83.5,394.
98.43,112.2,3.58,17.36,.8,.99
0.,8.2,2.36,20.
.5,.004,.5,8.
3000.,35840.,49857.,45285.
.00104,.00104,.0151,.0151
2900000.,29000000.,400000.
50.,25.,3.,2.,1.,0.5,.25
0.,340,341.,625.,770.,780.,800.
33,0,3,3,6,0,60,15,45
0.,0.,197.
.02,.12,9327.43,17000.,.0008
80,40,.00001,.0001,.015,0.
1.008,1.006,1.005
1.0025,1.002,1.002
1.04,1.009,1.004
.00002,.01,.9,1.1,.92,1.05,50
.0004,1.006
11.8,11.8,11.8,11.8,11.8,11.8,11.8,11.8,11.8,11.8,
11.8,11.8,11.8,11.8,11.8,11.8
47,7
11.8,11.8,11.8,11.8,11.8,11.8,11.8,7.53,.1,.1,4.07,
9.5,.1,.1,2.1,11.8,11.8,11.8,11.8,11.8,11.8,11.7,.1
9,10,11,13,14,15,23
```

APPENDIX D

COMPUTATION OF ULTIMATE MOMENT AND SHEAR CAPACITIES

D-1. Computation of M_{ult}:

The stress-block method was used to determine the ultimate moment capacity of the full composite beam. The force in the concrete slab is equal to the net tensile force in the steel beam. The interaction force developed between the steel beam and the concrete slab depends on the type of connection between them; for complete interaction, the net force is equal to the ultimate capacity of the connector, and for under-connected beams, the forces in both the steel beam and the concrete slab are less than the ultimate capacity of each item, and are controlled by the maximum force that can be transmitted by the connectors.

The capacity of the composite beam to sustain loads is limited by the capacity of its weakest component. The ultimate capacity of each component is computed. A check is first made to determine whether the number of connectors is sufficient for complete interaction to develop between the steel beam and the concrete slab. The number of shear connectors in the shear span is multiplied by the ultimate capacity of a single connector. The result is compared with the total tensile force the steel beam can sustain, which is the product of multiplying the cross-sectional area of the steel beam by the yield strength of the used steel. If the shear connectors can transmit the total force that can be resisted by the steel beam, then full interaction between the two components is possible. If the force that can be resisted by the steel beam is larger than the force that can be transmitted by the shear connectors, then partial interaction is the governing case.

Also, the force that can be resisted by the concrete slab is computed by multiplying the cross-sectional area of the slab by its yield stress. If the total compressive force that can be resisted by the concrete slab is larger than the tensile force that can be sustained by the steel beam, then full interaction is possible. However, the tensile force in the steel beam cannot exceed the compressive force in the slab for stability, therefore if the compressive force that can be resisted by the concrete slab is lower than the tensile force that can be resisted by the steel beam, then the tensile force in the steel beam is equal to the force in the slab.

To determine if complete interaction could be developed between the two components of the composite beam, the total load that can be transmitted by the shear connectors is computed. The force transmitted by the connectors is equal to

$$F=N\times Q_{ult} \qquad [D\text{-}1]$$

where 'F' is the total force that can be transmitted by the shear connectors.

'N' is the number of connectors in the shear span.

'Qult' is the ultimate capacity of a single connector.

The total force that can be resisted by the steel beam is equal to

$$T=A_s\times\sigma_{yb} \qquad [D\text{-}2]$$

where 'T' is the total tensile force in the steel beam.

'A_s' is the steel beam area.

'σ_{yb}' is the yield stress of the steel.

The total force transmitted by the shear connectors is then compared to the total force that can be resisted by the steel beam. If the total force that can be transmitted by the shear connectors is greater than or equal to the force that can be developed in the steel beam, then full interaction can develop in the composite beam. On the other hand, if the total force 'F' that can be transmitted by the shear connectors is less than the capacity of the composite beam, then only partial interaction can develop.

D-1.1. Full Interaction:

Figure D-1 shows the state of stresses at the mid-span of a composite beam at the ultimate loading stage. The total force that can be resisted by the steel beam is obtained from

$$T=A_s\times\sigma_{yb} \qquad [D\text{-}2]$$

For stability, the force 'T' must be balanced by an equal force 'C' in the concrete slab. The compressed depth of the concrete slab, 'a', is computed from

$$C=0.85\times B\times f_c'\times a \qquad [D\text{-}3]$$

where 'C' is the total compressive force in the slab.

'B' is the effective width of the slab ($16t_s+b_f$).

'f_c" is the yield stress of the concrete.

'a' is the compressed depth of the slab.

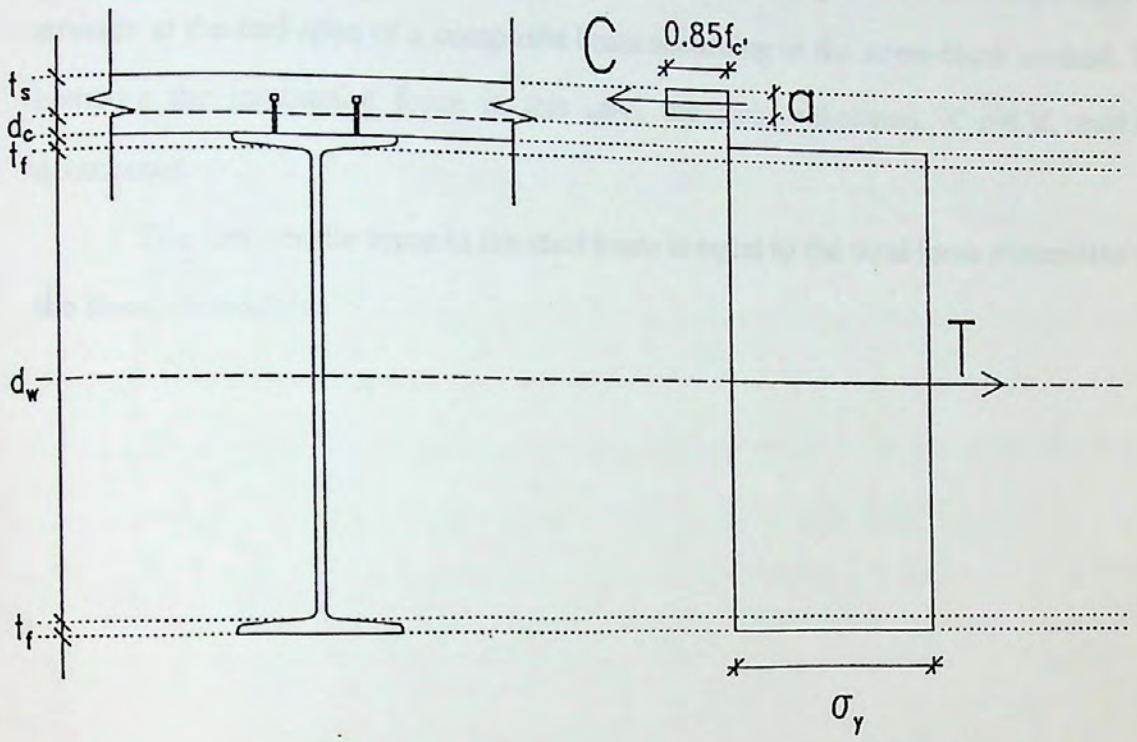

Figure D-1- State of Stresses in the Case of Full Interaction

Having computed the compressed depth of the slab, the ultimate moment capacity of the composite beam could be computed by taking the moments about the point of application of the compressive force in the slab.

$$M_{ult}=T\times\left(\frac{d_w+2t_f}{2}+t_s+d_c-\frac{a}{2}\right) \qquad [D\text{-}4]$$

where 'M_{ult}' is the ultimate moment capacity of the composite beam.

'T' is the total tensile force in the steel beam.

'd_w' is the depth of the steel web.

't_f' is the flange thickness.

'd_c' is the depth of the cellular decking.

't_s' is the thickness of the solid slab.

'a' is the depth of the compressed concrete.

D-1.2. Partial Interaction:

If the number of connectors is insufficient to transmit the total force in the steel beam to the slab, then partial interaction is in effect. Figure D-2 shows the state of stresses at the mid-span of a composite beam according to the stress-block method. To compute the interaction force in this case, the two unknowns, 'X' and 'a', must be determined.

The net tensile force in the steel beam is equal to the total force transmitted by the shear connectors.

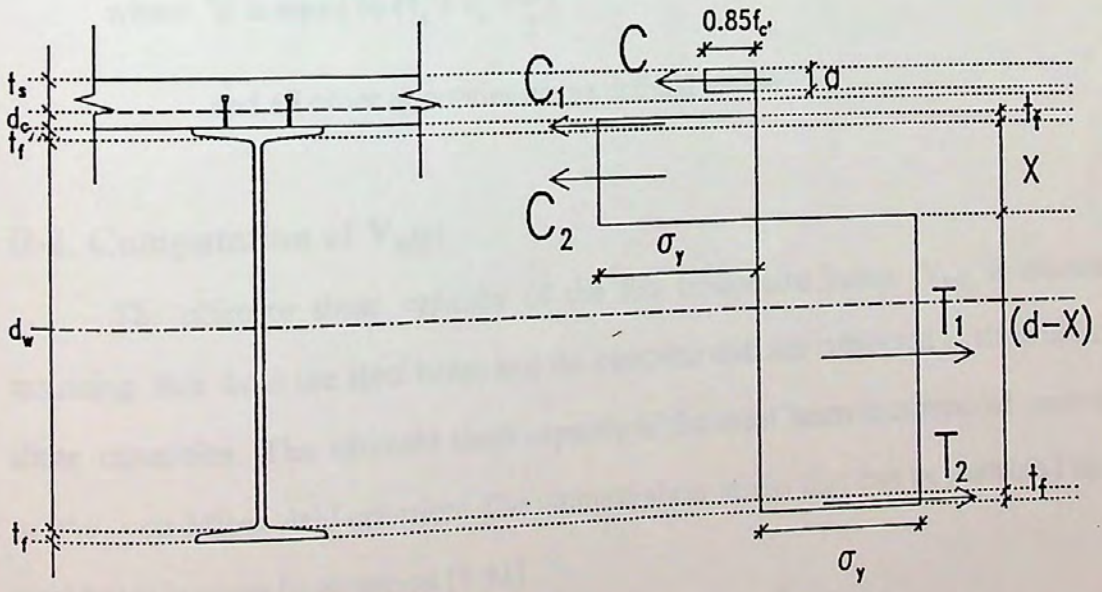

Figure D-2- State of Stresses in the Case of Partial Interaction

$$N \times Q_{ult} = \sigma_{yb}(A_f + X \times t_w - (A_f + (d_w - X)t_w))$$

$$N \times Q_{ult} = \sigma_{yb}(X \times t_w - (d_w - X)t_w) \qquad [D\text{-}5]$$

where 'A_f' is the area of the flange.

'd_w' is the depth of the web of the steel beam.

't_w' is the thickness of the web.

'N' and 'Q_{ult}' are as defined in equ. [D-1], and σ_{yb} is as defined in equ.[D-2].

From equation [D-5] 'X' is determined. For stability, the net tensile force in the steel beam is equal to the compressive force in the concrete slab, that is

$$\sigma_{yb}(X \times t_w - (d_w - X)t_w) = 0.85 \times B \times f_c' \times a \qquad [D\text{-}6]$$

The only unknown in equation [D-6] is the depth of the compressed concrete, 'a', and can thus be computed.

Computing the moments about the point of action of the compressive force 'C' of the concrete slab, the ultimate moment capacity is equal to (from figure D-2)

$$M_{ult} = \sigma_{yb}\left(-A_f\left(\frac{t_f}{2} + b\right) - X\left(\frac{X}{2} + t_f + b\right) + (d_w - X)\left(X + \frac{d_w - X}{2} + t_f + b\right) + A_f\left(\frac{t_f}{2} + d_w + t_f + b\right)\right)$$

$$M_{ult} = \sigma_{yb}\left(-A_f\left(\frac{t_f}{2} + b\right) - X\left(\frac{X}{2} + t_f + b\right) + (d_w - X)\left(\frac{d_w + X}{2} + t_f + b\right) + A_f\left(\frac{3t_f}{2} + d_w + b\right)\right)$$

..... [D-7]

where 'b' is equal to $\left(t_s + d_c - \frac{a}{2}\right)$.

and all other quantities are as defined earlier.

D-2. Computation of V_{ult}:

The ultimate shear capacity of the full composite beam, V_{ult}, is calculated assuming that both the steel beam and the concrete slab are subjected to their ultimate shear capacities. The ultimate shear capacity of the steel beam is computed according to the von-Mises yield criterion. The ultimate shear stress that can be sustained by the steel beam is given by equation [3.43]

$$\tau_{max} = \frac{\sigma_y}{\sqrt{3}} \qquad [3.43]$$

The ultimate shear capacity that can be resisted by the steel beam alone, V_{bmax}, can be obtained by multiplying the ultimate shear stress, τ_{max}, by the web area of the steel beam.

$$V_{bmax}=\tau_{max}\times t_w \times d_w$$

The ultimate shear capacity of the concrete slab, V_{smax}, is obtained from equation [3.35].

$$V_s=0.9t_s^2\sqrt{f_c} \qquad [3.35]$$

The ultimate shear capacity of the full beam is then obtained by adding the ultimate shear capacities of the steel beam and the concrete slab.

$$V_{ult}=V_{bmax}+V_{smax} \qquad [D-8]$$

NAME..AMGD..HASSANEIN.....

TITLE OF THESIS..NON-LINEAR..ANALYSIS..OF..COMPOSITE....
.....BEAMS..WITH..WEB..OPENINGS.....
.....

DEPARTMENT.CIVIL.ENG.....YEAR..95.... [Library no.....]

Please sign and date ONE of the following paragraphs:

1. The thesis may be consulted in the Library and photocopied.

Signed... [redacted] .....Date..17/8/89.....

OR

2. The thesis may be consulted in the Library, but may not be photocopied. The restriction on photocopying will cease two years after the date below, unless I apply for, and am granted, its renewal.*

Signed.....Date.....

OR

3. The thesis may neither be consulted nor photocopied without written permission from me, or from the appropriate Head of Department if I cannot be contacted. This restriction will cease three years after the date below, unless I apply for, and am granted, its renewal.*

Signed.....Date.....

* Application for renewal of restrictions will be considered by the Librarian, the appropriate Head of Department and the Chairman of the Academic Board or his nominee.